INFORMATION TO USERS

The most advanced technology has been used to photograph and reproduce this manuscript from the microfilm master. UMI films the original text directly from the copy submitted. Thus, some dissertation copies are in typewriter face, while others may be from a computer printer.

In the unlikely event that the author did not send UMI a complete manuscript and there are missing pages, these will be noted. Also, if unauthorized copyrighted material had to be removed, a note will indicate the deletion.

Oversize materials (e.g., maps, drawings, charts) are reproduced by sectioning the original, beginning at the upper left-hand corner and continuing from left to right in equal sections with small overlaps. Each oversize page is available as one exposure on a standard 35 mm slide or as a 17″ × 23″ black and white photographic print for an additional charge.

Photographs included in the original manuscript have been reproduced xerographically in this copy. 35 mm slides or 6″ × 9″ black and white photographic prints are available for any photographs or illustrations appearing in this copy for an additional charge. Contact UMI directly to order.

Accessing the World's Information since 1938

300 North Zeeb Road, Ann Arbor, MI 48106-1346 USA

Order Number 8820909

A quantitative investigation of crystalline and amorphous components of trans-polybutadiene

Wang, Peiguo, Ph.D.

City University of New York, 1988

U·M·I
300 N. Zeeb Rd.
Ann Arbor, MI 48106

PLEASE NOTE:

In all cases this material has been filmed in the best possible way from the available copy. Problems encountered with this document have been identified here with a check mark ✓.

1. Glossy photographs or pages ✓
2. Colored illustrations, paper or print _____
3. Photographs with dark background ✓
4. Illustrations are poor copy _____
5. Pages with black marks, not original copy _____
6. Print shows through as there is text on both sides of page _____
7. Indistinct, broken or small print on several pages ✓
8. Print exceeds margin requirements _____
9. Tightly bound copy with print lost in spine _____
10. Computer printout pages with indistinct print _____
11. Page(s) _____ lacking when material received, and not available from school or author.
12. Page(s) _____ seem to be missing in numbering only as text follows.
13. Two pages numbered _____. Text follows.
14. Curling and wrinkled pages _____
15. Dissertation contains pages with print at a slant, filmed as received ✓
16. Other _____

_____

_____

A QUANTITATIVE INVESTIGATION OF CRYSTALLINE AND AMORPHOUS COMPONENTS OF TRANS-POLYBUTADIENE

by

Peiguo Wang

A dissertation submmitted to the Graduate Faculty in Chemistry in partial fulfillment of the requirements for the degree of Doctor of Philosophy, The City University of New York.

1988

This manuscript has been read and accepted for the Graduate Faculty in Chemistry in satisfaction of the dissertation requirement for the degree of Doctor of Philosophy.

10/1/87
date

Arthur E. Woodward
Chairman of Examining Committee

11/17/87
date

A. M. Lesser
Executive Officer

R. W. Brotzman

Willaim Sweeney

Supervisory Committee

The City University of New York

Abstract

QUANTITATIVE INVESTIGATION OF CRYSTALLINE AND AMORPHOUS COMPONENTS OF TRANS-POLYBUTADIENE

by

Peiguo Wang

Adviser: Arthur E. Woodword

Polybutadiene lamellas containing 89% and 99% trans units were grown from solution and were investigated by the technique of surface epoxidation coupled with by C-13 NMR analysis. It was found that under proper suspension conditions all of and only monomer units in the surface (amorphous) part can be epoxidized. Since the resonances of the junction carbons between epoxidized and unepoxidized sequences can be separated from other resonances in the C-13 NMR spectrum, both the average crystalline stem length (A) and the average fold length (B) could be evaluated.

For the lamellas prepared from 99%-trans-polybutadiene, both A (17-24 monomer units) and B (5-9 monomer units) values increase with crystallization temperature, but they are not affected by the solution concentration It was found that cis units and chain ends are rejected from the crystalline core, leading to some larger folds with additional trans units. Correcting for this rejection effect yields a minimum fold length of three to four monomer units.

A general statistical treatment has been established for the calculation of the crystallinity and a characteristic tetrad ratio as functions of the crystalline stem length (A), the minimum fold length (B'), equivalent cis-units (q_1) and the degree of polymerization (X_n). Both calculated crystallinity and tetrad ratio fit the experimental data with a minimum fold length of three or four monomer units.

For lamellas prepared from 89%-trans-polybutadiene A-values do not change with crystallization temperature, solvent and solution concentration. The experimental point (A of 11 and crystallinity of 0.41) falls on a theoretical curve with a minimum fold length of three. Since three monomer units is the minimum length for folding in trans-polybutadiene lamellas, the results obtained from both 89% and 99% trans-polybutadiene samples strongly favor tight adjacent reentry.

In amyl acetate a critical at 10 °C gelation concentration for 89%-trans-polybutadiene is found to be 0.7% (w/v). A fold entanglement mechanism for gelation was proposed.

ACKNOWLEDGEMENTS

I wish to express, first of all, my sincere thanks to my mentor, Professor Arthur E. Woodward, in appreciation for his excellent guidance and his precious time given to me.

I would like to thank my supervising committee members, Dr. R. Brotzman and Dr. W. Sweeney for their valuable time and encouragement.

I would like use this chance to thank Dr. Renyuan Qian, It is under his guidance, I started my academic life.

I should also mention my wife, Ailin Wan, She shares my hardship and happiness in the whole program.

Finally, I would like to thank many friends for their friendly encouragement (Yuanze Xu and Hao Jian), and kind helps (Stella Huang running some NMR; Shoadao Wang operating x-ray scattering and Zhengyou Ding doing GPC experiment).

CONTENTS

TABLE LIST

FIGURE LIST

Chapter I

INTRODUCTION

Polymer crystallization has been an interesting research subject. The fact that polymers can be crystallized has been known since 1920's. However, until single crystals of polyethylene were grown, the concept of polymer crystallization was incorrect. Keller [1] , Fisher [2] and Till [3] obtained single crystals of polyethylene from solution in 1957. Under the electron microscope these crystals are platelets with rhombic shape and smooth edges, and with thickness of about 10 nm. The orientation of the molecular chains within the platelets has been determined by selected area electron diffraction [4,5] . A detailed analysis indicated that the chain axis is preferentially perpendicular to the wide surfaces of the crystals. Since the contour length of polyethylene molecular chain is much greater than the thickness of the platelets (For example, a polyethylene molecule with molecular weight of 24000 has contour length of 170 nm), the only possible chain arrangement is folding back and forth. Further investigation [6-9] showed that almost all flexible linear polymer chains which have enough chemical regularity can be crystallized as platelet-like single crystals (lamellas) in solutions. Later, the lamellar nature of melt crystallized polymers was revealed by small angle x-ray scattering, selected chemical etching and other techniques [10-13] . Thus, chain folding in polymer crystallization is well established. Wunderlich had summarized the research on the chain folded crystalline structure of synthetic polymers

earlier than 1972 [14].

However, various aspects concerning chain folding in polymer crystals have been the subject of much debate in recent years. The debate was summarized in terms of questions by Khoury [15] : (a) Does adjacent reentry or random reentry take place ? (b) To what extent does nonadjacent reentry manifest itself, if it doesn't manifest itself at all. (c) Are the folds in chains tight or loose ? (d) Are the chain ends incorporated into the interior of lamellas or are they excluded and exist as dangling cilia at fold surfaces ?

Three models are shown in Fig 1.1, they represent random reentry, tight adjacent reentry and loosen adjacent reentry folding respectively. The questions raised above can be converted to which model is correct ?

In fact all three models have experimental support. The first evidence for adjacent reentry came from morphological observations. Many single layers of solution grown polymer crystals at low supercooling have symmetric habits which are bounded by smooth or essentially smooth low-index crystalline planes. This symmetry reflects the unit cell symmetry. For example, polyethylene has an orthorhombic unit cell, its single crystals exhibit a lozenge or truncated lozenge shape with {110} or {100} crystalline plane as side planes [16] . In the case of polyoxymethylene which has an hexagonal unit cell, the simplest lamellar crystals are hexagonally shaped and are bounded by $\{10\bar{1}0\}$ faces [17]. Another related phenomenon is sectorization, i.e. the lamellas are inherently subdivided into a number

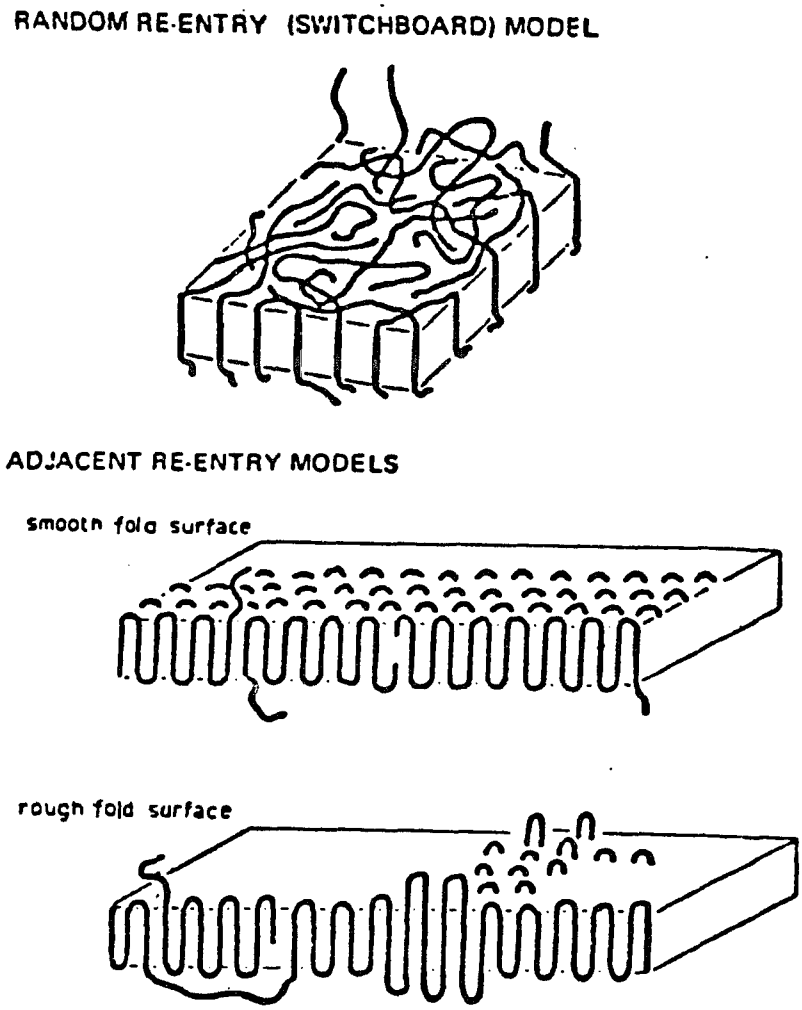

Fig 1.1 The different folding models. At the top is a model of the random reentry; in the middle is the model of tight adjacent reentry; and at the bottom is the model of loose adjacent reentry.

of distinct sectors. It was found that the cleavage easily takes place along the plane which is parallel to side crystalline planes [18] . All of these facts can be easily interpreted by adjacent reentry based on the assumption that the growth faces are fold faces as depicted in Fig 1.2.

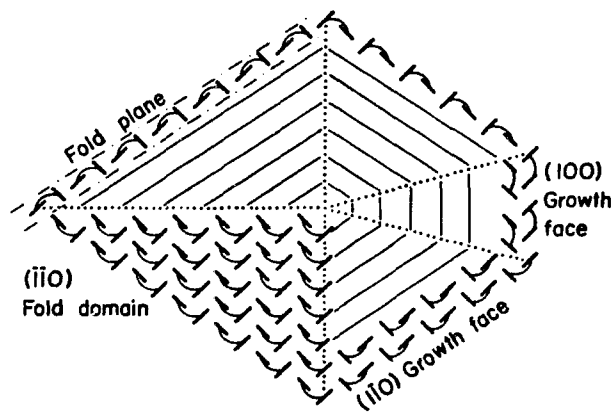

Fig 1.2 Adjacent reentry folding and sectorization in a lamella

Based on adjacent reentry Laurizen and Hoffman [19,20] , and Price [21] developed a kinetic theory of chain folded crystals. This theory gives a formula for the lamellar thickness of chain folded lamellas:

$$L = \frac{2\sigma_e T_m}{\Delta h_f \rho_c \Delta T} + \delta l \qquad (1.1)$$

where L is the average lamellar thickness; σ_e is the specific fold surface free energy; T_m is the melting or dissolution temperature; Δh_f is the heat of fusion; ρ_c is the density of the crystalline part; ΔT is the supercooling and δl is equal to $kT/b_0\sigma$ at melting temperature and increases initially slowly with supercooling (b_0 is the single molecular layer thickness; σ is the specific side surface free energy).

Equation (1.1) not only gives a correct L value, it has a proper mathematical form to describe the dependence of lamellar thickness on supercooling. Many modifications have been made in the kinetic theory, but the basic form of equation (1.1) is unchanged. Since the kinetic theory obtained success, the adjacent reentry model is widely accepted.

As indicated by Mandelkern [22], however, the success of equation (1.1) does not depend on adjacent reentry. There is some evidence favoring for random reentry. The density measurement is one of them.

Fisher [23] and Flory [24] measured the density of single crystal mats of polyethylene and found it corresponding to 15-20% of disordered or noncrystalline chains. Since only 5% of noncrystalline material is necessary for a regular folded structure, it was concluded that a random folded chain arrangement is preferred.

Lauritzen and Hoffman [25] attributed the higher amorphous fraction of single crystal mats of polyethylene to the existence of adsorbed layers on the surfaces of the mats. A loose adjacent reentry model (Fig 1.1 (b)) was also put forward as an explanation. Both suggestions was made to

retain the concept of adjacent reentry.

Strong evidence for random reentry came from neutron scattering experiments. Small angle neutron scattering can be used to obtain the average gyration radius of molecular chains. It is obvious that if adjacent reentry is true, the average gyration radius of molecular chains (R_g) in the crystalline arrangement should be proportional to its molecular weight. i.e the following formula should hold.

$$R_g = A_1 M \tag{1.2}$$

However, it seems that most experiments are not in agreement with equation (1.2). Using a small amount of deuterated polymer mixed with protonated polymer as a probe the small angle neutron scattering results of melt crystallized polyethylene [26] and polypropylene [27] showed that the root mean square gyration radius of the polymer molecular chains obey

$$R_g = A M^{\frac{1}{2}} \tag{1.3}$$

Not only is the form of the formula the same as that obtained from Gaussian statistics, but the constant A is close to its value in the melt, therefore, the molecular conformation of polymer chains in the crystal is

similar to that in the melt which is known to be a random coil. Meanwhile the neutron scattering function at large angles is not compatible with the regular folding mechanism. based on this experiment, random reentry is believed to be predominant in crystalline structures.

Flory [28] estimated the relaxation rate of polyethylene molecular chains with molecular weight of 10^5 at 120°C in the melt as about 1 second. At the same time the deposit rate of the polyethylene chain along a growing lamella is evaluated as about 50 - 500 μ per second or $10^5 - 10^6$ monomer unit per second. It is assumed that a molecule cannot disentangle completely, quickly enough to rearrange itself in a regular folded form.

Although most evidence of random folding came from melt crystallized polymers, Flory insisted that polymer crystals grown from solution should also have this folding behavior [28] . It is worth mentioning that some experimental results of gyration radii of molecular chains of polymer crystals grown from solutions obey equation (1.2). For example, Guenet [29] obtained a result of R_g with dependence of $M^{0.91}$ for isotactic polystyrene.

Results of another two experiments favor adjacent reentry. These experiments are selective oxidation followed by gel permeation chromatography (GPC) analysis by Williams [30,31] [30,31] and IR absorption of mixtures of polyethylene and deuterated polyethylene by Bank and Krimm [32] .

Using fuming nitric acid as an oxidant to cut folds of polyethylene monolayers grown from dilute solution, Williams [30] found that in the GPC spectra the material has three, latter two, and finally single well-defined low molecular weight species, corresponding to triple, double and single traverses of the crystals, and these species dominate the whole distribution curve. The higher molecular weight portion disappears rapidly with degradation time. Information about the folds comes from the comparison of molecular weight of double and single traverses. The ratio of the two molecular weights is always close to 2, with the double traverses about 5% larger. This result can only be indicative of adjacent folds with only small amount of material actually contained in each fold. However, the same technique revealed that the corresponding melt crystallized polymer has much more less regular folds [31]. But the final ratio of two low molecular weight species is again close to 2, indicating at least some relative tight adjacent chain folds.

Another experiment related to the folding mechanism is the observation of splittings in the infrared spectrum of polyethylene crystal mats [32]. The interaction between two different chains in one unit cell of pure polyethylene splits the infrared-active interchain CH_2-bending mode into two components at 1463 and 1473 cm^{-1}. The equivalent CD_2 mode at higher mass has the components of 1084 and 1094. Since in a unit cell with both deuterated and nondeuterated polyethylene chains adjacent reentry and random reentry result in different kinds of symmetry, the

splitting behavior found for the crystals is different. A comparison of the splitting of crystal mats of polyethylene mixed with deuterated polyethylene with the splitting of crystals of $C_{36}H_{74}$ and $C_{36}D_{74}$ mixture showed that solution crystallized polyethylene has adjacent reentry along the {110} plane. Meanwhile melt crystallized polyethylene has a splitting like that of the crystals with random reentry. Earlier Bank and Krimm attributed the splitting to regular folding but along the {200} plane [33], Latter, they attributed the behavior to random reentry of the crystals [34].

It is worth noting that in both the IR and neutron scattering experiments the segregation of deuterated and nondeuterated polymer chains takes place. making analysis difficult.

In summary, for both adjacent reentry and random reentry folding some evidence has been given. However, it seems that for solution crystallized polymers adjacent reentry predominates, while for melt crystallized polymers random reentry is more favorable.

There are some theoretical estimations of the percentage of adjacent reentry. Flory and Yoon [35] developed a lattice model which predicts that about 70% of chains reenter the same lamellas from which they emerge. However, even in favorable circumstances only about 20% of these chains are engaged in adjacent folds with immediate reentry. In contrast, the Gambler's Ruin Model developed by Guttman, DiMarzio and Hoffman [36] estimated the fraction of crystalline stems involved in tight adjacent reentry in semicrystalline polymers to be at least 2/3.

After summarizing the conflicted results related to the folding mechanism, Mandelkern [22] indicated that "A measure of the distribution of disordered sequence length (loop length) and what tendency there is, if any, for preferential adjacent reentry would be helpful". Until recently there is no reported experiment which can directly determine fold length accurately. This thesis will use an experimental technique which allows an accurate determination of the average fold length as well as the crystalline stem length for trans polybutadiene. Using this technique a series of results have been obtained. The following chapters will present and discuss those results.

Most research on morphology and structure of polymer crystals has been focused on polyethylene due partially to its chemical simplicity. In fact trans polybutadiene (TPBD) also has advantages, these include chemical simplicity, ease of crystallization and possibility of quantitative chemical modification. Natta and Corradini [37] found that TPBD has two thermo-reversible crystalline forms, and obtained the crystalline parameters of these forms by x-ray crystallography. Latter, Iwayanagi et al [38] and Suehiro et al [39] revised the parameters of the high temperature form. Takayanagi and his colleagues [40] studied the transition between the two forms by electron microscopy, infrared absorption and dynamic mechanical properties. They concluded that the low temperature form of TPBD has loose folds while the high temperature form has tight folds, which means that adjacent reentry is predominant. Based on calculations

of the normal vibration modes Hsu, Moore and Krimm [41] assigned the infrared and Raman spectra of crystalline TPBD. Using infrared spectroscopy Oyama et al [42] investigated the TPBD lamellas and concluded that for the low temperature form a fold has an average of 2-3 trans conformation monomer units and 2-3 gauche-conformation monomer units. While for the high temperature form the fold has 0-1 trans monomer units and 2-3 gauche monomer units. Finter and Wegner [43] investigated morphology of TPBD crystals by small x-ray scattering and scanning differential calorimetry. Marchetti and Martuscelli [44] studied the TPBD lamellas by bromination, but the reaction did not appear to be completely selective with the crystalline part of TPBD reacting also. The thermal properties of crystalline TPBD were measured by Wunderlich and his colleagues [45] . Much research on TPBD have been done in this laboratory by Woodward and his colleagues [46-55] . Various physical methods like IR [46,47], Raman [48], ESR spin-probe [49], differential scanning calorimetry (DSC) [50] and broad-line nuclear magnetic resonance (NMR) [51] as well as chemical etching methods like epoxidation and bromination were employed in investigation of TBPD lamellas.

Broad line proton NMR measurement of wetted crystalline TPBD was carried out by Eng and Woodward [51] , they found that the mobile part (amorphous part) decreases significantly when the transition from the low temperature form to the high temperature form takes place.

A recent study of TPBD lamellas by solid state NMR was done by Schilling, Bovey, Tseng and Woodward [53]. They found that in the spectra for a TPBD sample which contains less than 1% cis units using scalar decoupling and magic angle spinning the resonances of the crystalline component and the amorphous component can be separated. Thus, the crystallinity can be evaluated as 73% which is in good agreement with estimates from density. They found also that the cis-units are concentrated into the amorphous part.

A earlier comparison of the crystallinity obtained from different methods is shown in Table 1.1 [46].

Table 1.1

The crystallinity of TPBD lamellas calculated from various methods

Crystn. Condition	DSC	NMR	IR	Epoxidation
Heptane (76°C)	(.8)	.6	.8	.86
Toluene (50°C)	.6	.5	.5	.81
Benzene (35°C)	.6		.5	.73

Although the results obtained from different methods have large deviations, an approximate crystallinity of TPBD lamellas is in range of

0.6-0.8. It appeared that the technique of surface epoxidation had higher accuracy.

First using the technique of surface modification Stellman and Woodward [53,54] studied the amorphous component of TPBD lamellas. The reaction used was epoxidation of double bonds at the surface with m-chloroperbenzoic acid (MCPBA) in suspension. In earlier studies the reaction extent was monitored by measuring the loss of MCPBA by iodometric titration. It was found that in suspension liquid of benzene at 6°C it took 4-5 days to reach equilibrium, and that about 14-27% double bonds were reacted leading to an average value of the fold length of 2.5-5 monomer units.

Further, Wichacheewa and Woodward [55] studied the kinetics of epoxidation of TPBD lamellas in suspension. The percentage of epoxidation was determined by obtaining the mole ratio of MCPBA to its product m-chlorobenzoic acid (MCBA) using IR spectroscopy. The IR absorption ratio at 1700 cm^{-1} and 1735 cm^{-1} which corresponds to the carbonyl stretching bands of MCPBA and MCBA, respectively, was calculated with a calibration curve obtained from known mixtures of the two compounds. It was found that the epoxidation is a second order reaction and that in toluene reaction needs 3-5 days for completion.

In work by Tseng and Woodward [55,56] epoxidation in suspension was followed by proton NMR analysis of the reacted polymer directly. Combining the proton NMR results with lamellar thickness from small

angle x-ray scattering or electron micrograph the fold length of TPBD lamellas was determined as 3-5 monomer units.

More recently C-13 NMR was used by Schilling, Bovey, Tseng and Woodward [57,58] to analyzed the surface-epoxidized TPBD chain sequences Since the resonance for the junction carbon atoms can be separated from other resonances, both the crystalline stem length (A) and the fold length (B) can be obtained simultaneously and directly. Epoxidation percentage, fe, therefore, can be obtained too by the formula fe = B/(A+B). However, prior to the present work only three samples of TPBD lamellas were analyzed by this method. Only one of them gave a result for the epoxidation amount that was in agreement with the density measurement.

A similar technique was developed for trans polyisoprene (TPI) [59-62]. A recent research using epoxidation followed by C-13 NMR by Xu and Woodward [61] showed that an average fold length of TPI lamellas is about 9 monomer units , and that the epoxidation fraction is in agreement with the density measurement. Other chemical modifications on polydiene also were tried. Wichacheewa and Woodward [52] studied the bromination of TPBD lamellas in suspension at 0°C in dark. It was found that about 23% double bonds can be brominated.

Research on TPI lamellas by the technique of hydrochlorination followed by C-13 NMR analysis was completed by Tischler and Woodward [62]. In that research they found that only about half of the non-

crystalline fraction calculated from the density measurement can be hydrochlorinated, and an average fold length is about 5 monomer units. However, recent evidence [63] showed that the hydrochlorination done by Tischler was not complete, and a complete hydrochlorination may give a similar fold length as epoxidation did.

In Chapter II the synthesis, fractionation, crystallization and surface epoxidation of a 1% cis- content TPBD sample will be described. Through the analysis of the C-13 NMR spectra for surface-epoxidized TPBD lamellas the unepoxidized block length, A, as well as the epoxidized block length, B, can be evaluated. In addition the percentage of epoxidation can also be obtained. It was found that after a certain amount of time surface epoxidation reaches equilibrium, that in various suspension systems the same equilibrium values of A, B and fe are obtained, and that fe values are matched with the amorphous fraction calculated from density measurement. It means that all and only amorphous part can be epoxidized. Based on this fact, the block lengths, A, and B are the crystalline stem length and the fold length respectively. In the experimental region both the fold length and crystalline stem length increases with crystallization temperature, but both of them are independent of solution concentration. Evidence was obtained that showed that all cis-units and chain ends are rejected from the crystalline core, it is expected that the rejection of cis-units will bring trans-units to the amorphous part, therefore, leading to a larger average fold length. After a cis-units correction the length of the

folds that contain trans-units only is about 3 monomer units. This result favors the adjacent reentry mechanism.

In Chapter III, based on the assumptions of random placement of cis-units, complete rejection of cis-units and chain ends from the crystalline core, and tight adjacent reentry with a fixed minimum fold length, a statistical treatment for crystallinity and a tetrad ratio of the monomer sequences will be set up. The comparison of this statistical treatment with the experimental results suggests that the minimum fold length of TPBD lamellas is 3-4 monomer units which is in agreement with the conclusion reached in Chapter II.

In order to test the conclusion that the length of the folds which contain trans units only is 3-4 monomer units, a commercial polybutadiene sample which contains 10% cis-, 1.5% 1,2-, and 89% trans- units was subjected to the tests of surface epoxidation, DSC and x-ray scattering. In Chapter IV the results of those tests will be reported. For this high cis content sample, in dilute solution single layers can be obtained. The results of surface epoxidation showed that both the crystalline stem length and the fold length are independent upon crystallization solvent, temperature and concentration. Using the statistical treatment the minimum fold length for this sample was determined to be 3 monomer units again. It was found that about 1/20 of the total cis-units enter the crystalline core, and that this small fraction of cis-units in the crystalline core have a significant effect on the thermal properties of the lamellas. It was found

also that a three dimensional gel structure is easily formed for the high cis polybutadiene, and the critical gelation concentration is between 0.3%-0.7%. Based on the large fold length a gelation mechanism of fold entanglement fold will be discussed.

Chapter II

A QUANTITATIVE INVESTIGATION OF 99%-TRANS-POLYBUTADIENE LAMELLAS

2.1 INTRODUCTION

Surface epoxidation has been used in this Laboratory for more than 15 years to investigate solution grown polydiene lamellas and their aggregates [53-61]. This is a non-destructive chemical modification technique based on the assumption that only and all the surface part (amorphous part) of the lamellas, consisting of folds and cilia, can be epoxidized when lamellas are suspended in a proper liquid containing the epoxidation agent for a particular amount of time. After surface epoxidation the polymer chains become block copolymers with alternating epoxidized and unepoxidized blocks, these two kinds of blocks represented the original folds (cilia) and the crystalline stems, respectively. In the proton nuclear magnetic resonance (H-NMR) spectrum, the protons of these two blocks have different chemical shifts. Therefore, the percentage of reacted part (amorphous part) can be evaluated. Recently, the C-13 NMR technique has been developed to characterize the products of surface-epoxidized polydienes [57,58]. Since the resonance of junction carbons between epoxidized and unepoxidized units can be separated in the C-13 NMR spectra, the average lengths of the

two kinds of blocks can be evaluated simultaneously. Thus, this method becomes an unique one in investigation of lamellar structure of polymers. However, for trans-polybutadiene (TPBD) only three samples have been analyzed by this method to date. Only one of them gave results which can match that obtained from density measurement. Therefore, it was believed interesting to investigate TPBD lamellas by this method systematically. In this chapter a set of results from a systematic investigation on the effects of crystallization temperature, crystallization concentration and molecular weight for a trans-polybutadiene sample by the technique of surface epoxidation followed by C-13 NMR analysis will be reported.

2.2 EXPERIMENTAL

2.2.1 Sample Synthesis

The TPBD samples for this research were synthesized in this Laboratory. The polymerization was carried out in the presence of rhodium ions in water emulsion [64]. The reaction is believed to be ionic [65], and, like the Zieglar-Natta reaction, the products are highly sterospecific [64]. Totally, 18 batches of TPBD were polymerized in an attempt to obtain

Table 2.1 Synthesis Conditions

Code	[$RhCl_3$]/[1,3 BD]	[DSS]/[1,3 BD]	Temp.°C	Time (Days)
SB-6	.005	.05	50	4
SB-7	.005	.025	50	4
SB-8	.005	.025	60	4
SB-9	.005	.025	50	4
SB-11	.00125	.025	22	21
SB-13	.00125	.0125	25	70
SB-14	.0025	.0125	50	4
SB-15	.0025	.0125	50	4
SB-16	.0025	.0125	50	4
SB-17	.0025	.0125	50	7
SB-18	.0025	.0125	50	7
SB-19	.0025	.0125	50	7
SB-20	.0025	.0125	50	7
SB-21	.001	.0125	50	20
SB-22	.0025	.0125	50	10
SB-23	.0025	.0125	50	9
SB-24	.001	.0125	40	18
SB-25	.00125	.025	50	25

1,3 BD, 1,3 butadiene; DSS, dodecyl sodium sulfate;

samples with different molecular weights. The details of the polymerization conditions are listed in Table 2.1. The yield of the polymerization is around 60%. The intrinsic viscosity of the products in toluene at 30 ℃ are 43-52 cm^3/g corresponding to molecular weight of $1.6–2.0\times10^4$ [66]. Their polydispersity index is about 2.5-3.0.

C-13 NMR spectroscopy showed that except for the batch SB-6 all the polymers synthesized have about 99% trans- and 1% cis- content, and that there is no 1,2 component.

2.2.2 Fractionation

The Successive Solutional Fractionation method [67,68] was used. Every time 40 gm TPBD was dissolved in 2000 ml of a mixture of toluene and heptane at 60-70℃ in the presence of antioxidant (A.O. 2246); the solution was cooled to room temperature with stirring for one day to bring about crystallization. Then the temperature of the system was raised to 40℃, and kept there for one day, during which time the lower molecular weight fraction redissolved. This fraction, then, was separated by filtering at 40℃ and drying. The remaining polymer solid was extracted by a better solvent by increasing the content of toluene. The fraction number and the solvent content are as follows:

Fraction No.	1	2	3	4
Tol./Hep. (v/v)	5/95	10/90	15/85	20/80
Fraction No.	5	6	7	8
Tol./Hep. (v/v)	25/75	30/70	35/65	40/60

Six different fractionations were carried out. Each fraction was kept separate, and its molecular weight was measured by intrinsic viscosity in toluene at 30° C with constants α=.753 and K=.0293 [66]. The polydispersity index of the fractions of one run was determined by gel permeation chromatography (GPC) in toluene at 60°C using polystyrene standards for reference. For all the fractions the polydispersity index (M_w / M_n) is about 1.5-1.8 and viscosity average molecular weight is 2000-36000.

2.2.3 Crystallization

Two crystallization procedures were employed: direct and precooling crystallization. By direct crystallization TPBD was dissolved in solvent at T_d (80-90 ° C in amyl acetate or 60-70° C in cyclohexane) for about 20 minutes, then the solution was placed in a water bath at a crystallization temperature T_c. By the precooling procedure TPBD was dissolved at T_d (as indicated above). The solution then was cooled to zero °C for a few minutes until some crystals appeared clearly. It was rewarmed to T_r until the crystals just redissolve completely. Finally, it was quickly placed in a water bath at a crystallization temperature T_c (T_c value, see 2.3.7)for one day. When amyl acetate was used as solvent T_r = 49-58° C, and when

cyclohexane was used T_r = 24-34°C. After filtering and washing with fresh solvent a part of the crystal preparation was dried at 0°C for one week for density measurement.

2.2.4 Surface Epoxidation

After filtering the crystals were transferred to precooled suspension liquid containing epoxidation agent, m-chloroperbenzoic acid, for 7-15 days. The partially epoxidized TPBD was recovered, washed with fresh solvent many times, and dried at 0°C. The epoxidation was found by C-13 NMR to be a highly selective and quantitative reaction:

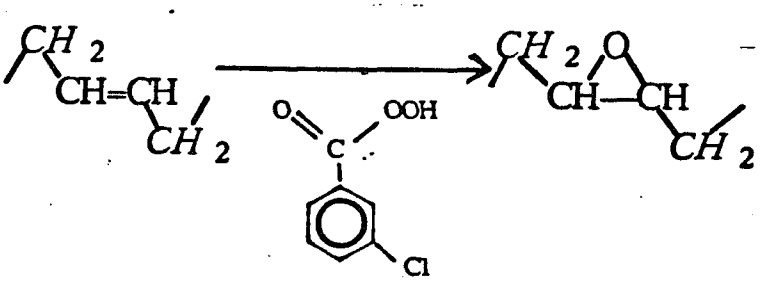

2.2.5 C-13 NMR Measurement

A 200 MHz IBM/Bruker NMR spectrometer was used to obtain C-13 spectra. The samples were dissolved in $DCCl_3$ in 5-10% concentration (w/v). The operation conditions are : high power proton decoupling mode; 90° pulse; window width of 8000 kHz; memory of 32 K; delay time of 10 seconds (5 times the longest T_1); inner reference of TMS, accumulation of 2000-5000.

2.2.6 Density Measurement

Determination of the density of TPBD mats was carried out with a water-ethanol density gradient column at room temperature. The weight fraction of the crystalline part (crystallinity) was calculated based on the two phase model using an amorphous density of .874 and a crystalline density of 1.03 g / cm^3 [69].

2.2.7 Transmission Electron Microscopy

A Philips EM-300 transmission electron microscope was used for observation of TPBD single crystals. The procedure is as follows. One drop of TPBD crystal suspension was put on a carbon coated copper grid. After evaporation of solvent the grid was shadowed by Au/Pd (80/20) at an angle $\alpha=\tan^{-1}(1/3)$. For hedrites and complex TPBD structures, a Cambridge Stereoscan S4 scanning microscope was used. The crystals were fixed with OsO_4 in suspension for one hour. After washing one drop of the fixed suspension was placed on an aluminum plate. Upon solvent evaporation this was decorated with Au/Pd (80/20).

2.3 RESULTS

2.3.1 Morphology

As long as T_r is well controlled, The TPBD crystals (with molecular weight 7000-36000) grown from .05% solution by the precooling procedure are always single layers as shown in Fig 2.1. They are 1.5μ times 2.5 μ hexagons. When crystallized in amyl acetate and T_c is above 50 ℃ the lamellas become larger and regular (Fig 2.1(c)). Sometimes there are overgrowths (see Fig 2.1 (d)). After epoxidation the shape and the edges of the single layers are not changed (Fig 2.1 (d)).

TPBD crystals grown from ≥1% solution by direct cooling are multilamellar ones. Their morphology depends on T_c, molecular weight, and solution concentration (Fig 2.2 (a)-(d)).

Fig 2.3 is the picture of a group of hedrites which were grown form .05% amyl acetate without precooling. Compared to Fig 2.1 (a), it is clear that seeding by the precooling procedure is important in obtaining single layers.

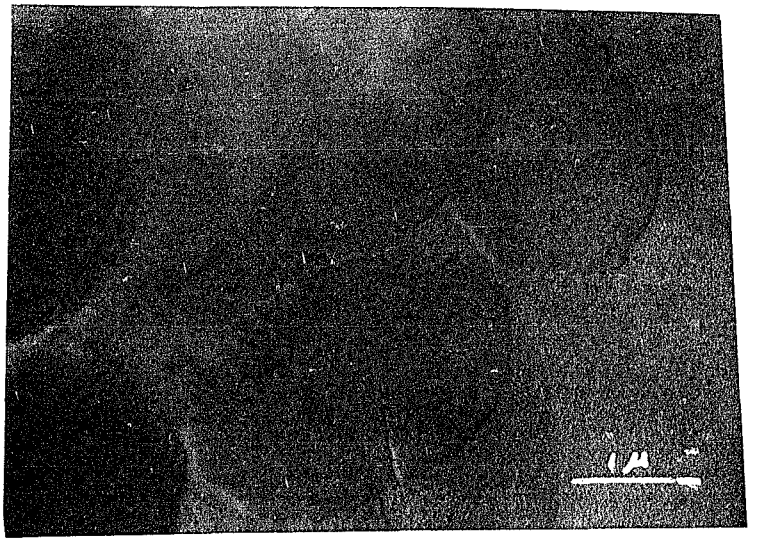

Fig 2.1 (a) Transmission electron micrograph of single lamellas of 99%-trans-polybutadiene grown from 0.05% amyl acetate at 30 ℃ by the seeding procedure.

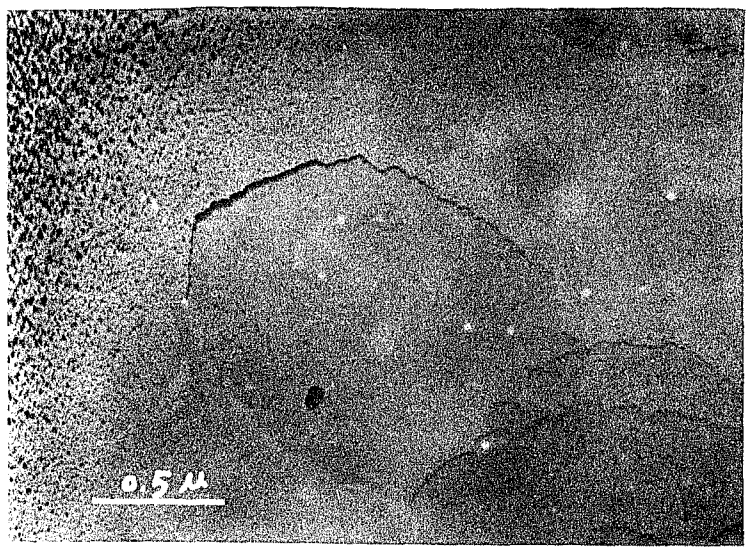

Fig 2.1 (b) Transmission electron micrograph of single lamellas of 99%-trans-polybutadiene grown from 0.05% cyclohexane at 30 °C by the seeding procedure.

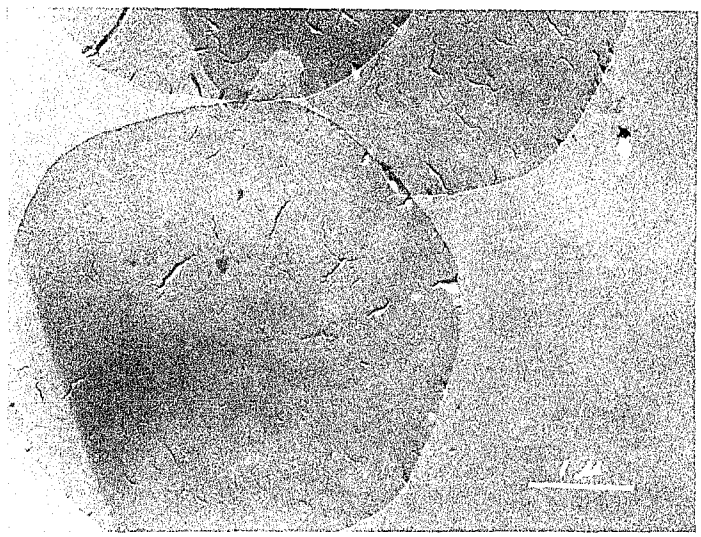

Fig 2.1 (c) Transmission electron micrograph of single lamellas of 99%-trans-polybutadiene grown from 0.05% amyl acetate at 50 °C by the seeding procedure.

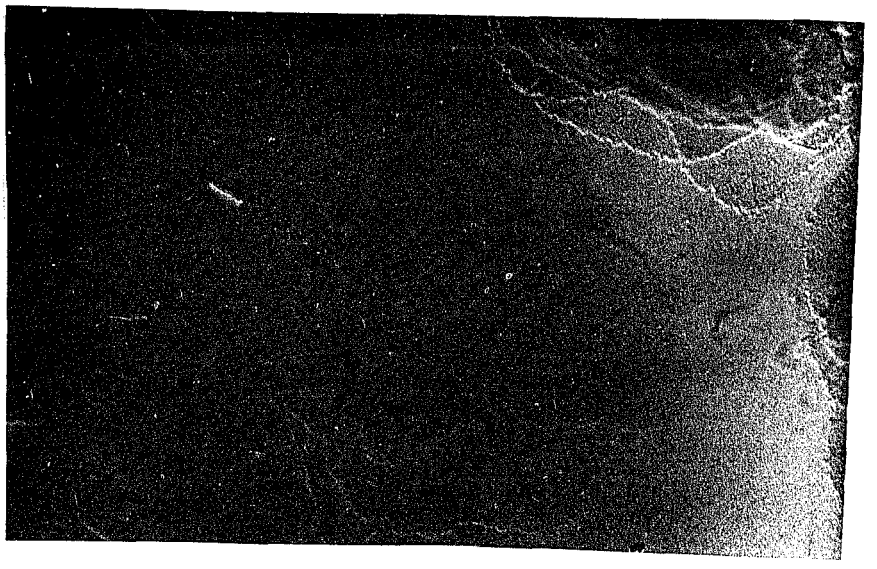

Fig 2.1 (d) Transmission electron micrograph of epoxidized single lamellas of 99%-trans-polybutadiene grown from 0.05% amyl acetate at 30 °C by the seeding procedure.

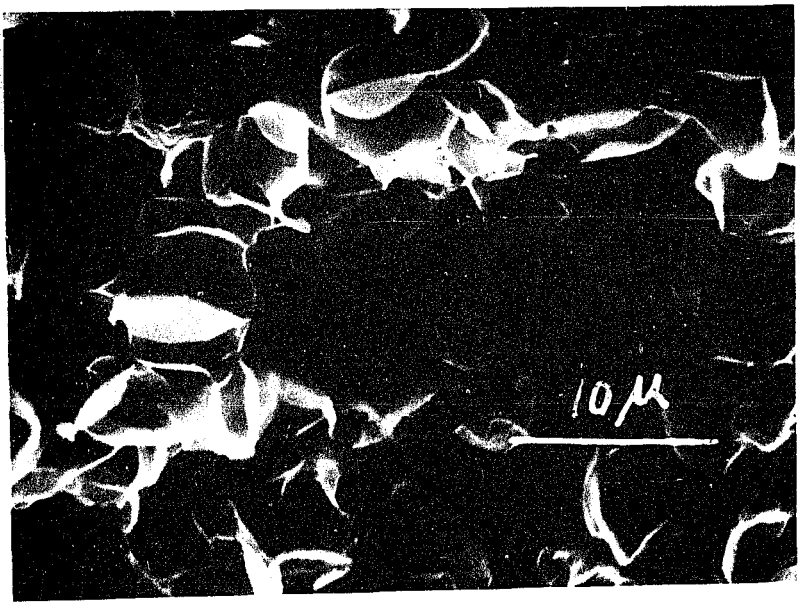

Fig 2.2 (a) Scanning electron micrograph of hedrites of 99%-trans-polybutadiene grown from .05% amyl acetate solution at 30°C by the direct cooling procedure.

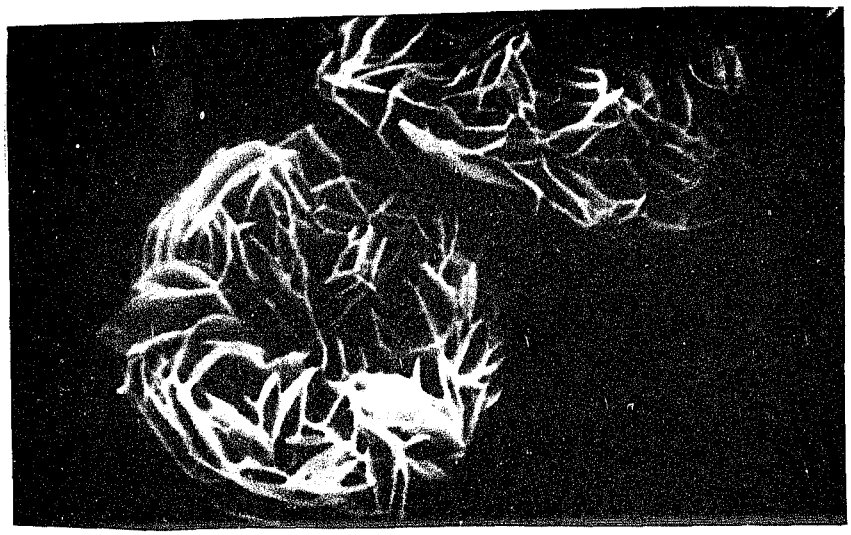

Fig 2.2 (b) Scanning electron micrograph of hedrites of 99%-trans-polybutadiene grown from 1% amyl acetate solution at 30°C by the direct cooling procedure.

Fig 2.2 (c) Scanning electron micrograph of hedrites of 99%-trans-polybutadiene grown from 2% amyl acetate solution at 30°C by the direct cooling procedure.

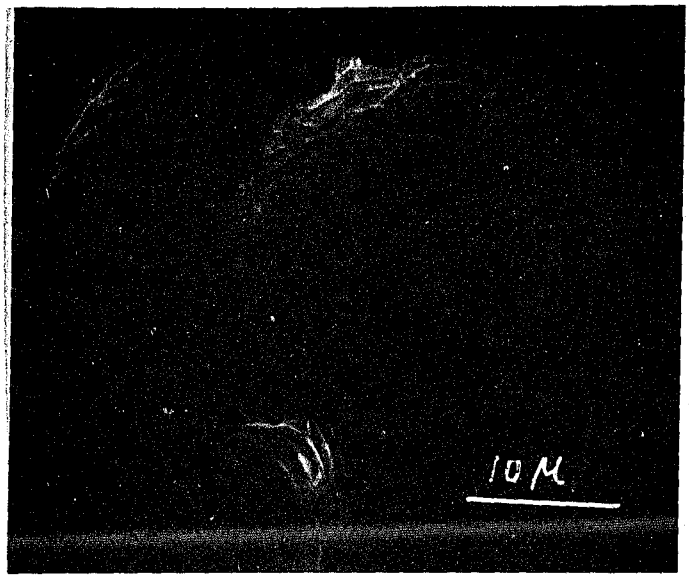

Fig 2.2 (d) Scanning electron micrograph of hedrites of 99%-trans-polybutadiene grown from 2% amyl acetate solution at 30°C by the direct cooling procedure.

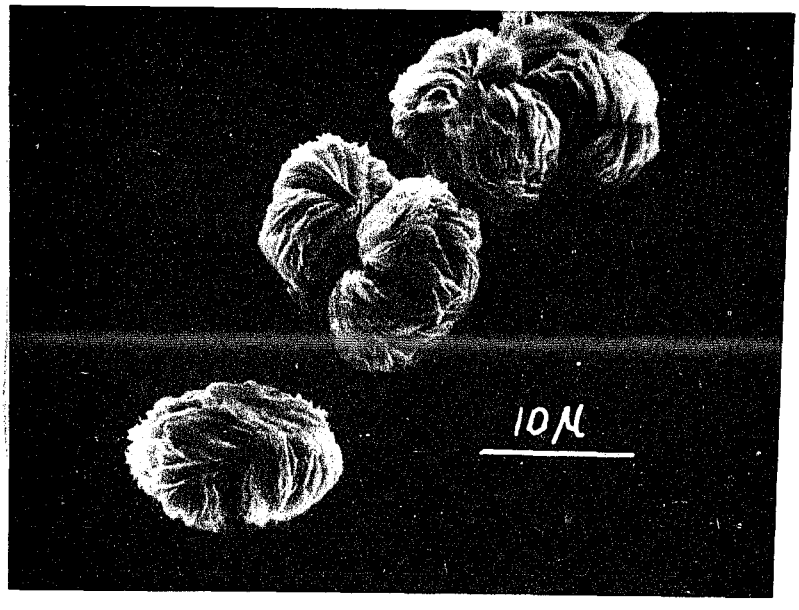

Fig 2.3 Scanning electron micrograph of hedrites of 99%-trans-polybutadiene grown from 0.05% amyl acetate solution at 40°C by the direct cooling procedure.

The total lamellar thickness (L) of single layers can be estimated from the shadowing length (l) measured from electron microscope pictures by the formula:

$$L = l\frac{tg(\alpha)}{X} = \frac{l}{3X} \tag{2.1}$$

where X is magnification, and α is shadowing angle.

For the single layer grown from amyl acetate at 30° C nine lamellar thickness measurements data are available. they are 9.2, 13.0, 16.0, 13.1, 9.7, 15.9, 16.0, 16.0, and 10.0 nm. The average is 13 $\pm$ 3 nm.

2.3.2 NMR Spectrum Assignment and A, B Values

Earlier work [57] gave the detailed assignments for the block copolymer of epoxidized and unepoxidized TPBD. The relative assignments are listed as Table 2.2.

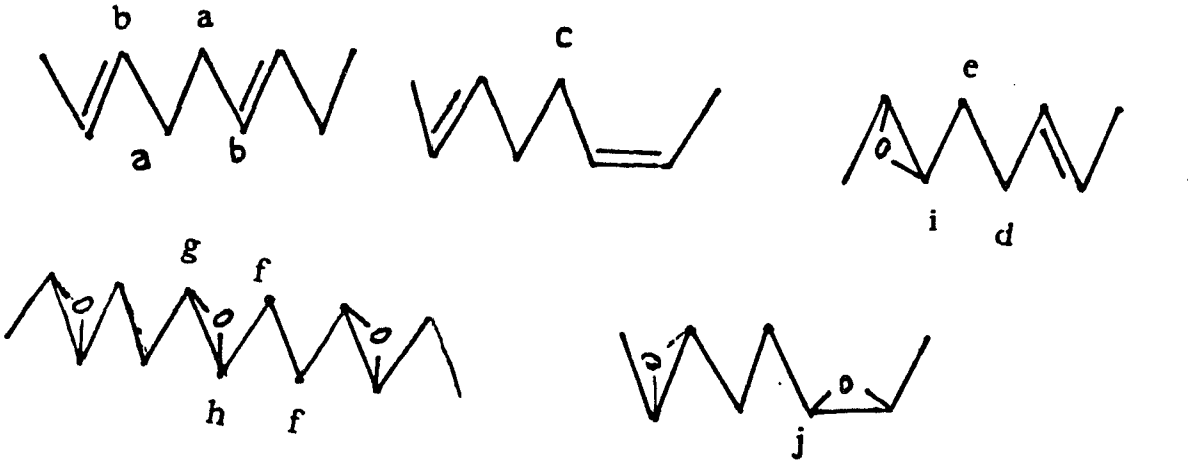

Table 2.2

Principal Assignments of C-13 NMR Spectra

No. of carbon	Chemical Shift (ppm)
a	32.7
b	130.0
c	27.4
d	32.1, 32.2 *
e	29.1
f	28.5, 28.8 *
g	129.3,129.4 *
h	130.6, 130.7 *
i	57.9, 58.2, *
j	56.4, 56.9 *

*, diasteroisomers

Supposing that all and only the monomer units in the amorphous part can be epoxidized (latter on this will be proved), the epoxidized blocks are the original fold segments, and the unepoxidized blocks are the crystalline stems. Since in the NMR spectrum the resonances of junction carbons (carbon d and carbon i, or carbon g and carbon h) can be separated from other resonances, both crystalline stem length (A) and fold length (B) could be obtained by

$$A = \frac{[a]+[d]}{[d]} \tag{2.2}$$

or,

$$A = \frac{[b]+[g]}{[g]} \tag{2.2a}$$

$$B = \frac{[f]+[d]}{[d]} \tag{2.3}$$

or,

$$B = \frac{[i]+[g]}{[g]} \tag{2.3a}$$

here [a],[b]...[g] are the integral intensity of the corresponding peaks. When formulas (2.2), (2.2a) and (2.3) are used, since only the same kind of

carbons are involved, the NOE effect doesn't have to be considered. In formula (2.3a) the different kinds of carbons appear. Therefore, a consideration of NOE effect is needed. However, it was found that the differences in NOE values due to different kinds of carbons are less than 2%.

Another dependent quantity, the epoxidation fraction fe, can be obtained from A and B values:

$$fe = \frac{B}{A+B} \tag{2.4}$$

An actual C-13 NMR spectrum of surface-epoxidized TPBD is shown in Fig 2.4 (a) and (b). Based on equation (2.2), (2.3) and (2.4) and the integral intensity of the relative peaks, A, B and fe values can be evaluated. Repeat of the tests showed that A and B have a relative error of about 5%, and fe a relative error smaller than 2%.

2.3.3 Completeness of Surface Epoxidation

To verify the basic assumption that only and all of the monomer units in the amorphous part can be epoxidized, different suspension systems were employed. Fig 2.5 is a plot of A, B and fe values versus epoxidation time for the lamellas grown from dilute cyclohexane solution in three different systems. Triangles represent the results when toluene is used as suspension liquid and the mole ratio (MR) of epoxidation agent, meta-chloroperbenzoic acid (MCPBA), to the double bonds of the polymer

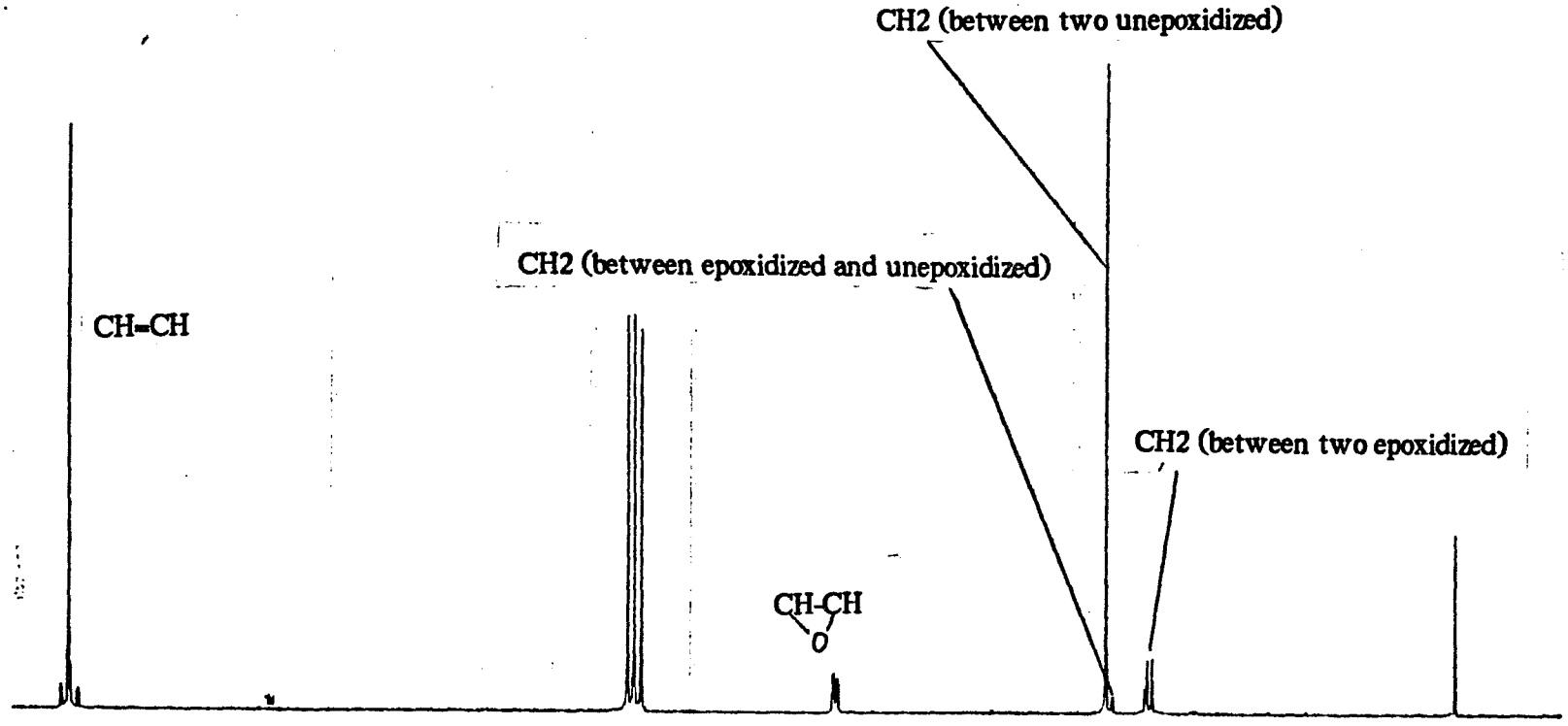

Fig 2.4 (a) Cabons-13 NMR spectrum of surface-epoxidized 99%-trans-polybutadiene.

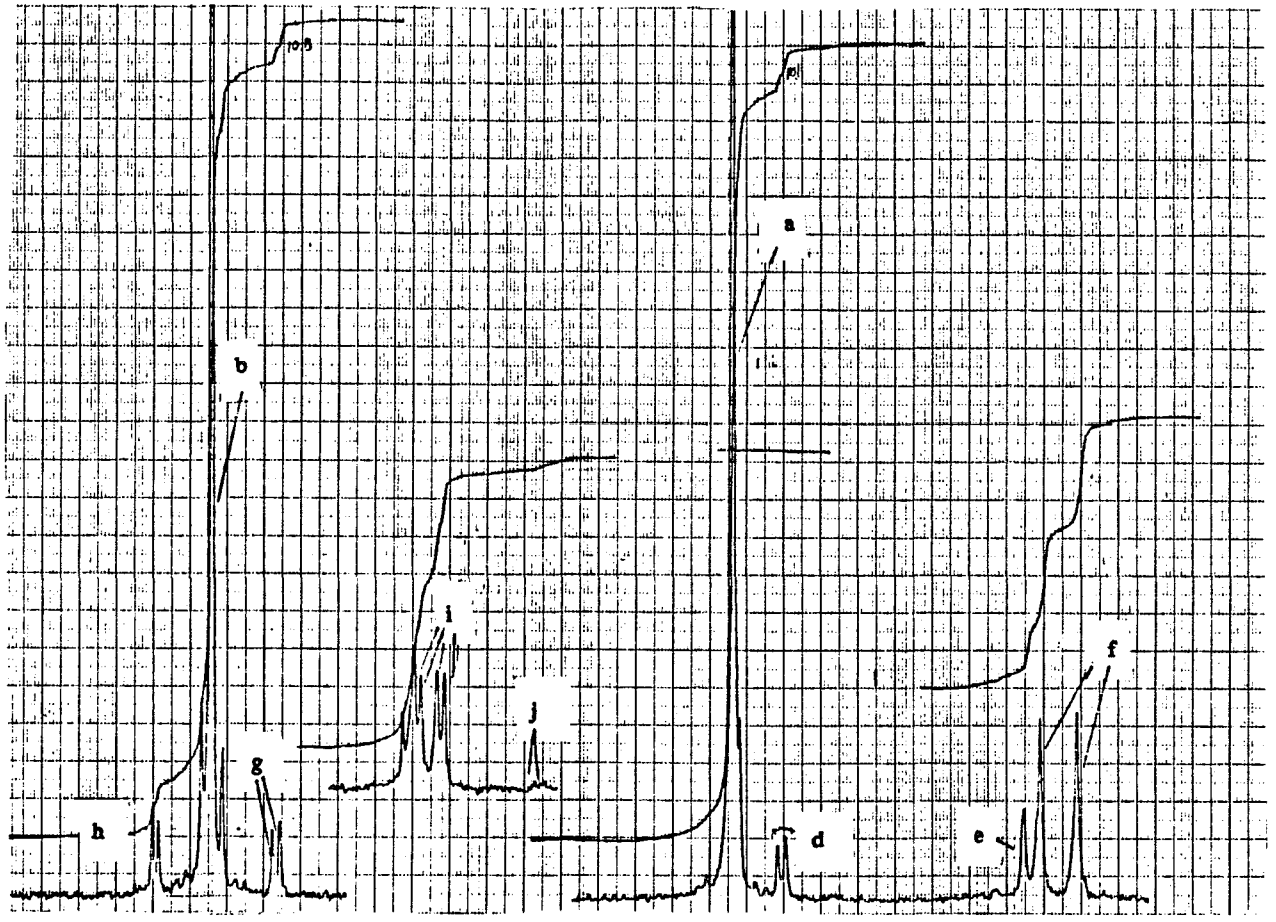

Fig 2.4 (b) Expanded cabons-13 NMR spectrum of surface-epoxidized 99%-trans-polybutadiene.

is 0.8. The squares and stars represent the results when amyl acetate is used as suspension liquid and MR is 1.2 and 1.9, respectively. Fig 2.5 shows that

(a) Leveling off is reached for each system;

(b) The leveling off values are the same (A = 18.0, B = 6.1, fe = .25);

(c) The equilibrium fe value is very close to (1-Wc) = .26, where Wc is the crystallinity from density measurement.

These results support the basic assumption that all and only the amorphous part is epoxidized under the reaction conditions chosen. In amyl acetate it takes 15 days to complete surface epoxidation, in toluene 7 days are enough.

A similar plot is shown in Fig 2.6 for crystals grown from dilute amyl acetate solution at 30°C in four suspension systems (amyl acetate, MR 0.9; amyl acetate, MR 1.2; toluene, MR 0.6; chloroform/ether 3:1 by volume, MR 1.3). Again, the same equilibrium values with A of 20.3, B of 7.3 and fe of 0.25 are obtained from different systems; again fe is close to the non- crystalline fraction (1-Wc), .26, from density measurements.

For the rest of this work the standard epoxidation conditions for lamellas grown from amyl acetate (or cyclohexane) are selected as suspension in amyl acetate with MR of 1.2 (or 1.9) for 15 days.

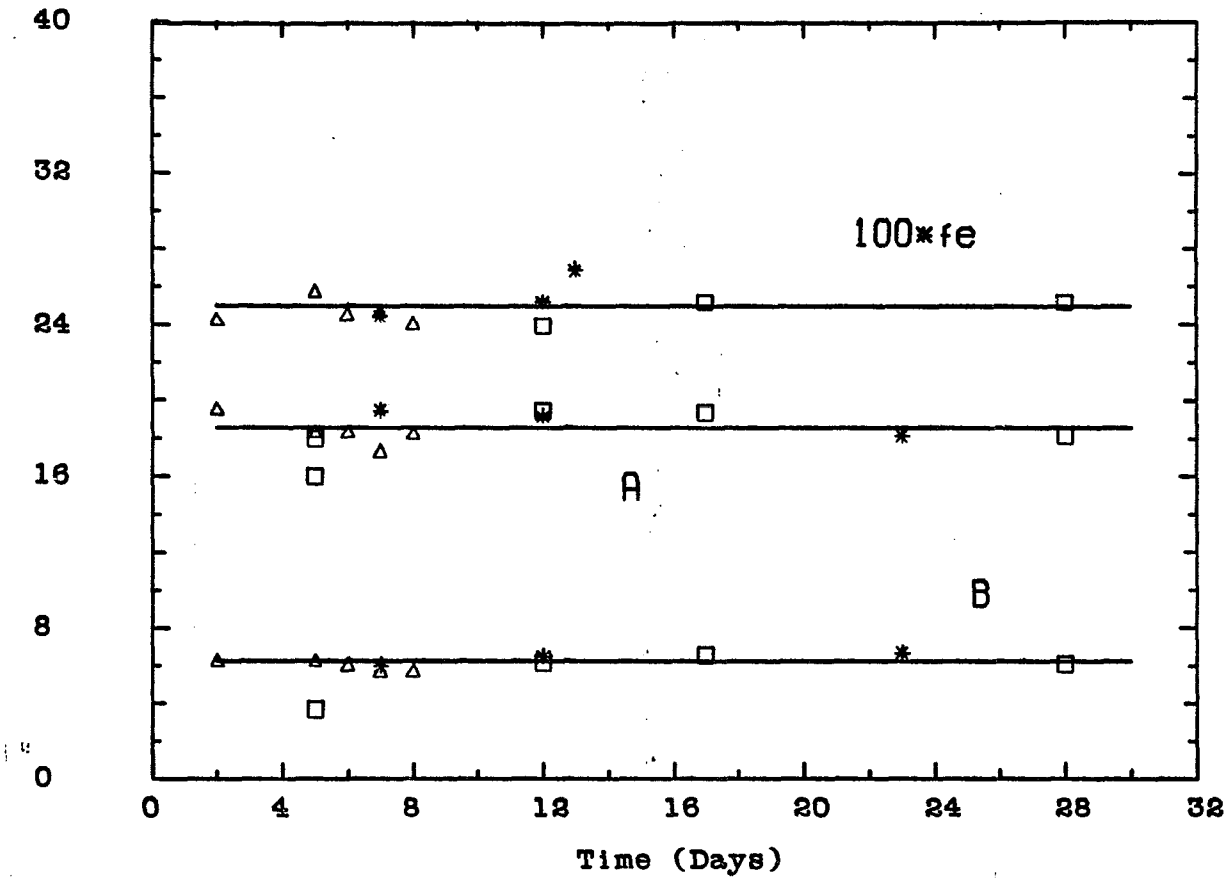

Fig 2.5 Effect of time and MR on surface epoxidation. Crystals grown from 0.5% cyclohexane solution at 10°C. Squares, epoxidized in amyl acetate with MR of 1.2; asterisk, epoxidized in amyl acetate with MR of 1.9; triangles ,epoxidized in toluene with MR of 0.8.

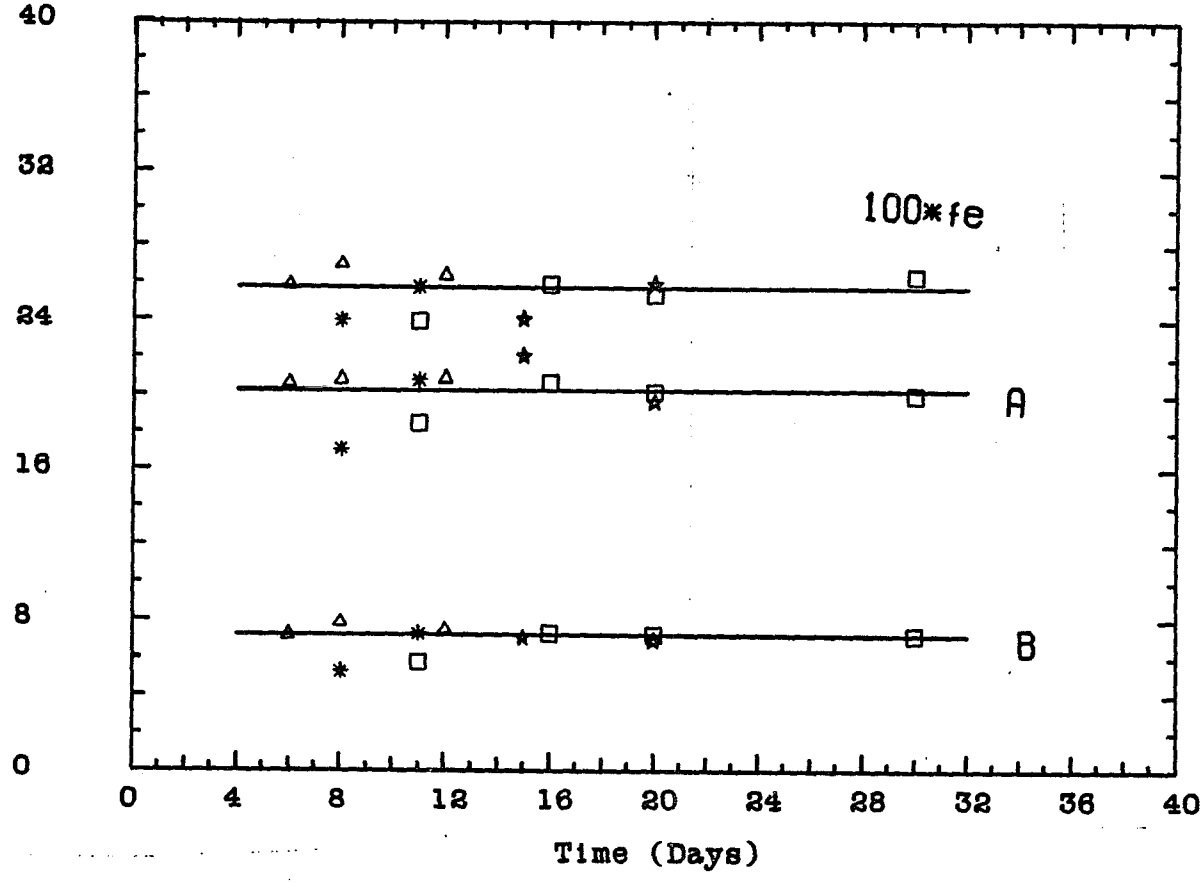

Fig 2.6 Effect of time and MR on surface epoxidation. Crystals grown from 0.5% amyl acetate solution at 10°C. Squares, epoxidized in amyl acetate with MR of 0.9; asterisk, epoxidized in amyl acetate with MR of 1.2; triangles ,epoxidized in toluene with MR of 0.8; stars, epoxidized in chloroform/ether (3:1) with MR of 1.3.

Table 2.3

A Values for Lamellas Grown from AA 30°C

No. of test	X_n	q	Crys. Conc. (g/100cc)	A
68	160	.01	.05	20.0
69	160	.01	.05	20.0
86	300	2.5	.05	19.8
114	120	3.0	.05	20.5
127	300	.01	.05	20.7
128	300	.01	.05	20.2
130	300	.01	.05	20.8
131	300	.01	.05	20.0
151	440	.01	.05	20.8
162	276	.008	1	20.6
164	276	.008	1	20.6
180	276	.011	.05	19.8
188	300	.01	.05	20.0
193	350	.008	.05	20.3
198	350	.008	1	20.8

Crys. Conc., crystallization concentration; q, cis-content;
X_n , degree of polymerization; AA, amyl acetate.

2.3.4 A Comparison of Total Lamellar Thickness

The A values for the lamellas grown from dilute amyl acetate solution at 30° C are listed in Table 2.3. The A value does not change with molecular weight, with concentration of crystallization solution or with cis-content. The average A value from 19 measurements are 20.3 monomer units.

Referring to Fig 2.7, the total lamellar thickness (L) of a single layer of TPBD can be evaluated from A and fe values by the formula (2.5):

$$L = AR\left(1 + \frac{f_e \rho_c}{(1 - f_e)\rho_a}\right)\cos\theta \qquad (2.5)$$

where R is the repeat distance of the TPBD unit cell along the crystalline stem direction (0.483 nm). ρ_c and ρ_a are the densities of the crystalline and amorphous part (1.03 and 0.874 g / cm^3, respectively). and θ is the tilt angle of the TPBD crystalline stem with respect to the lamellar surface (114 °, see [37]).

When fe = .25 (This value is unchanged almost for all samples, see Fig 2.5 and Fig 2.6) and A = 20 are put into eq. (2.4), L = 13 nm is obtained, the same as the result from electron microscopy (See 3.3.1). This agreement is further evidence for the assertion that the surface epoxidation is a reliable method.

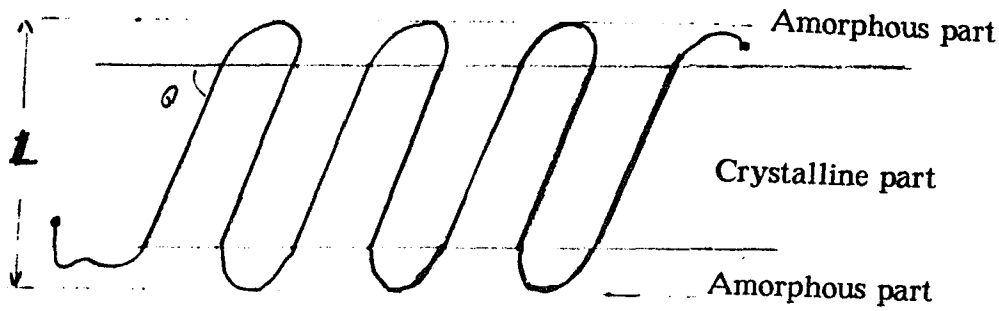

Fig 2.7 A schematic representation of a lamellar structure

2.3.5 Measurements of Chain Ends and Cis-Units

The C-13 NMR resonance for the CH_2 carbon in cis polybutadiene units is at 27.4 ppm. Prior to epoxidation this can be used as a indicator of the existence of cis-component. For all the samples except those from SB-6 the cis-content is about 1.0%. A small peak at 17.9 ppm is also found in the C-13 NMR spectra as shown in Fig 2.4. It is known that CH_3 carbons attached to a trans-double bond have a chemical shift around 17.7 ppm [70]. Thus, the resonance of 17.9 ppm can be attributed to CH_3 carbon atoms of TPBD chain ends. If the assignment is true, the ratio of peak intensities at 32.7 and 17.9 ppm should be equal to the number average degree of polymerization. The data in Table 2.4 confirm this conclusion for four fractions. In converting the viscosity average degree of polymerization to number average degree of polymerization, it is assumed that the viscosity average is close to weight average, and that the polydispersity index of all the fractions is 1.5.

Table 2.4

A Comparison of Molecular Weights

No. of test	$\overline{M}_\eta$	$\overline{X}_\eta$	[32.7]/[17.9]
49	12000	148	130
50	25000	310	360
190	27000	330	370
205	16000	197	116

After epoxidation both peaks of 27.4 and 17.9 ppm disappear completely, as shown in Fig 2.8 (b). This means that the cis-component and chain ends stay in the amorphous part, and thus, attached double bonds can be epoxidized. According to the assignment of Schilling et al [57], epoxidized cis double bonds have a resonance at 57.9-58.3 ppm (See Table 2.2 peak j). This peak can be used for the estimation of cis-content, q, by equation (2.6)

$$q = \frac{[j]}{[j]+[i]} \times f_e \qquad (2.6)$$

where j and i are epoxidized cis- and trans- olefinic carbons (see Table 2.2)

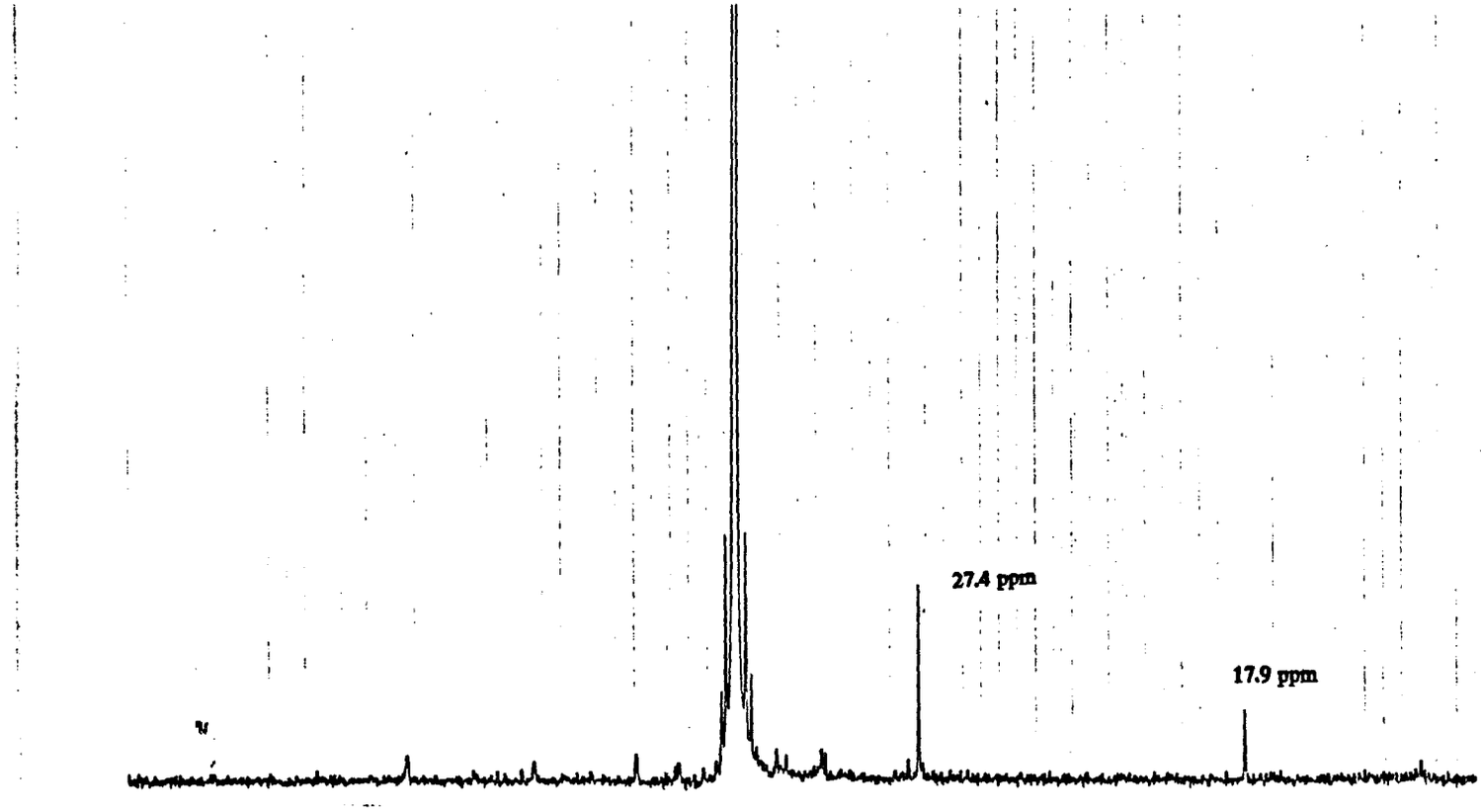

Fig 2.8 (a) A cabon-13 NMR spectrum (in the range of 0-30 ppm) for unepoxidized 99%-trans-polybutadiene. The resonances at 27.4 and 17.9 ppm exist clearly.

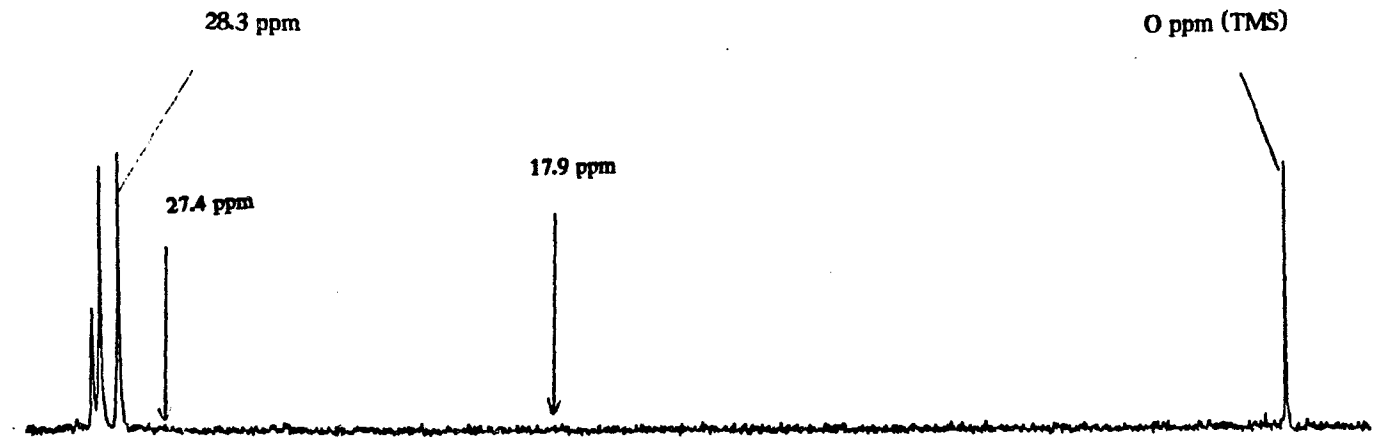

Fig 2.8 (b) A cabon-13 NMR spectrum (in the range of 0-30 ppm) for epoxidized 99%-trans-polybutadiene. The resonances at 27.4 and 17.9 ppm disappear.

2.3.6 The Effect of Molecular Weight

A, B and fe obtained using fractions with different molecular weights for lamellas grown from cyclohexane (T_c = 10°C) and amyl acetate (T_c = 30°C) are given in Table 2.5. It is observed that A remains constant within ± 0.5 for a four-fold change in molecular weight. B decreases with molecular weight for cyclohexane grown preparations. For amyl acetate grown lamellas there is no consistent change in B with X_n. The meaning of the terms of (x-A-B-2)/(A+B) and (BA+2A)/(A+B) appeared in Table 2.5 will be discussed later (See 3.4.1)

Table 2.5 Effect of Molecular Weight

Xsunn	Cry. Cond	A	B	(x-A-B-2)/(A+B)	(Bx+2A)/(A+B)
100	Cyclohexane	16.6	5.7	3.5	26
120	10°C	16.6	5.6	4.6	34.4
380		15.5	5.1	16.9	93.1
440		15.4	5.0	19.7	105.7
160	Amyl acetate	20.0	7.0		
280	30°C	20.4	7.3		
300		20.4	7.2		
320		20.3	7.3		
440		20.8	7.5		

2.3.7 The Effect of Crystallization Temperature

Table 2.6 lists A, B and fe values of single crystals grown from .05% cyclohexane solution and .05% amyl acetate solution from a sample with X_n of 440 at various crystallization temperatures, Tc. A similar set of the results is represented in Table 2.7 for another sample with X_n of 300. Fig 2.9 and Fig 2.10 are the corresponding plots for Table 2.6 and Table 2.7. It can be seen that both A and B increase with T_c. However, fe seems to remain unchanged. In Table 2.6 some crystallinity data are also available. We can see again that $fe \approx 1-Wc$ The meaning of the quantity of B' which appeared in Table 2.6, Table 2.7, Fig 2.10 and Fig 2.11 will be discussed latter. Using the formula (2.4), The total lamellar thickness which corresponds to 15 - 22 monomer unit is in the range of 10 - 15 nm. This result means that all the crystals obtained belong to the regime 1 after Finter and Wegner's definition [43].

2.3.8 The Effect of Concentration

The morphologies of crystals from dilute solution and from concentrate solution are completely different, as discussed in Section 3.3.1. However, A, B and fe do not change with concentration, as shown in Table 2.8 and Fig 2.11.

Table 2.6

Effect of Crystallization Temperature I

No	T_c (° C)	A	B	fe	Wc	B'
124	10	15.5	5.0	.25		2.8
149	15	16.5	5.6	.25	.73	2.9
145	20	18	6.0	.25	.73	3.1
147	25	19	6.5	.26	.74	3.0
148	27	20.5	6.9	.25	.73	2.8
166	20 AA	19	6.3	.25	.74	2.7
151	30 AA	21	7.5	.26		3.2
167*	40 AA	23	6.8	.23	.77	3.0

X_n = 440; crystallized in .05% cyclohexane solution, or in .05% amyl acetate solution (AA).
Wc, crystallinity from density measurement.

Table 2.7

Effect of Crystallization Temperature II

No. of test	T_c (°C)	A	B	fe	B'
186	20	19	7.2	.28	3.0
187	30	20	7.6	.27	3.0
188	40	22	8.2	.27	2.6
189	45	23.5	9.2	.28	3.0

X_n = 300; crystallized in .05% amyl acetate.

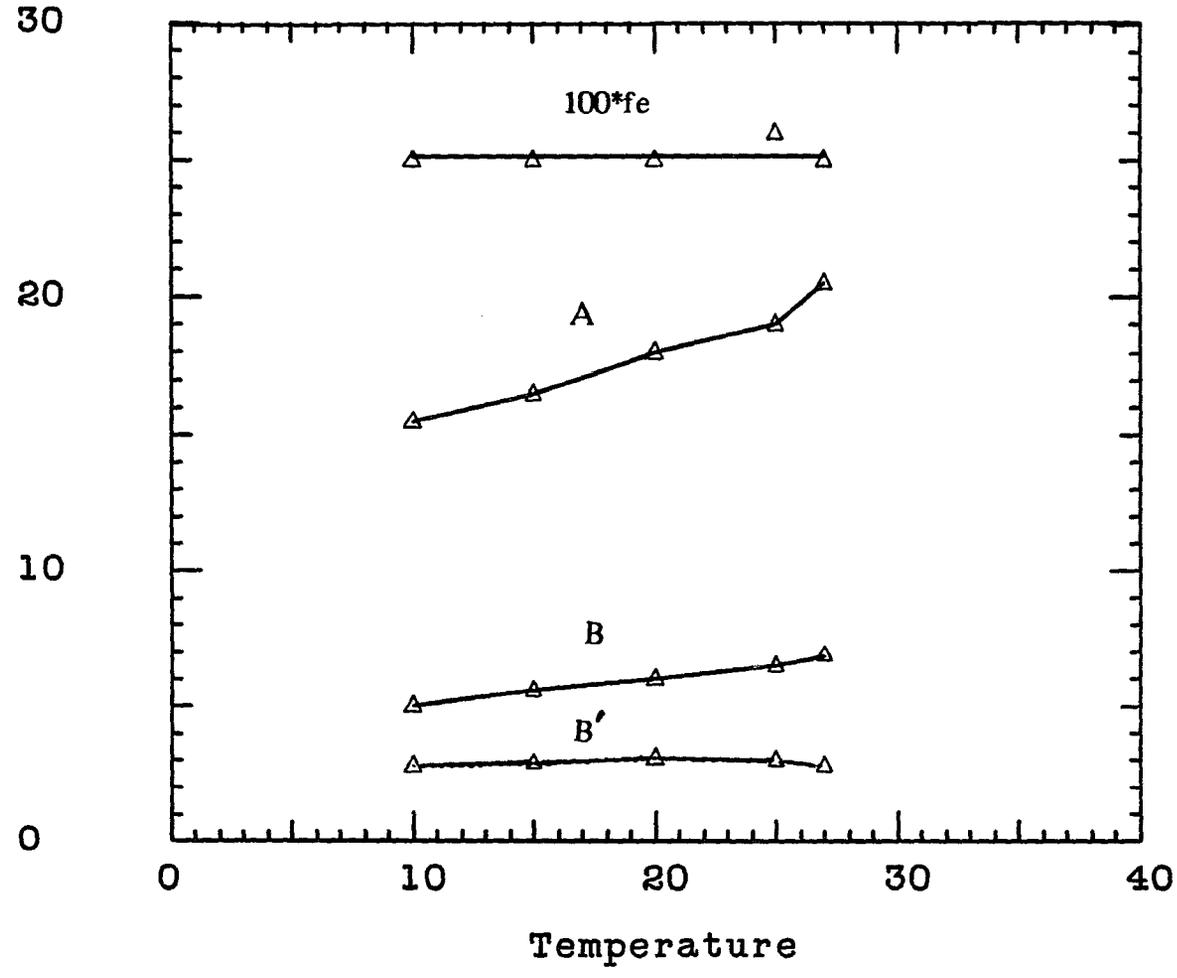

Fig 2.9 The effect of crystallization temperature I. Crystals grown in .05% cyclohexane solution, and the sample is with X_n of 440

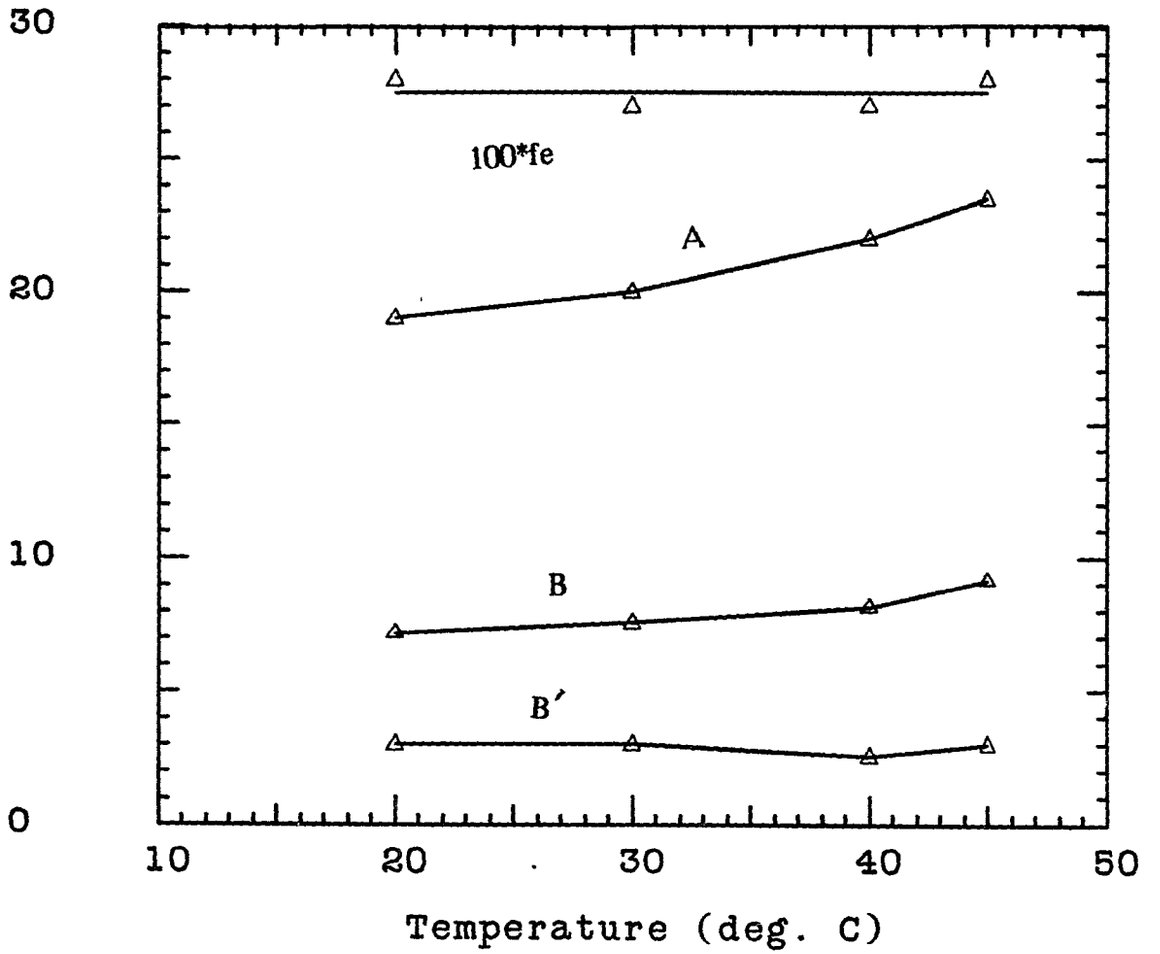

Fig 2.10 The effect of crystallization temperature II. Crystals grown in .05% amyl acetate solution, and the sample is with X_n of 330

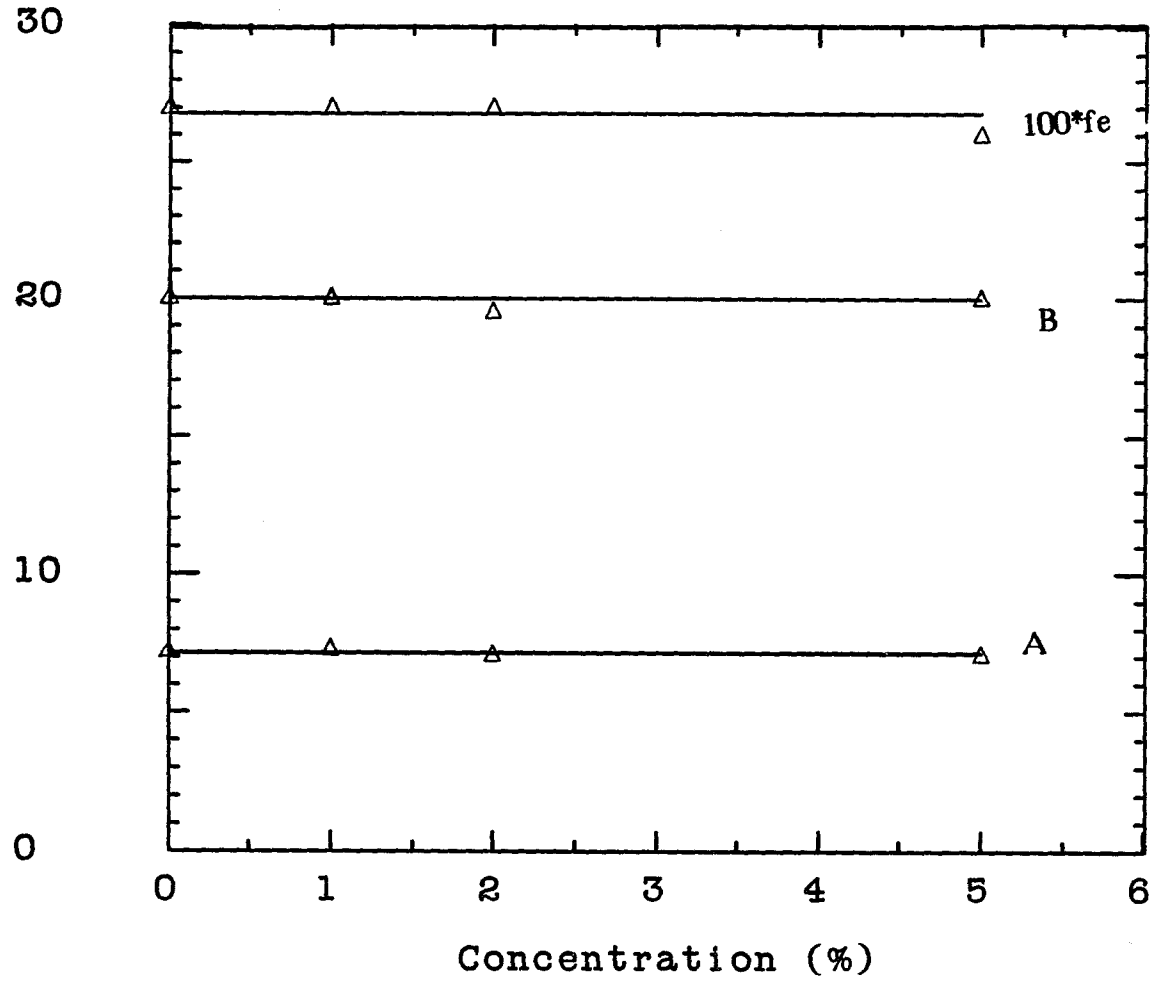

Fig 2.11 The effect of solution concentration. Crystals grown in .05% amyl acetate, and the sample is with X_n of 330

Table 2.8

Effect of Concentration

No. of test	Conc. (%)	A	B	fe	Wc
180	1.0	20	7.3	.27	.73
181	2.0	19.5	7.1	.27	.73
185	5.0	20	7.1	.26	

All crystallized in amyl acetate at 30°C

2.4 DISCUSSION

2.4.1 A Estimation of Cilium Length

As discussed in Section 2.3.5, the molecular chain ends of crystalline TPBD are rejected from the crystalline core as shown in Fig 2.7. The chain sequence which starts with a chain end and stays in amorphous part is called a cilium. Based on the folding model the average length of the cilia can be estimated. Tseng and Woodward [54] had estimated the average cilium length using proton NMR and small angle x-ray scattering data. Based on the C-13 NMR data more accurate estimation of cilium length can be obtained.

Let C the total chain end length (total monomer units in chain ends per chain)

C' =C-2

B" the average fold length after chain end correction

Fn the average fold number per chain

x the number average degree of polymerization

According to the model in Fig 2.7, a molecular chain which can fold itself Fn times forms Fn+1 crystalline stem traverses, Fn folds and two cilia. From the mononer unit balance, we have

$$(Fn+1)A + FnB^{*} + C = x \tag{2.7}$$

Meanwhile, B and B" have a relation:

$$B^{*} Fn + C' = B(Fn+1) \tag{2.8}$$

Both sides of eq. (2.8) represent the total monomer units in the amorphous part but in different notation. C' is introduced since the chemical shift of the carbon nuclei in the two terminal units fall outside the resonances of eq (2.3). In eq (2.3) the length of the cilia, C, is counted

into the B value. Introducing C' and B" eq. (2.8) separates these two quantities.

Recombining the eqs (2.7), (2.8) and eliminating Fn, leads to

$$\frac{Bx+2A}{A+B} = B'' \frac{x-2-A-B}{A+B} + C \qquad (2.9)$$

Thus, a plot of (Bx +2A)/(A+B) versus (x-2-A-B)/(A+B) will give slope B" and intercept C. Fig 2.12 is this kind of plot based on the data of Table 2.5 From this plot B"=4.8, and C=11 are obtained. This result hints that cilium length is approximately equal to the crystalline stem length. However, It must be noted that to obtain reliable C and B" a set of precise data is needed. Our results (both A, B and X) are not precise enough for this kind of treatment. A larger error for x is expected due to the method used and the refractionation which may take place in crystallization, particularly, for the low molecular fractions. This is why for the amyl acetate grown lamellas this kind of treatment gives a meaningless result.

2.4.2 Cis-Content Correction

As shown before, the cis-component is rejected from the crystalline core completely or at least to the experiment limit. Since each cis-unit causes up to (A-1) trans monomer units to be rejected into the amorphous

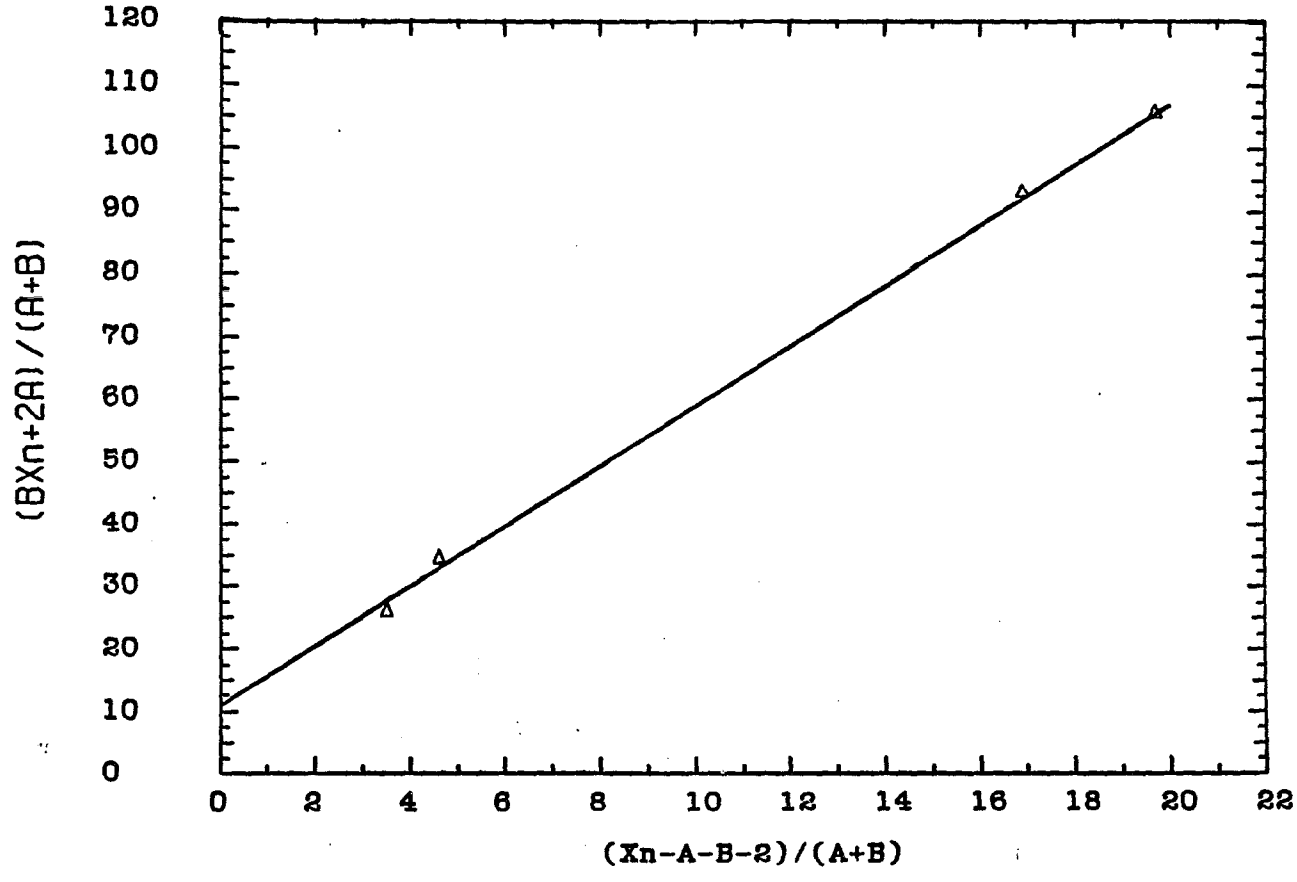

Fig 2.12 The plot for chain end correction

part, this effect is important even for very low cis-content samples. This effect leads to a larger B value. However, a "minimum fold length" B' which is the length of the folds that contain trans units only can be obtained by the following correction. Let the probability of the cis-unit appearing be q. Then, for a chain with degree of polymerization x there are qx cis units. Supposing that each cis-unit brings A/2 (a average number of 0 to A) trans monomer units to the amorphous part, there are qxA/2 monomer units per chain which will be transferred to the amorphous part due to the rejecting effect of the cis-units. Since each chain has x /(A + B) stems, the monomer units in the amorphous part due to cis-effect per stem is

$$\frac{qxA\ /\ 2}{x\ /\ (A+B)} = qA\ (A+B)/\ 2 \qquad (2.10)$$

We can correct the B value by

$$B' = B - qA\ (A+B)/\ 2 \qquad (2.11)$$

Here B is the fold length from C-13 spectrum directly, while B' corresponds to the B value in the case where there are no cis-units. A chain end correction can be combine together with the cis unit correction. If a chain end is equivalent to a cis-unit, each chain end brings A/2 units

to the amorphous part. Instead of qx, there are qx+2 = x(q + 2/x) equivalent cis-units per chain. In other words equivalent cis-content q' is q + 2/x. Therefore the total correction will be

$$B' = B - q'A\,(A + B)/2 \qquad (2.12)$$

Returning to Table 2.6, Table 2.7, Fig 2.9 and Fig 2.10 it is striking that after this cis and chain end correction all the B'-values are around three monomer units. Except Test 167 in Table 2.6 the q value of all the test is taken as 1.0% which is an average value. For Test 167, the measured q value is 0.7%. For this test the experimental (1-fe) and Wc values are significantly larger than for the others, In Table 2.6 the B-'value of this test was calculated using q of 0.7%. It can be seen that 1.0% cis content can increase B by 2-3 fold depending on the A value. After a similar cilium correction the earlier result of the fold length of TPBD lamellas grown from dilute solution, which was obtained by combining the results of small angle x-ray scattering and epoxidation followed by proton NMR measurement, was found to be 3 to 6 monomer units [55]. Since the cis correction introduced here was not considered that time, that result appears consistent with our result. As given by Oyama et al., three monomer units are needed to form a tight adjacent fold in TPBD lamellas [42], The present results strongly favor tight adjacent reentry for TPBD lamellas grown from solution.

2.5 CONCLUSIONS

The method of surface epoxidation followed by C-13 NMR analysis is effective in investigation of crystalline TPBD grown from solution. Both the crystalline stem length (A) and the fold length (B) can be obtained simultaneously by this and no other method to our knowledge.

Cis-units and chain ends are rejected from the crystalline core of TPBD. Therefore, crystallinity is determined by the cis-content and the molecular weight and the A value.

The A value ranges from 15 -22 monomer units under our experimental conditions. The corresponding total lamellar thickness is 10-15 nm, which is in agreement with the results from electron microscopy.

The B value is affected by the A value, the molecular weight, and particularly cis-content. After correction by the formula $B' = B - q'A(A+B)/2$, the minimum fold length is about three monomer units. This result strongly favors the tight adjacent reentry model.

Crystals with different morphologies, but from the same Tc, have almost the same A and B values.

Chapter III

A STATISTICAL TREATMENT TO THE CRYSTALLINITY AND CHARACTERISTIC TETRAD RATIO OF THE FOLD LENGTH

3.1 INTRODUCTION

In Chapter II, both the average crystalline stem length (A) and the average fold length (B) of trans-polybutadiene crystals (TPBD) grown from solution were obtained though surface epoxidation followed by C-13 NMR measurement. It was found that after a correction is made for folds containing cis-units and rejected trans units, the fold length B' for a fold containing trans units only is about three for all the preparations from the different solvents, different concentrations and different crystallization temperatures. The parameter B' is given by $B- q'A(A+B)/2$, where q' is an "equivalent" cis-content. This value for B' suggests that TPBD lamellas or their aggregates grown from solution have a prevalence of tight adjacent folds. However, the formula used above is valid only at low cis-content which does not address the situation of two or more cis-units in a single fold. Thus, to treat the case of high cis-content a more general statistical model is needed. In such a model instead of a molecular chain, the segment which is a piece of a molecule chain between two successive non-crystallizing monomer units will be considered. The basic idea is as follows. Due to the rejection of the cis units and chain ends, the two ends of

each segment stay in the amorphous part. Therefore, if tight adjacent reentry takes place, a segment with a length that falls into the range of n(A+B') to (n+1)(A+B')-1 monomer units can fold n times and form n+1 crystalline stems and n tight folds, where n is an integer, A is the crystalline stem length and B' is the minimum fold length. An average of nA dividing by the average segment length will give the crystallinity. Thus, a comparison of the crystallinity calculated from the model with the experimental results will test this folding mechanism.

According to the assignments of Schilling et al [57] the resonances of CH_2 carbons in OOOO and DOOO sequences in epoxidized and unepoxidized TPBD block copolymer have a chemical shift difference of .05 ppm, where O and D represent epoxidized and unepoxidized units, respectively. These two resonances should separate in a high field instrument, making possible an estimation of the ratio of their integral intensities. This quantity, is related to the distribution of fold length. If the cis-content is zero and the real fold length is three (or four), the tetrad ratio of [OOOO]/[DOOO] would be zero (or 0.5). With increasing cis content the ratio should increase significantly due to trans unit rejection from the crystalline core. Therefore, this tetrad ratio can provide another check on the folding model. This chapter will give a statistical treatment to calculate the crystallinity and the tetrad ratio of [OOOO]/[DOOO]. A comparison of the calculation with the experimental results presented in the previous chapter will be given.

3.2 EXPERIMENTAL

Except for the characteristic tetrad ratio of [OOOO]/[DOOO], the other experimental data used below is taken from Chapter II, mainly from Table 2.5 and Table 2.6. The tetrad ratio of [OOOO]/[DOOO] were measured for two samples. One of these was grown from .05% cyclohexane solution at 10°C, and the other was grown from .05% amyl acetate solution at 30°C. For both samples the precooling procedure, as described in 2.2.1, was used. The crystals of these two samples were surface-epoxidized in amyl acetate suspension containing dissolved m-chloroperbenzoic acid at a mole ratio of 1.5 for 14 days. The surface-epoxidized TPBD lamellas, after washing and drying were dissolved in deutrochloroform, and NMR measurements were carried out on those two samples using a JEOLCO NMR instrument with the following parameters: frequency of 100 MHz; window width of 16 KHz; memory of 64 KHz; delay time of 10 sec. (five times the longest T_1); accumulation scans of 4000; mode of high power proton decoupling. The spectra were expanded in the region of 28.8 ppm. The integral intensities of the resonances at 28.83 and 28.88 ppm were measured.

3.3 THE STATISTICAL TREATMENT

3.3.1 Assumptions and Definitions

There are three assumptions in the statistical treatment given below:

1. The cis-units are randomly distributed.

2. All the cis-units and chain ends are rejected from the crystalline core.

3. The folding involves adjacent reentry. If there are no cis units, all the folds have a fixed minimum length, B'.

According to the work of Clougue [71], Assumption 1 is likely. Assumption 2 was confirmed in Chapter II. The cis correction made in Section 2.4.1 suggests that Assumption 3 is possible and B' is about three or four monomer units.

We define a 'segment' as a piece of a molecular chain between two successive noncrystallizing units which can be cis-units, 1,2 units or chain ends as shown in Fig 3.1 (a dot represents a noncrystallizing unit).

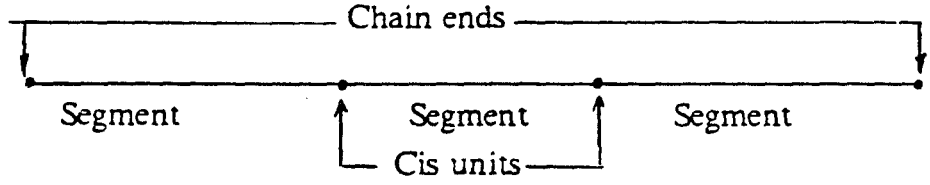

Fig 3.1 The segments in a molecular chain

According to the tight adjacent reentry fold model the conformation of a chain in a lamella can be represented as Fig 3.2. The crystalline part is in the middle, the amorphous part, consisting of folds and chain ends, is on both sides.

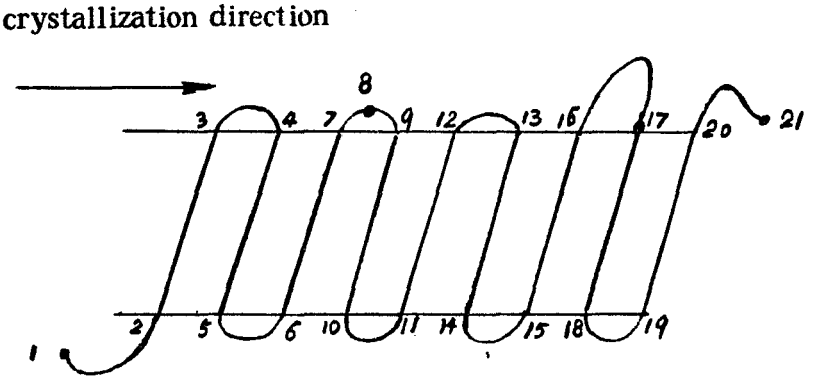

Fig 3.2 Conformation of a molecular chain in the adjacent reentry folding model. 1, 21 are two chain ends; 17 is a rejected cis unit, 8 is a interior cis unit. 1-8, 8-17, 17-21 are three segments in this chain. 1, 8 and 17 (8, 17 and 21) is the head (tail) of the segments. 1-2, 8-9 and 17 (7-8, 16-17 and 20-21) are the head parts (tail parts) of the segments. 3-4, 5-6, 12-13, 14-15 and 18-19 are regular folds. 7-8-9 and 16-17 are irregular folds.

In this treatment below attention will be directed to segments instead of molecular chains, because it is much easier to count how many monomer units in a segment are rejected to the amorphous part. The head of a

segment is defined as a noncrystallizing unit, and the tail of a segment is another noncrystallizing unit. The chain sequence which stays in the amorphous part and connects to the head (tail) is called the head (tail) part. For any crystallizing segments forming a new crystalline stem a total of (A+B') monomer units is needed, among them A is for the crystalline stem, and B' for a regular fold. If the remaining length is less than (A+B'), this part becomes a rejected tail part. Thus, a rejected tail part could be as long as (A+B')-1. According to Assumption 3 the head part is shorter than B', unless the head is a chain end, then, this head part has a length between 0 to A-1.

Based on the location of the heads, the segments can be classified as one of three kinds. In the first one the heads of the segments are rejected cis units, and they stay just outside the crystalline core (Segment a). In the second kind, the heads are interior cis units. they are removed from the crystalline core by g monomer units (Segment b). According to Assumption 2, g runs from 1 to B'-1, where B' is the minimum fold length. In the third kind the heads of the segments are chain ends (Segment c). The three kinds of segment are represented in Fig 3.3.

According to the model (Fig 3.2), the amorphous part consists of folds and cilia. the crystalline part consists of crystalline traverses. The folds without cis unit are termed regular, and those with cis units irregular.

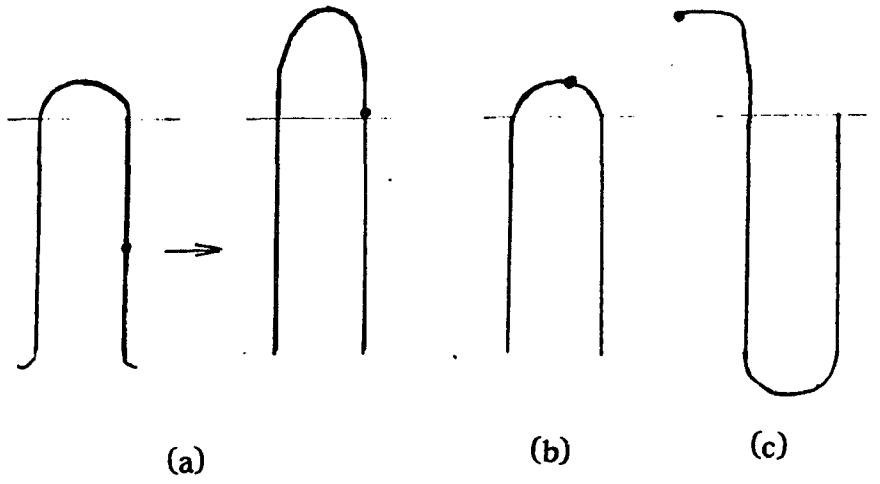

Fig 3.3 Three kinds of segments

3.3.2 Calculation of Crystallinity

The crystallinity of polymer lamellas can be given by the average number of monomer units in the crystalline core divided by the average total number of units per segment. The number of monomer units in the crystalline core for three kinds of segments will be evaluated below.

Let the probability that a trans unit appears in a segment be p (p = $1-q_1$ = 1-q+1/x, q_1 is the fraction of equivalent cis-units, q is the fraction of cis-units, and x is the degree of polymerization. see Section 3.5.3), then, according to the assumption of random placement of cis-units the probability that the segment contains i trans monomer units is

$$p^i(1-p) \qquad (3.1)$$

The first type of segment to be considered starts with a rejected unit (see Fig 3.3 Segment a). When the segment length falls in the region between n(A+B')-B' and (n+1)(A+B')-B'-1, only nA monomer units can enter the crystalline core. Thus, the average number of crystalline monomer units per segment (S_{01}) is given by:

$$S_{01} = \sum_{n=1}^{m} (nA) \sum_{j=0}^{(A+B')-1} p^{(n(A+B')-B'+j)}(1-p) \qquad (3.2)$$

where m is equal to the integer of x/(A+B'). This number determines the longest segment having m(A+B') monomer units. In eq. (3.2) there is a double summation; one summation (n) counts the possible number of folds (1 to m), and the other (j) the possible tail length (0 to A+B'-1). The double summation considers all possible probability distributions of segment length, which has been normalized by the factor of (1-p).

In the case of the segment starting with an interior cis unit (Segment b), another g monomer units in the head part contribute nothing to the crystallinity; the average crystalline monomer units per segment (S_{02}) is

$$S_{02} = \frac{1}{(B'-1)} \sum_{g=1}^{B'-1} \sum_{n=1}^{m} (nA) \sum_{j=0}^{(A+B'-1)} p^{(n(A+B')-B'+g+j-1)}(1-p) \qquad (3.3)$$

where 1/(B'-1) is a normalization factor for the summation to g.

For the segment starting with an ending group (Segment c), before entering the crystalline core there could be up to (A-1) monomer units that stay in the amorphous part. Therefore, the corresponding crystalline monomer units per segment (S_{03}) is

$$S_{03} = \frac{1}{A}\sum_{g=0}^{A-1}\sum_{n=1}^{m}\sum_{j=0}^{(A+B'-1)} p^{(n(A+B')-B'+j+g)}(1-P) \tag{3.4}$$

For a molecular chain with degree of polymerization of x have qx cis units, there are qx+1 segments per molecular chain on the average (see Fig 3.1). The probability that a segment starts with a chain end is k_1 = 1/(1+qx). Referring to Fig 3.3 (a), It is seen that the probability of segment (a) appearing is k_2 = A/(A+B'), and the probability of segment (b) appearing is $1-k_2$ = B'/(A+B') when the head of the segment is not a chain end. Combining all the possibilities, the average number of crystalline monomer units per segment is

$$S_0 = k_1 S_{03}+(1-k_1)(k_2 S_{01}+(1-k_2)S_{02}) \tag{3.5}$$

Meanwhile the total average length of a segment is

$$S = \sum_{i=0}^{x}(i+1)p^i(1-p) \tag{3.6}$$

where (i+1) includes a noncrystallizing unit per segment.

Finally, the crystallinity, χ, is

$$\chi = \frac{S_0}{S} \tag{3.7}$$

3.3.3 Calculation of the Tetrad Ratio

Under the proper epoxidation conditions only and all the monomer units in the amorphous part are epoxidized. After epoxidation a molecular chain of TPBD becomes a block copolymer chain, as follows:

..DDOOODD..DDOOOOOOOODD..DDOOODD..DDDOOODD..

where D and O represent unepoxidized and epoxidized monomer units, respectively. DD..DD represents the unepoxidized crystalline stem. and O..O sequences are the epoxidized folds. In general we have

$$\frac{[OOOO]}{[DOOO]} = \frac{S_4}{S_3} \tag{3.8}$$

where S_4 is the average number of OOOO sequences per segment, and S_3 is the average number of DOOO sequences per segment.

All the DOOO and OOOO sequences come from regular folds, head parts and tail parts. According to our definition, the chain sequence

which stays in the amorphous part and connects to the head (tail) is called the head (tail) part. The contribution from each parts can be counted separately. The case of B'=3 is to be considered first. For that case, the regular folds do not contribute any OOOO sequences, but each of them contributes two DOOO sequences. The tail part could contribute one DOOO sequence, and the head part contributes nothing. For any kind of segments the number of regular folds is one less than the number of crystalline stems, the latter is expressed by $\frac{S_{01}}{A}$. Thus, the average number of DOOO sequences per segment is given by:

$$S_{31} = 2(\frac{S_{01}}{A}-1)+\sum_{n=1}^{m}\sum_{j=3}^{(A+B'-1)} p^{(n(A+B')-B'+j)}(1-p) \qquad (3.9)$$

The first term of the right side of eq. (3.9) counts the contribution of regular folds, and the second term counts the contribution from the tail part.

Similarly, we have eq. (3.10) and eq.(3.11) for the segments which start with an interior cis unit (Segment b) and which start with a chain end (Segment c), respectively.

$$S_{32} = 2(\frac{S_{02}}{A}-1)+\frac{1}{(B'-1)}\sum_{g=1}^{B'-1}\sum_{n=1}^{m}\sum_{j=3}^{A+B'-1} p^{(n(A+B')+g+j-B')}(1-p) \qquad (3.10)$$

$$S_{33} = 2\left(\frac{S_{03}}{A}-1\right)+\frac{1}{A}\sum_{g=0}^{A-1}\sum_{n=1}^{m}\sum_{j=3}^{A+B'-1} p^{(n(A+B')+g+j-B'-1)}(1-p) \qquad (3.11)$$

$$+\frac{1}{A}\sum_{g=3}^{A-1}\sum_{n=1}^{B'-1} p^{(n(A+B')+g+j-1)}(1-p)$$

In eq. (3.11) the head part could contribute one DOOO sequence if the length of the head part is longer than three monomer units. Taking the average of the three kinds of segments, we have

$$S_3 = k_1 S_{33}+(1-k_1)(k_2 S_{31}+(1-k_2)S_{32}) \qquad (3.12)$$

In counting the number of OOOO sequence per segment when B' value is three monomer units, regular folds have no contribution, a contribution could only come from the tail parts, and the head part of the segments which start with chain ends. An OO..OO sequence with j successive O units contributes (j-3) OOOO sequences. Therefore, for the segments (a) and (b) we have

$$S_{41} = \sum_{n=1}^{m}\sum_{j=4}^{A+B'-1}(j-3)p^{(n(A+B')-B'+j)}(1-p) \qquad (3.13)$$

$$S_{42} = \frac{1}{(B'-1)}\sum_{g=1}^{B'-1}\sum_{n=1}^{m}\sum_{j=4}^{A+B'-1}(j-3)p^{(n(A+B')-B'+j+g)}(1-p) \qquad (3.14)$$

For the segments (c), both the head part and the tail part can have a contribution to the OOOO sequence. the expression, therefore, is

$$S_{43} = \frac{1}{A}\sum_{n=0}^{m}\Big(\sum_{g=4}^{A-1A+B'-1}\sum_{j=0}^{}(g-3) \tag{3.15}$$

$$+\sum_{g=o}^{A-1A+B'-1}\sum_{j=4}^{}(j-3)p^{(n(A+B')-B'+g+j-1)}(1-p))$$

Combining these three cases, similar to eq. (3.5), the final expression for the average number of OOOO sequences per segment is

$$S_4 = k_1 S_{43}+(1-k_1)(k_{21}S_{41}+(1-k_2)S_{42}) \tag{3.16}$$

The tetrad ratio, then, can be obtained by substituting eq. (3.12) and eq. (3.16) into eq. (3.7).

When the B' value is four (five), each regular fold contributes one (two) OOOO sequence, and the head part in segments (b) may contain one DOOO sequence. Thus, a relative correction must be made in S_{41}, S_{42}, S_{43} and S_{32}. For the first three terms an additional term of $(B'-3)(\frac{S_0}{A}-1)$ is needed, Meanwhile, S_{32} becomes

$$S'_{32} = S_{32}+\frac{1}{(B'-1)}\sum_{g=3}^{B'-1}\sum_{n=1}^{m}\sum_{j=3}^{A+B'-1}p^{n(A+B')+g+j-B'}(1-p) \tag{3.10a}$$

3.4 COMPARISON OF CALCULATIONS AND EXPERIMENTS

3.4.1 Comparison of Crystallinity

The program for the calculation of crystallinity and characteristic tetrad ratio are attached in Appendix I. A comparison of the calculated and experimentally determined crystallinity is shown in Fig 3.4 and Fig 3.5. The calculated curves for an equivalent cis content (q_1) of 0.01 and a degree of polymerization (x) of 330 and 440 respectively, and for minimum fold length (B') of 3, 4 and 5, as marked, were obtained as function of the crystalline stem length (A). These calculated results are tabulated in Table 3.2, 3.3 and 3.4. The experimental results are taken from Table 2.5 and Table 2.6 of Chapter II for samples crystallized at various temperatures using two different solvents. The comparison shows that all experimental points scatter between the curves with B'=3 and B'=4. This result is in agreement with those obtained using the equation: B'= B-q'A(A+B)/2 (See eq. 2.12). This is not surprising, because for low cis-content samples the statistical treatment should be consistent with the cis correction formula ,eq. (2.12). As a matter of fact, eq. (2.12) can be reformed as

$$B = \frac{B' + \frac{q'A^2}{2}}{1 - q'A/2} \qquad (2.12a)$$

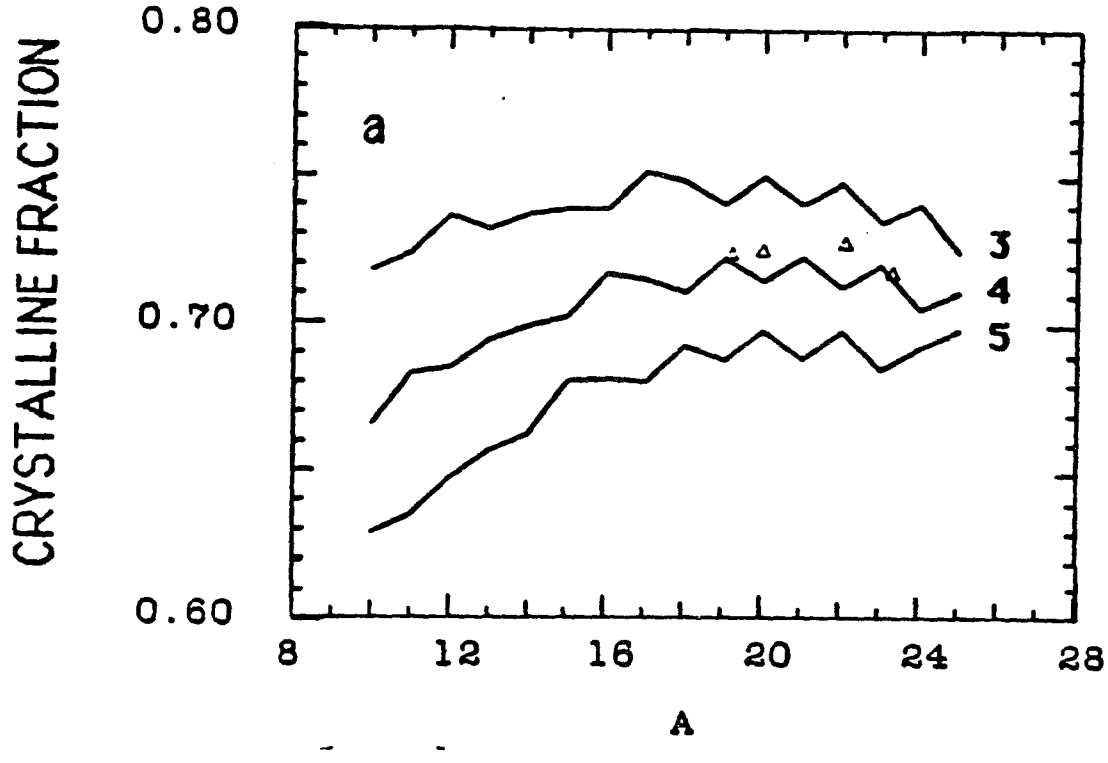

Fig 3.4 A comperison of calculated and experimental crystallinity as a fuction of the crystalline stem length (A). The experimental data come from the samples with X_n of 330 and grown in .05% amyl acetate solution.

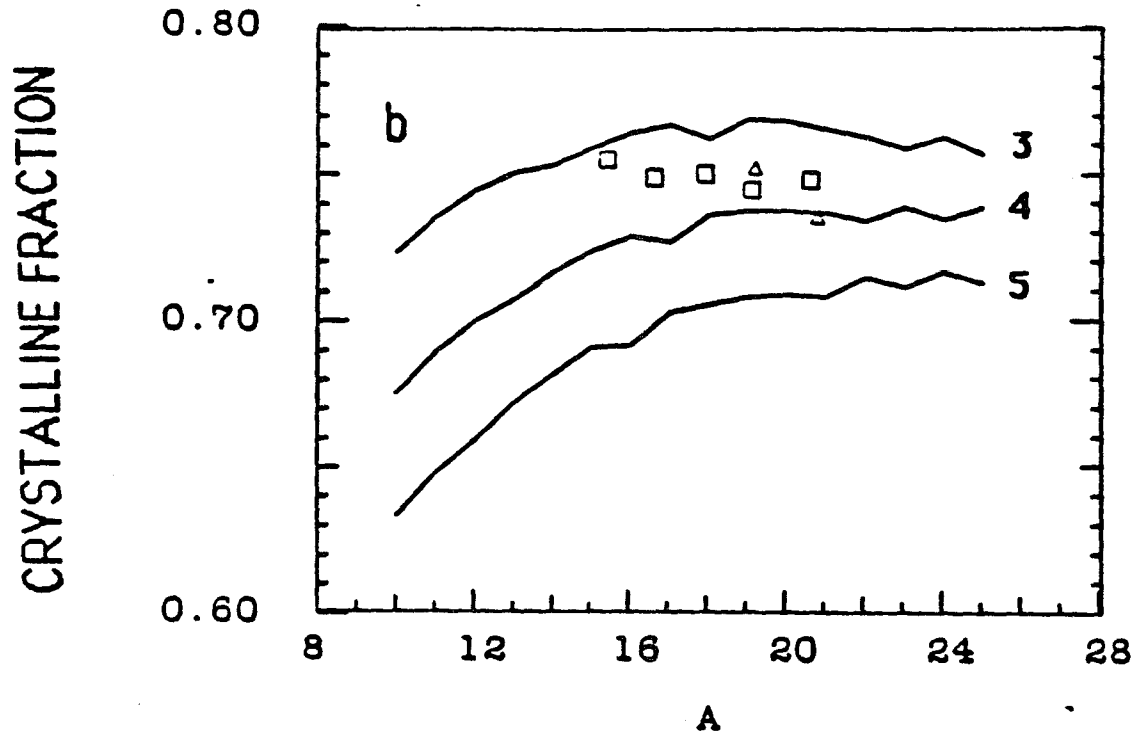

Fig 3.5 A comperison of calculated and experimental crystallinity as a fuction of the crystalline stem length (A). The experimental data come from the samples with X_n of 440 and grown in .05% cyclohexane solution.

Using B'=3, A=15-24 and a q' value of .016 (remember, q'=q + 2/x) the B value can be calculated from eq. (2.12 a). When the calculated B and the corresponding A are put into eq. (2.4), fe = B/(A+B), the correct crystallinity value, (1-fe), about 0.75, is obtained; that value is the same as that from the statistical treatment.

In Chapter IV the method developed here for calculation of crystallinity will be compared with the experimental results obtained for a high cis content TPBD sample.

3.4.2 Comparison of the Characteristic Tetrad Ratio

According to the earlier assignment [57], the peaks at 28.8 and 28.4 ppm belong to CH_2 carbons within OO sequences with splitting due to the presence of diasteroisomers. At higher fields both peaks split into doublets. The peak at 28.8 ppm splits into the a doublet at 28.83 and 28.88 ppm (in the earlier results they are assigned as 28.90 and 28.95 ppm). The resonance of the CH_2 carbons in the DOOO sequences contribute to both peaks (28.88 and 28.83 ppm), and the resonance of the CH_2 carbons in the OOOO sequences contributes only to the resonance at 28.83 ppm. Therefore,

$$R = Area\,(28.83m)\,/\,Area\,(28.88) = \frac{0.5[DOOO]+[OOOO]}{0.5[DOOO]} \qquad (3.17)$$

or,

$$[OOOO]/[DOOO] = \frac{(R-1)}{2} \qquad (3.17a)$$

The pertinent part of a C-13 NMR spectrum of surface-epoxidized TPBD at 100 MHz is given in Fig 3.6. Values of A, R and tetrad ratio were obtained from 100 MHz C-13 NMR spectra for two samples of 99% trans-polybutadiene. One of these was crystallized from .05% cyclohexane solution (CH) at 10°C and the other from .05% amyl acetate solution (AA) at 30°C using the precooling method. In calculating the tetrad ratio from the spectrum a deconvolution procedure was used. The results are given in Table 3.1. Considerable uncertainty in R is evident due to the presence of a small peak at 28.93 ppm, with the values shown being an average with or without the area under this resonance.

In Table 3.2, Table 3.3 and Table 3.4 the results of the statistical calculation of tetrad ratio, [OOOO]/[DOOO], as function of A and B' are given, using q = .010 and x= 330, values found experimentally for these samples. Although the A value for the two samples varies by about 30% (A = 15.5 and 20), the best fitting with the experimental tetrad ratios shows that the minimum fold length B' is about four monomer units

Table 3.1 Experimental Results from 100 MHz C-13 NMR Spectra

Cry. Solv.	T_c (° C)	A	R	[OOOO]/[D000]
CH	10	15.5	3.6 ±0.4	1.3 ±0.2
AA	30	20	4.0 ±0.4	1.5 ±0.2

CH, cyclohexane; AA, amyl acetate.

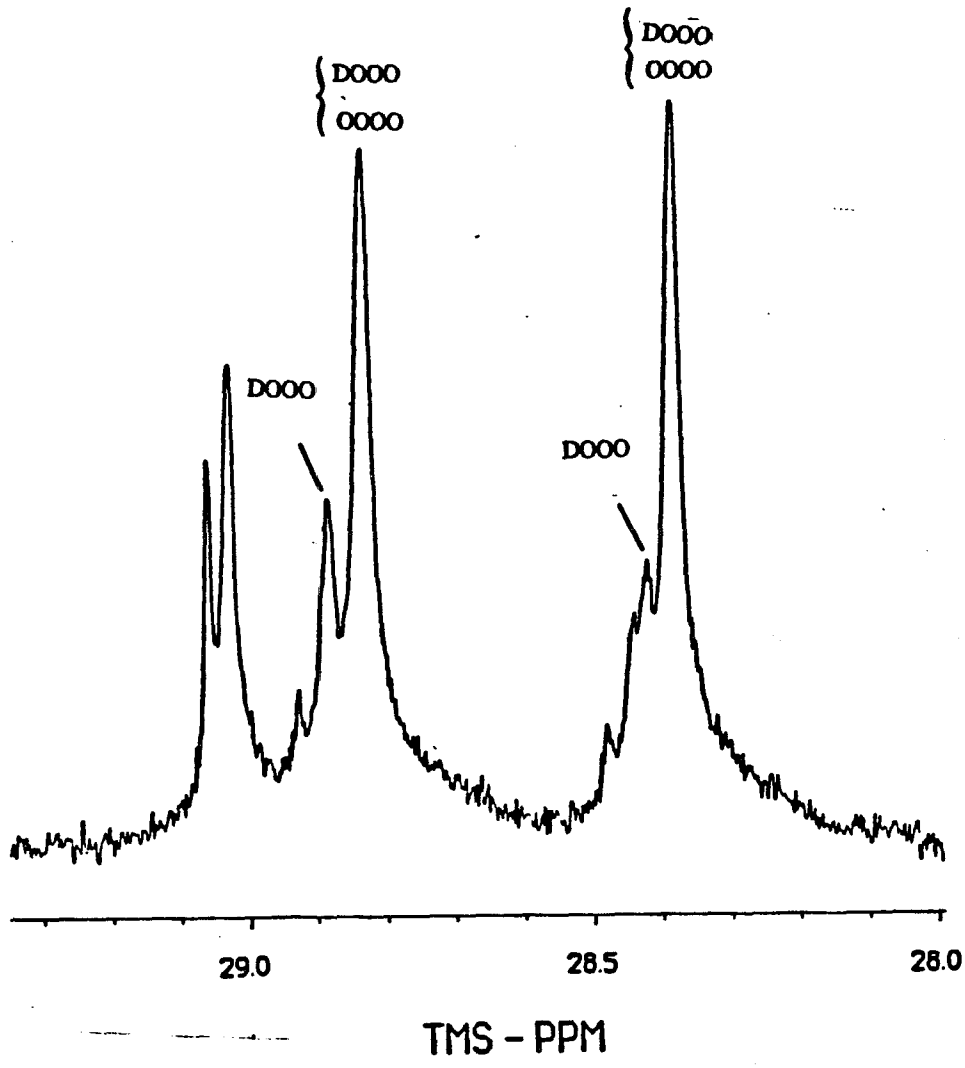

Fig 3.6 Expanded C-13 NMR spectrum of surface-epoxidized 99%-trans-polybutadiene at 100 MHz in the range of 28.8 ppm. The sample was grown from .05% cyclohexane solution at 10°C.

Table 3.2

The Calculated Crystallinity and Tetrad Ratio with B'=3

A	S0	S3	S4	S	χ	[OOOO]/[DOOO]
10	5.310	10.309	3.177	73.162	0.726	0.308
11	4.935	9.692	3.576	73.162	0.742	0.369
12	4.558	9.060	3.957	73.162	0.748	0.437
13	4.216	8.490	4.324	73.162	0.749	0.509
14	3.951	8.070	4.689	73.162	0.756	0.581
15	3.709	7.692	5.043	73.162	0.760	0.656
16	3.488	7.349	5.383	73.162	0.763	0.733
17	3.285	7.036	5.711	73.162	0.763	0.812
18	3.097	6.747	6.025	73.162	0.762	0.893
19	2.922	6.478	6.325	73.162	0.759	0.976
20	2.803	6.326	6.638	73.162	0.766	1.049
21	2.651	6.093	6.913	73.162	0.761	1.135
22	2.548	5.966	7.203	73.162	0.766	1.207
23	2.414	5.759	7.454	73.162	0.759	1.294
24	2.284	5.555	7.688	73.162	0.749	1.384
25	2.205	5.465	7.948	73.162	0.754	1.455

Table 3.3

The Calculated Crystallinity and Tetrad Ratios with B'=4

A	S0	S3	S4	S	χ	[OOOO]/[DOOO]
10	4.992	9.687	7.795	73.162	0.682	0.805
11	4.611	9.054	7.808	73.162	0.693	0.862
12	4.266	8.482	7.841	73.162	0.700	0.924
13	3.998	8.062	7.949	73.162	0.710	0.986
14	3.754	7.683	8.068	73.162	0.718	1.050
15	3.530	7.340	8.194	73.162	0.724	1.116
16	3.325	7.027	8.324	73.162	0.727	1.185
17	3.135	6.739	8.456	73.162	0.728	1.255
18	2.958	6.470	8.585	73.162	0.728	1.327
19	2.838	6.320	8.783	73.162	0.737	1.390
20	2.684	6.087	8.909	73.162	0.734	1.464
21	2.580	5.961	9.101	73.162	0.741	1.527
22	2.444	5.755	9.220	73.162	0.735	1.602
23	2.313	5.552	9.326	73.162	0.727	1.680
24	2.233	5.462	9.510	73.162	0.733	1.741
25	2.156	5.375	9.687	73.162	0.737	1.802

Table 3.4

The Calculated Crystallinity and Tetrad Ratios with B'=5

A	S0	S3	S4	S	χ	[OOOO]/[DOOO]
10	4.992	9.687	12.034	73.162	0.682	1.242
11	4.611	9.054	11.674	73.162	0.693	1.289
12	4.266	8.482	11.368	73.162	0.700	1.340
13	3.998	8.062	11.212	73.162	0.710	1.391
14	3.754	7.683	11.091	73.162	0.718	1.443
15	3.530	7.340	10.996	73.162	0.724	1.498
16	3.325	7.027	10.923	73.162	0.727	1.554
17	3.135	6.739	10.865	73.162	0.728	1.612
18	2.958	6.470	10.818	73.162	0.728	1.672
19	2.838	6.320	10.897	73.162	0.737	1.724
20	2.684	6.087	10.869	73.162	0.734	1.786
21	2.580	5.961	10.958	73.162	0.741	1.838
22	2.444	5.755	10.938	73.162	0.735	1.901
23	2.313	5.552	10.911	73.162	0.727	1.965
24	2.233	5.462	11.016	73.162	0.733	2.017
25	2.156	5.375	11.114	73.162	0.737	2.068

3.5 DISCUSSION

3.5.1 Adjacent Reentry

It was shown above for TPBD that the experimental results of two different quantities, crystallinity and NMR tetrad ratio, are in agreement with the calculations based on a tight adjacent reentry model. It appears, therefore, that the molecular chains in TPBD lamellas grown from solution arrange themselves with tight adjacent reentry.

The statistical treatment shows that in the experimentally accessible range the crystallinity is almost independent of A. this is in agreement with experiment and is due to the increase of the B-value with increasing A-value. The change in B-value is caused by an increasing in the length of trans sequences ejected from the crystalline core due to rejection of cis units during crystalization since that length is a function of A-value. As will be shown in Chapter IV, TPBD samples with higher cis-content have sharper decreases in crystallinity with increasing the crystalline stem length.

3.5.2 A Comparison with Melt Crystallized Polyethylene

Since the treatment established above is general, it should be applicable to other random copolymer systems. Some results given by Pakula provided a chance for such a comparison. Pakula measured the total lamellar thickness by small angle x-ray scattering and crystallinity by heat of

fusion for melt crystallized polyethylene which contains 7% short branches (35 CH_3 per 1000 carbons) [72]. The data cited from Pakula's plot are listed in Table 3.5. Plots of crystallinity versus A for B'=4, 5 and 6 using the experimental values of q (7%) and X_n (1000) are given in Fig 3.7. Pakula's results are represented by the black points with error boxes. Although the experimental uncertainty is large, the assumption of adjacent folding with B'= 4 fits the experimental results.

Harrison and Juska estimated the number of carbon atoms of a tight adjacent fold of polyethylene using the CPK precision space filling model [73]. A visual inspection of the models indicated that the number of carbon atoms involved in a fold is approximately 9 to 11. The average of this result is close to that found in the present treatment.

Table 3.5

Pakula's data for a melt crystallized polyethylene

Crystalline length (nm)	Crystalline length (mers)	Crystallinity
4.60	18.0	41.4
4.74	18.6	40.5
4.87	19.1	40.0
5.07	19.9	38.5
5.26	20.6	37.6
5.70	22.4	34.5

mers, monomer units.
mers = nm/c, c (.255 nm) is unit cell parameter of polyethylene along chain direction

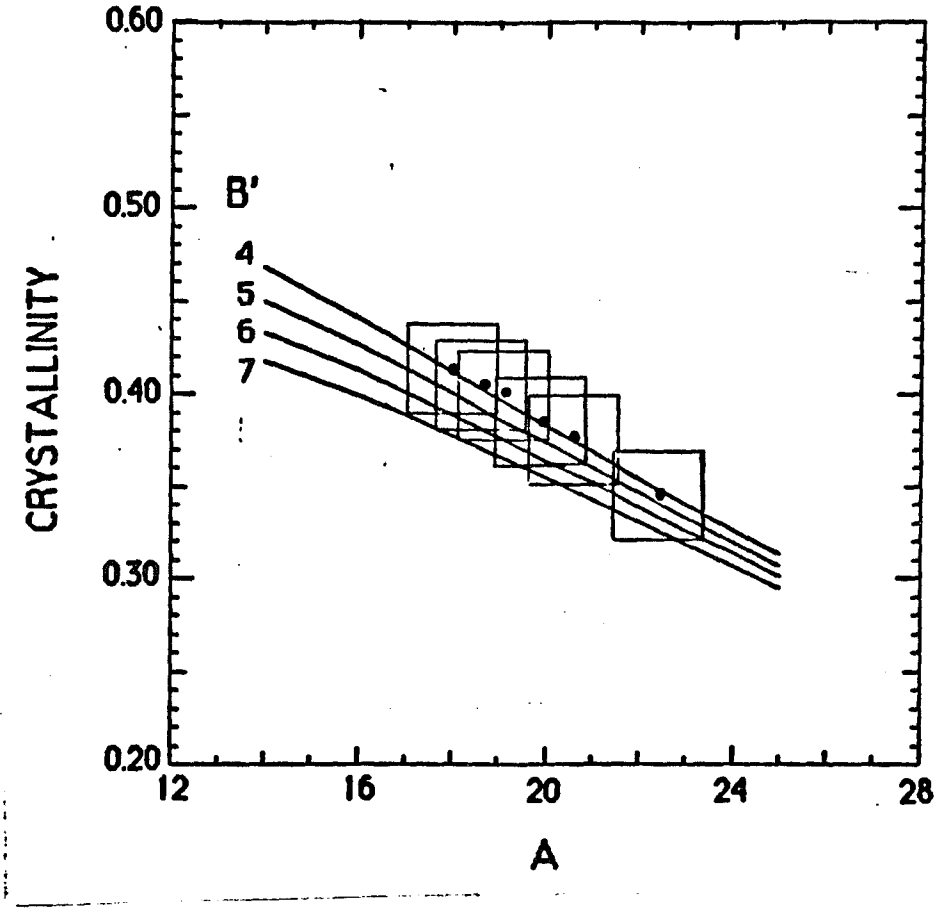

Fig 3.7 A comparison of calculaed and experimental crystallinity as a fuction of the crystalline stem length for melt crystallized polyethylene which contains 7% short branthes [64].

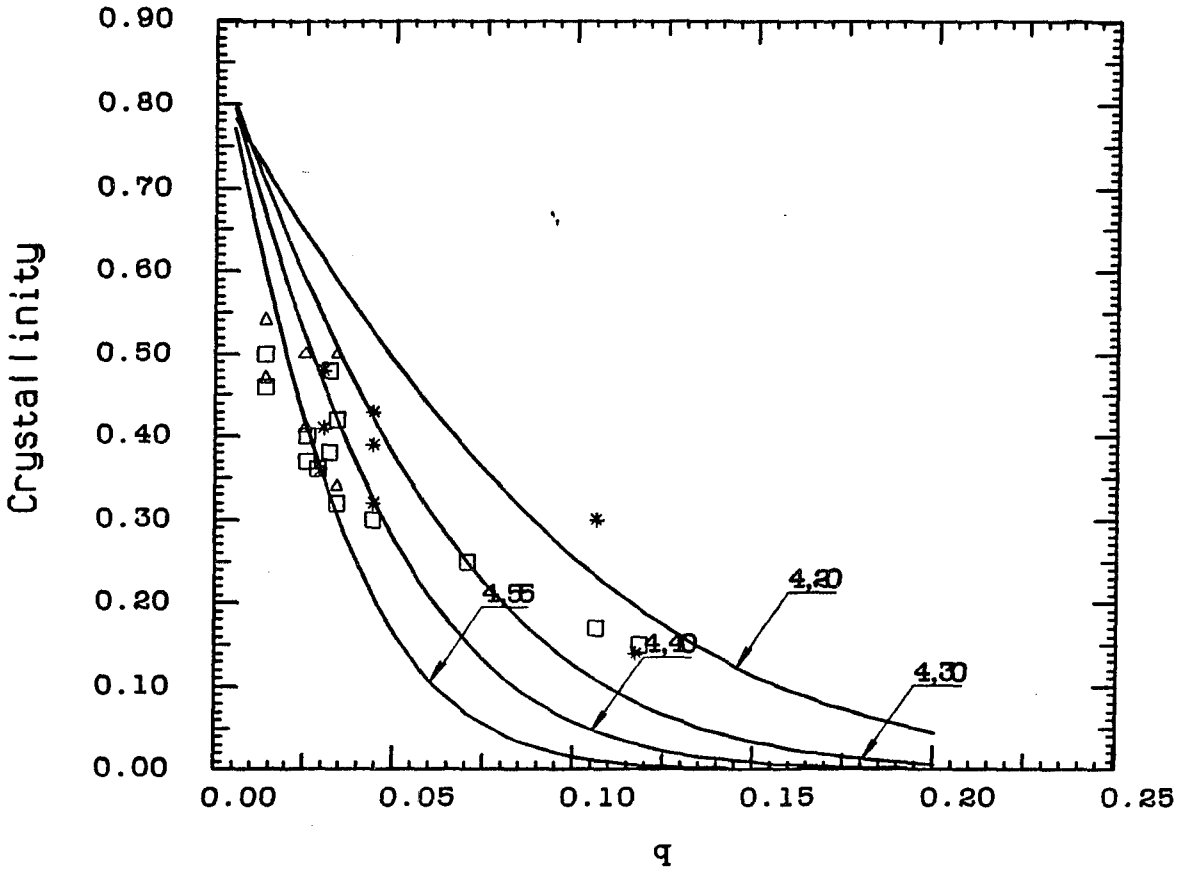

Fig 3.8 A comparison of calculated and experimental crystallinity as a function of short branches for melt crystallized polyethylene. Triangles are for slow cooled samples with A-values of about 40-50; squares are for quenched samples with A-value of about 25-30; and asterisk are for results without A-value [74]. Each theoretical curve is maked by a pair of numbers, they are the minimum fold length (B') and the crystalline stem length (A).

A recent work by Mandelkern (76) provides another chance to compare the model with experimental results. For a series of melt crystallized polyethylene specimen with various contents of short branches Mandelkern obtained the crystalline thickness by the analysis of the low-frequency Raman longitudinal-acoustic vibrational mode, and the crystallinity by measurement of density and enthalpy of fusion. In Fig 3.8 the solid curves are the calculated crystallinity versus the content of short branches with B' and A values, respectively, as parameters; the squares, triangles and stars represent the experimental results. It is worth noting that for large q and A values, the crystallinity is insensitive to B'. For example, the curves with parameters of B'=6 and A=40, and B'=8 and A=40 coincide with the curve with B'=4 and A=40.

3.5.3 Equivalent Cis Content q_1

The probability of equivalent cis-units, $q_1 = q + 1/x$, is not the same as the equivalent cis-unit content, $q' = q+2/x$, used in the Section 2.4.2. This is because a cis-unit can be met from two directions along the chain, while a chain end only from one direction. Another way to compare cis-units and chain ends is to connect two chain ends of a molecular chain to form a ring. By doing this the lengths of the segments within the molecular chain do not change, but two chain ends now is equivalent to a cis unit. The validity of expression for the q_1 can be proven in the calculation of the average segment length. Using statistics the average segment length

S is given by:

$$S = \sum_{i=1}^{x} p^{i-1}(i)(1-p) = \frac{1}{1-p} = \frac{1}{q_1} = \frac{1}{q+\frac{1}{x}} \tag{18}$$

On the other hand a molecular chain with x monomer units has qx cis-units, and qx + 1 segments. Therefore, an average segment length S is

$$\frac{x}{xq+1} = \frac{1}{q+\frac{1}{x}} \tag{19}$$

We see that the two expressions are exactly same. In other words the expression of probability of equivalent cis-unit, q_1 = q+ 1/x, is correct.

3.5.4 A Simpler Model for The Tetrad Ratio

Instead of the statistical treatment a simpler model can be set up to check all the formulas and procedures. It can be started with the case of B'= 3. As discussed in Section 3.3.3, all the DOOO and OOOO sequences come from regular folds and head parts and tail parts. According to our definition, the chain sequence which stays in the amorphous part and connects to the head (tail) is called the head (tail) part. Now we can count the contribution from each part. For the case of B'= 3, the regular folds do not contribute any OOOO sequences, but each of them contributes two DOOO

sequences. It is known that a molecular chain with a fractional cis-content, q, and degree of polymerization, x, has (qx+1) segments. The average segment length, thus, is x/(xq+1), and the average number of crystalline stems per segment are (x /(xq + 1)) / (A + B') = x/((xq+1)(A+B')), where (A+B') is the sum of monomer units of a crystalline stem and a minimum fold. Since the number of folds per segment are one less than the number of crystalline stems per segment, and each fold contributes two DOOO sequences, the number of DOOO sequences per segment from regular folds is 2[x/((qx+1)(A+B'))-1].

The tail part has an average length ((A+B'-1) +1)/2=(A+B')/2; it contributes one DOOO sequence and ((A+B')/2-3)) OOOO sequences. When the head of a segment is a chain end, it has an average length (0+A)/2=A/2, and contributes one DOOO sequence and $(\frac{A}{2}-3)$ OOOO sequences. But, when the head is not a chain end, its length is smaller than three, there is not any contribution to DOOO and OOOO sequences. The probability that the head of a segment is a chain end is $k_1 = 1/(qx+1)$, the average contribution from the head part to DOOO (or OOOO) sequence is k_1(or $k_1 A/2-3$). Therefore, the contribution from the head and tail part to the DOOO sequence is $1+k_1$. Together, the total number of DOOO sequences per segment is given by:

$$N_3 = 2[x / ((qx+1)(A+B'))-1] + (1 + k_1) \qquad (3.18)$$

The number of OOOO sequences per segment is given by:

$$N_4 = \frac{(A+B')}{2} - 3 + k_1 \left(\frac{A}{2} - 3\right) \tag{3.19}$$

Finally, the tetrad ratio of [OOOO]/[DOOO] is

$$N_4 / N_3 = \frac{((A+B')/2 - 3) + k_1 (A/2 - 3)}{2x / ((qx+1)(A+B')) - 1 + k_1} \tag{3.20}$$

When the minimum fold length, B', is four (five), each regular fold has one (two) contribution(s) to an OOOO sequence, but still contributes two DOOO sequences. Compared to the case of the minimum fold length of 3, the tetrad ratio of [OOOO]/[DOOO] is approximately increasing by 0.5 (1.0) for each A value.

Eq. (3.20) for q=.010, x=330, B'=3 gives the tetrad ratio of 0.85 (A=15) and 1.5 (A= 20). This is in agreement with the results calculated from eq. (3.12) (see Table 2).

Chapter IV

A QUANTITATIVE INVESTIGATION OF CRYSTALLINE 89%-TRANS-POLYBUTADIENE

4.1 INTRODUCTION

In Chapter II a series of polybutadiene (PBD) samples which contain about 1% cis- and 99% trans-units (99%-trans-PBD) were crystallized from solution, and the lamellas obtained were studied by surface epoxidation followed by C-13 NMR techniques. It was found that under the proper conditions, all and only the amorphous part of the crystals can be epoxidized and that both the crystalline stem length (A) and the fold length (B) can be obtained. It was also found that all the cis-units and chain ends can be epoxidized, therefore, must be rejected from the crystalline core. This fact leads to a correction of the fold length: $B' = B - q'A(A+B)/2$, where B' is the corrected fold length, and q is the cis-content. After this correction all the B' values are about 4 $\pm$1 monomer units. This result strongly favors the adjacent reentry mechanism.

To confirm this conclusion it would be the better to test a TPBD sample which doesn't contain any cis-component. In that case the measured fold length would be the real fold length. Nevertheless, it is difficult to

prepare an absolute trans-polybutadiene sample. The alternative way, then, is to test a higher cis-content TPBD sample. According to this idea a commercial TPBD sample which contains 89.5%-trans, 10%-cis, and 1.5%-1,2 additive components has been tested. This sample (latter, it will be called 89%-trans-PBD) has a molecular weight of 200,000, or ten times greater than that of 99%-trans-PBD. Thus, the use of this sample will also furnish a chance to examine any effect of the molecular weight.

As the cis content is increased in a cis/trans random copolymer, the probability of the presence of more than one cis units in a fold increases. This will cause the B' value from the simple correction formula : $B'=B-A(A+B)/2$ to deviate from real value. Therefore it is necessary to use the statistical treatment developed in Chapter III to find a B' value which should be valid for any cis content unlike the simple equation which is only valid at low cis content.

In this Chapter, a comparison of crystallinity as calculated from the statistical treatment with that obtained experimentally for 89%-trans-PBD crystals grown from solutions will be given. Results of surface epoxidation, differential scanning calorimetry, x-ray scattering and electron microscopy carried out on 89%-trans-PBD lamellas will also be reported. It was found in the course of this work that a small percentage of cis-units enter the crystalline core and that a gel structure can be formed. A discussions of these phenomena will be given.

4.2 EXPERIMENTAL

4.2.1 Polymer

The 89%-trans-PBD sample used here was kindly provided by GEN Corp., where it is called trans-4 rubber. The basic characters of 89%-trans-PBD sample are as follows: $\overline{Mn}$ =2.0×10^5 (corresponding to degree of polymerization, x_n, of 3700), $\overline{Mw}$ / $\overline{Mn}$ = 2.5, the fraction of cis-unit = .10, the fraction of 1,2 units = .015.

4.2.2 Crystallization

Single lamellas of 89%-trans-PBD were prepared from .05% (w/v) amyl acetate solution at 10 ℃, and in .05% diethylketone solution at 10 ℃ and 20 ℃ by the self-seeding procedure. Lamellar structures of 89%-trans-PBD were made at higher concentration in amyl acetate solution using concentrations of .1%, .3%, .7%, and 1%.

4.2.3 Density Measurement

These measurements were carried out as given in Chapter II.

4.2.4 Differential Scanning Calorimetry (DSC) Measurement

Completely dried unepoxidized and epoxidized 99%-trans-PBD and 89%-trans-PBD crystalline samples were subjected to DSC measurement using a DuPont 1090 instrument at a heating rate of 10 ℃/min. The melting point and the heat of fusion were calculated by the instrument's

computer.

4.2.5 Transmission Electron Microscopy (TEM)

Transmission electron microscopy were carried out on 89%-trans-PBD lamellas. The method has been described in Chapter II. All samples from 89%-trans-PBD were reacted with O_sO_4 prior to shadowing in order to prevent melting during that step. A smaller shadowing angle, α, was used with $tg\alpha = 1/4$.

4.2.6 X-Ray Scattering

X-ray scattering was carried out on the dried crystalline mats made from lamellas of 89%-Trans-PBD prepared from .05% and 1% amyl acetate solutions at 10°C and the mats of 99%-trans-PBD grown from .05% and 1% amyl acetate solutions. A Cu target, 32 mA, 40 kV and one-hour exposure were used.

4.2.7 Surface Epoxidation and C-13 NMR

Similar surface epoxidation and C-13 NMR techniques as described in Chapter II were employed . Due to a higher amorphous fraction in the 89%-trans-PBD lamellas, a higher mole ratio of meta-chloroperbenzoic acid to double bonds (MR) of 3 was selected.

4.3 RESULTS

4.3.1 Morphology

89%-trans-PBD can be crystallized only with an irregular overgrown lamellar morphology in dilute amyl acetate solution as shown in Fig 4.1. These lamellas are elongated with pointed ends and have about a 10 μ length and a 4 μ width. When crystallized in diethylketone solution at .05% concentration, single layers can be obtained as shown in Fig 4.2. The lamellar thickness of that preparation was estimated from the shadowing length as 11 nm (an average from six edge measurements).

A three dimensional gel structure can be formed when 89%-trans-PBD is crystallized from .7% and 1% amyl acetate solution at 10°C. Gelation can be easily judged by the naked eye. The critical concentration of gelation for 89%-trans-PBD in amyl acetate solution at 10 °C is between .3% and 0.7% (w/v). The lamellar nature of the gel is apparent from the transmission electron micrograph in Fig 4.3. As a comparison Fig 4.4 shows lamellas of 89%-trans-PBD crystallized from .3% amyl acetate solution at 10°C which is below the critical gelation concentration. The lamellas in this picture are isolated from each other.

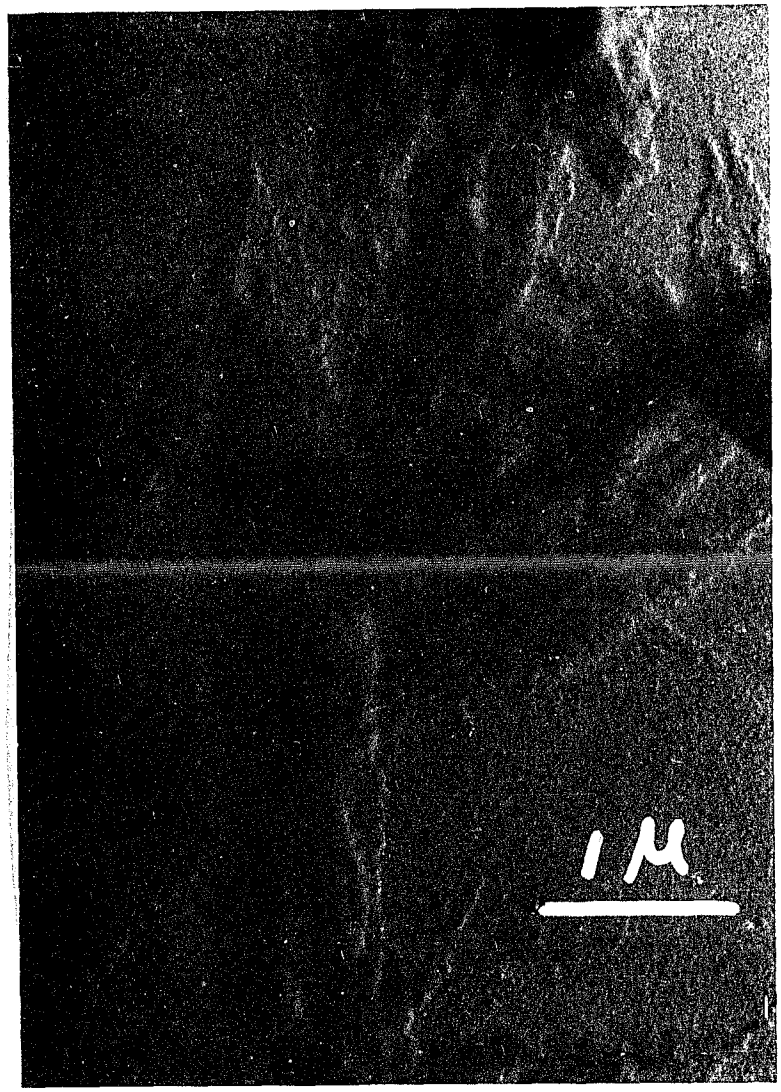

Fig 4.1 Transmission electron micrograph for 89%-trans-polybutadiene crystallized in .05% amyl acetate solution at 10 °C. The crystals are overgrown lamellas.

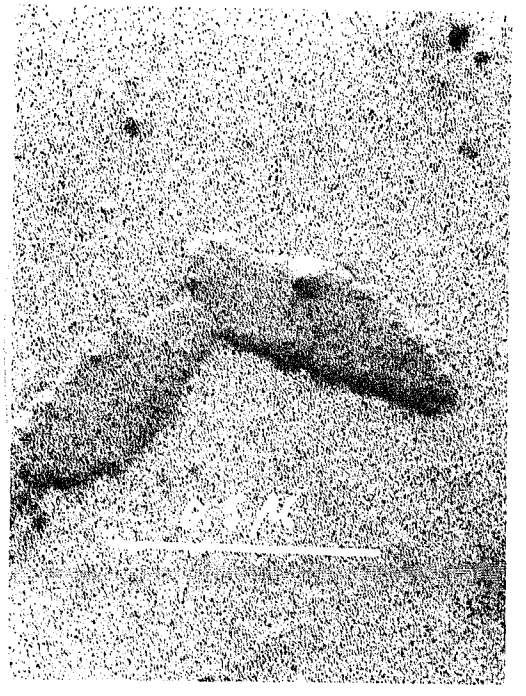

Fig 4.2 Transmission electron micrograph for 89%-trans-polybutadiene crystallized in .05% diethyl ketone solution at 10 °C. The crystals are manifested as single layers.

Fig 4.3 Transmission electron micrograph for 89%-trans-polybutadiene crystallized in 1% amyl acetate solution at 10 °C. The structure appears as connected lamellas.

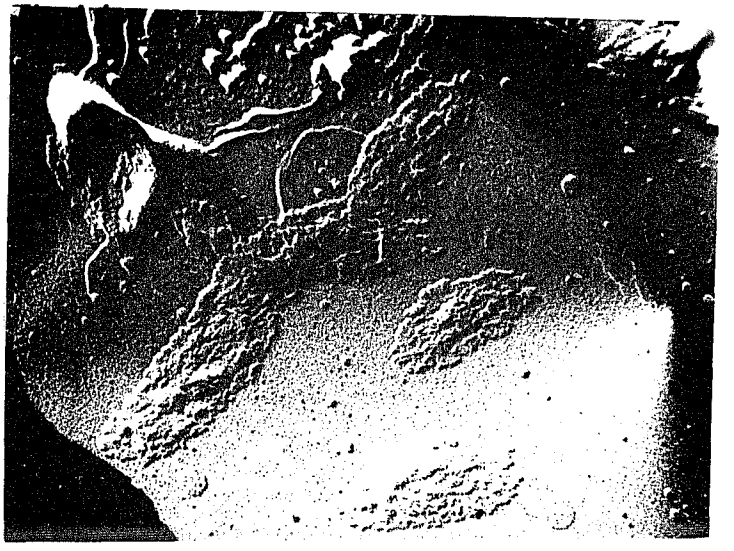

Fig 4.4 Transmission electron micrograph for 89%-trans-polybutadiene crystallized in .3% amyl acetate solution at 10 °C. The crystals are seperated each other.

4.3.2 Surface Epoxidation

4.3.2.1 Assignments

The C-13 NMR spectrum of unreacted 89% trans-PBD in solution is given in Fig 4.5 and shows the presence of trans-1,4, cis-1,4, and 1,2 components. Based on the work of Schilling et al. [57] and of Clouge et al [71], the spectrum can be assigned as given in Table 4.1. From the relative intensity of the C-13 NMR spectrum cis-1.4 and 1,2 contents are estimated as 10% and 1.5%, respectively.

Table 4.1

C-13 NMR Assignments for Polybutadiene

No. of Carbons	Chemical Shift (ppm)
01	43.6
02	38.3
03	34.4
04	30.3
05	114.6
06	142.9
07	128.7
08	131.5
09	130.8
10	130.0
11	32.7
12	130.0
13	27.4
14	129.4

The solution C-13 NMR spectrum for surface-epoxidized 89%-trans-PBD lamellas was obtained. The peaks at 114 and 143 ppm attributed to the olefinic carbons in a 1,2 unit in the unepoxidized polymer disappear in this spectrum, suggesting that all detectable 1,2 units are at the lamellar surfaces and can be epoxidized completely. The methylene part of this spectrum is given in Fig 4.6. The resonances are numbered according to the assignments in Table 4.1 and 4.2. It is observed that a small resonances at 27.4 ppm is still present. As assigned in Table 4.1, this resonance represents methylene carbon atoms between a trans and a cis unit. It is suggests that a small amount (about 5%) of the cis units are present in the crystalline core and are unavailable for a suspension reaction. The principal resonances that appear in the spectrum of the suspension-epoxidized product of 89% trans-PBD are associated with the trans-1,4 and cis-1,4 units. All of these assignments have been given previously. The resonances positions of various methylene carbon atoms are shown in Table 4.2.

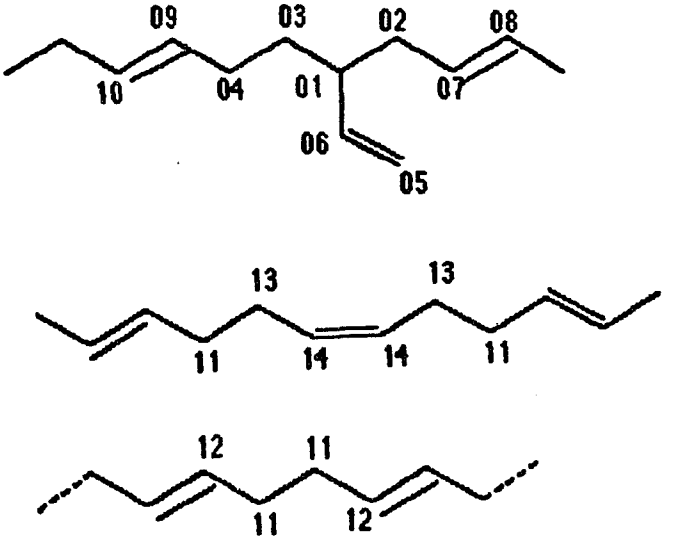

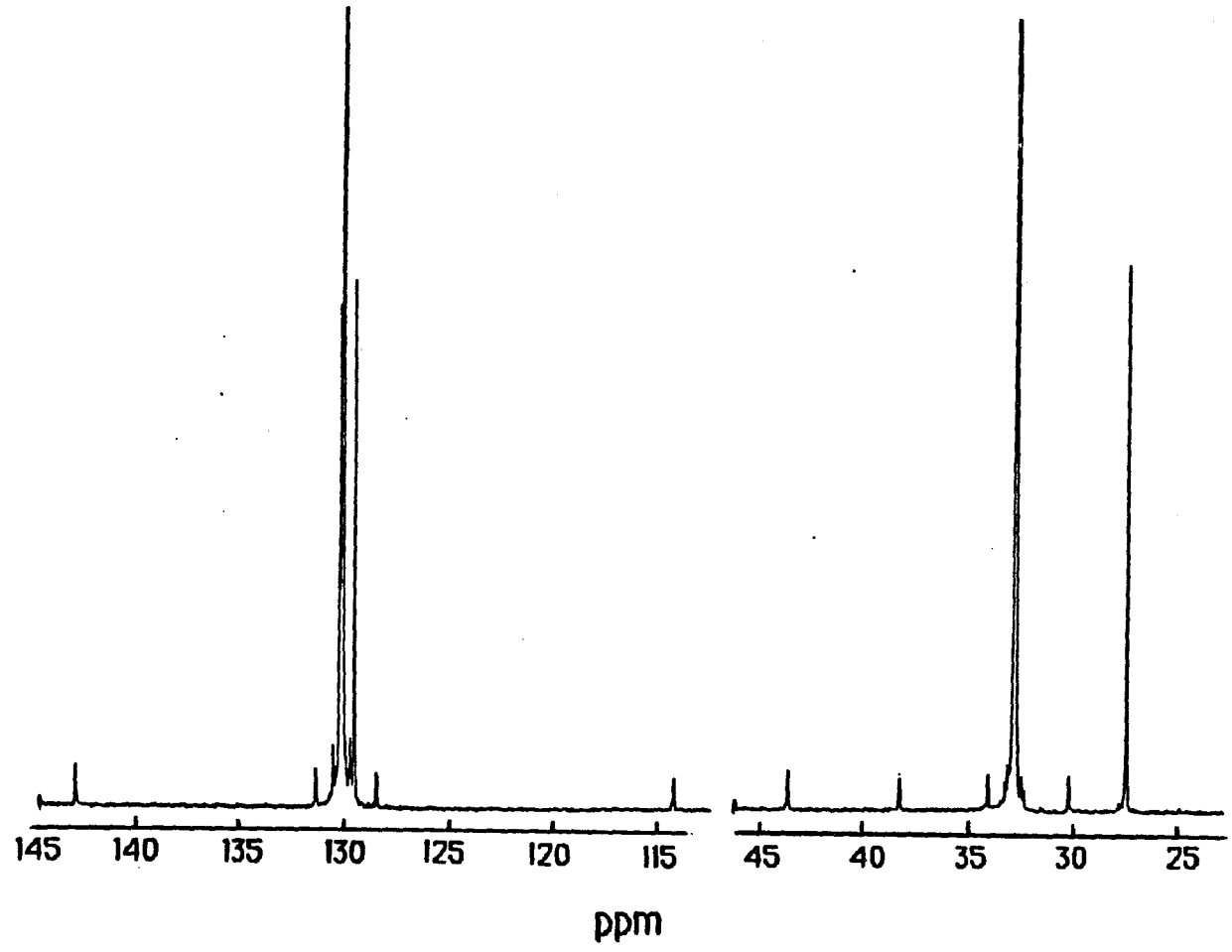

Fig 4.5 The cabon 13 NMR spectrum for unepoxidized 89%-trans-polybutadiene in DCl_3 solution at 50.32 MHz.

Table 4.2

Assingments of Methylene Carbons of Surface-Epoxidized Polyethylene

No. of Carbon	Position (ppm)
15	28.3, 28.8
16	29.0, 29.4
17	24.3, 24.7
18	29.0
19	32.2
20	29.8
21	28.0
22	25.3

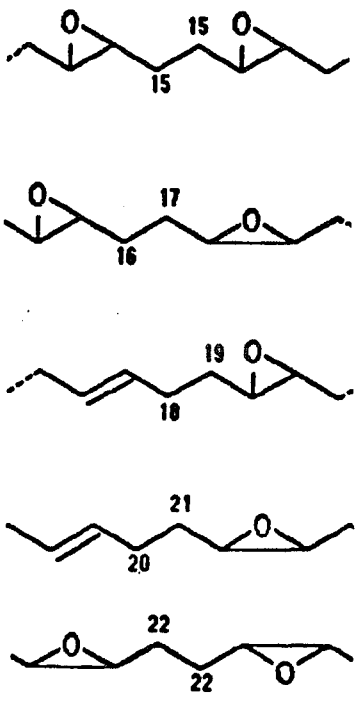

Small resonances at 23.9, 25.0, 25.8, 27.3, 27.8, 31.3 and 31.8 ppm are associated with epoxidized 1,2 units (carbon atoms 23-30, as shown below). These resonances have not been assigned and will not be used in the quantitative analysis given below. Since 1,2 units are present only to 1.5%, the error involved in ignoring them is small ($<3\%$ for A and B).

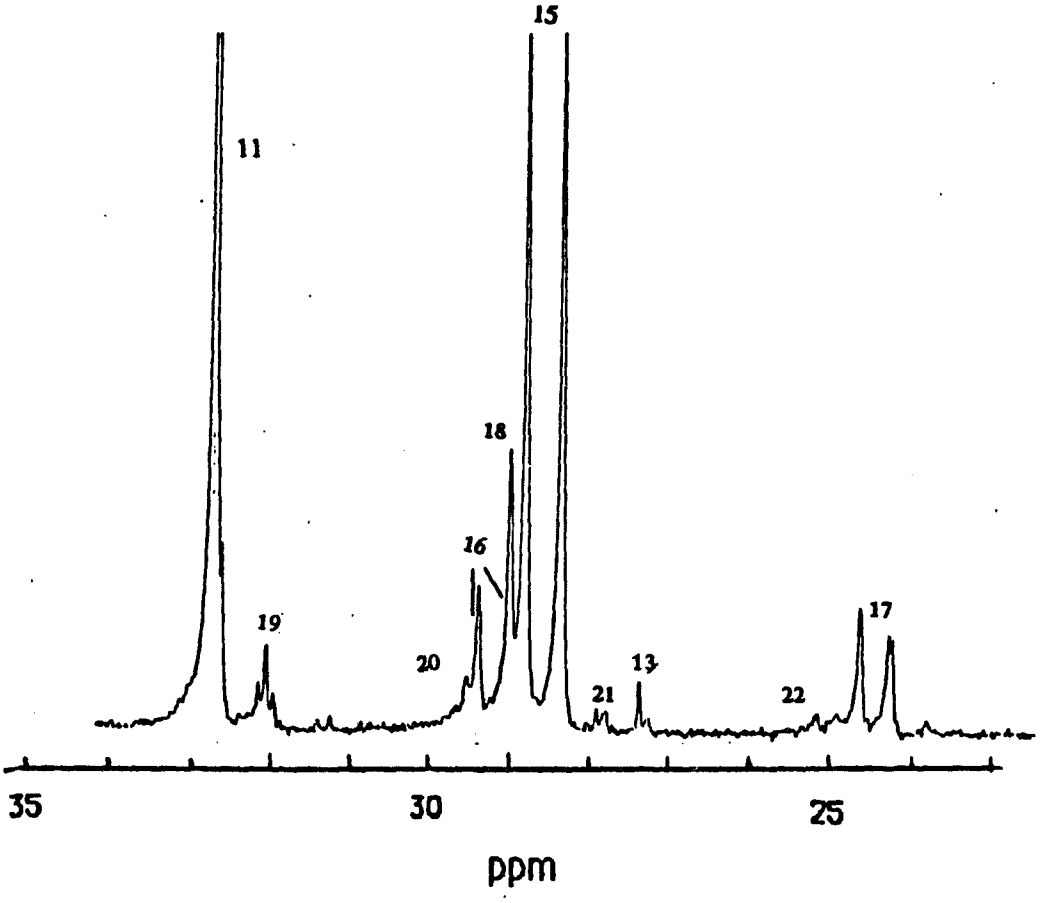

Fig 4.6 The cabon-13 NMR spectrum in CH_2 region for surface-epoxidized 89%-trans-polybutadiene in DCl_3 solution at 50.32 MHz.

4.3.2.2 Calculation of A and B

Based on the same principle as developed by Schilling et al [57] (See Section 2.3.2) along with the above assignments the crystalline stem length, A, the fold length, B, and the epoxidation fraction, fe, can be calculated by the formulas:

$$A = 1 + \frac{[11] + [13]}{[19] + [21] + [27]} \tag{4.1}$$

$$B = 1 + \frac{[15] + [16] + [17] + [22]}{[19] + [21] + [27]} \tag{4.2}$$

$$fe = \frac{B}{A + B} \tag{4.3}$$

where carbons 19, 21 and 27 are junction carbons between one unepoxidized trans-unit and one epoxidized trans-, epoxidized cis-, or epoxidized 1,2 unit. The quantitative value of [21] is about 1/4 of [19], and [27] is about 1/30 of [19], Therefore, ignorance of [27] doesn't make a big difference in formulas (4.1) and (4.2). Since the position of carbon 27 is unknown, in our latter calculation only [19] + [21] is used as junction intensity. There are two carbon atoms (18 and 19) that represent a junction between a trans-butadiene section and epoxidized trans-butadiene section, and two others (20 and 21) representing a junction involving an epoxidized cis-

butadiene. It is only necessary to use one of each pair in calculation of A and B; resonances 19 and 21 are chosen because there is no overlap of these with other resonances.

4.3.2.3 Equilibrium of Surface-Epoxidation

It was found that equilibrium of epoxidation of 89%-trans-PBD lamellas is reached after 12 days when suspended in amyl acetate containing MCPBA (at concentration of .01g/cm^3 and with mole ratio of MCPBA to double bond (MR) of 3). Table 4.3 lists the A, B and fe results as a function of reaction time. Fig 4.7 is the corresponding plot. The other epoxidation experiments have been carried out under the same conditions.

Table 4.3

Equilibrium of Surface Epoxidation

Rea. Time (Days)	A	B	fe
9	11	15	.57
12	11.5	15	.58
13	11.5	16	.58
14	10.5	15.5	.59
16	10.5	15.5	.59
20	10.5	16.0	.60

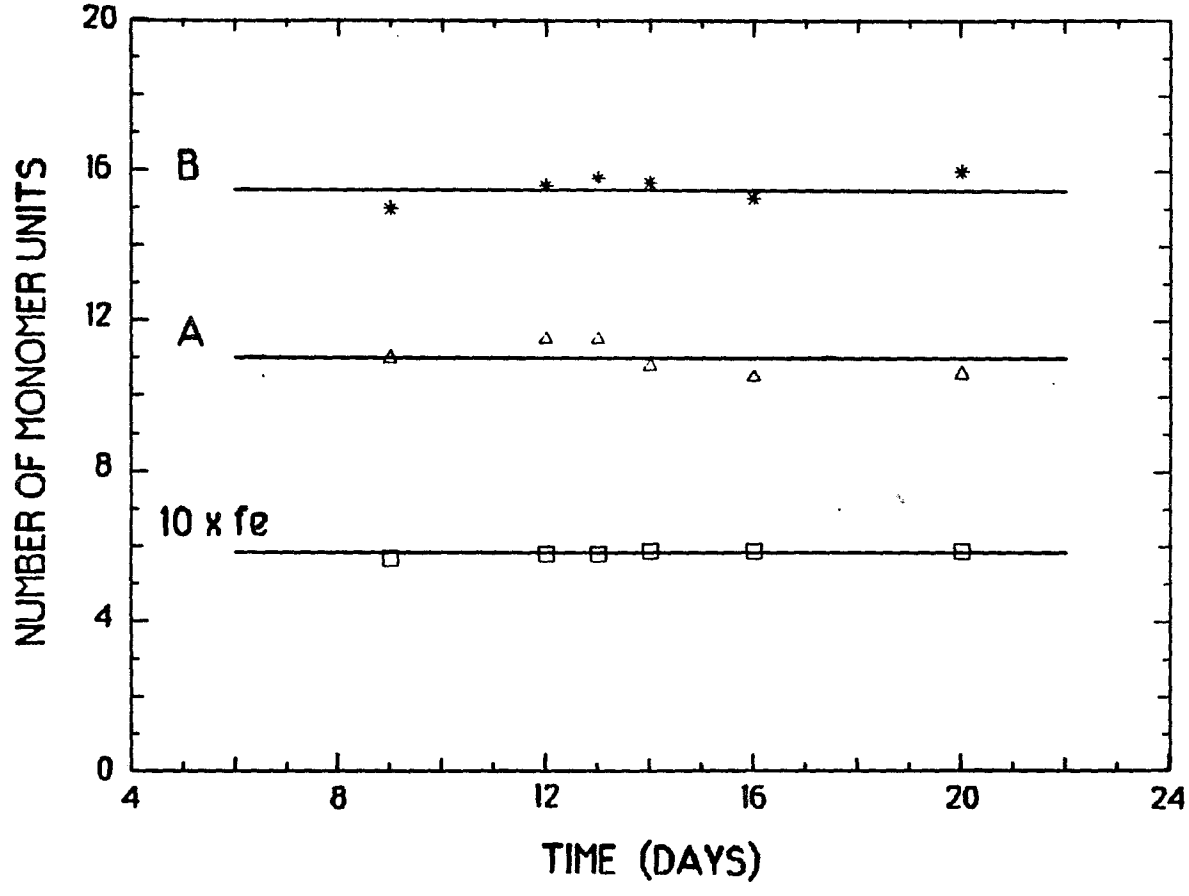

Fig 4.7 A, B and fe versus epoxidation time for 89%-trans-BPD. MR=3.0lybutadiene

4.3.2.4 Results of Surface-Epoxidation

The effects of crystallization concentration, solvent and temperature on the lamellar thickness and crystallinity of 89%-trans-PBD were investigated. The results for samples crystallized from amyl acetate solution at concentration of .05, .7 and 1% at 10°C and from .05% diethylketone at 10°C and 20°C are given in Table 4.4. For the five preparations considered, the A values are constant at 11 ± 1 monomer units, and the B values are constant at 16 ± 1 monomer units.

Table 4.4

Block Lengths from Surface Epoxidation

Crystallization Conditions.	A	B	fe
AA .05% 10°C	11	15.5	.59
AA .7% 10°C	12	16	.58
AA 1% 10°C	11.5	17	.59
DEK .05% 10°C	11	16	.59
DEK .05% 20°C	10.5	15	.59

AA, amyl acetate; DEK, diethylketone.

. The total lamellar thickness L can be estimated from A and fe through the formula (4.4).

$$L = RACOS\ \Theta\left(1 + \frac{f_e \rho_c}{(1 - f_e)\rho_a}\right) \tag{4.4}$$

where R is the repeat distance of the butadiene unit cell along the crystalline stem and is equal to 0.483 nm [39]; ρ_c is the density of the crystalline part of TPBD and is equal to 1.03 g/cm^3; ρ_a is the density of the amorphous part of 89%-trans-PBD; and Θ is the tilt angle of the molecular chain with respect to the lamellar surface, is equal to 114°.

Putting A = 11, fe = 0.59, and ρ_a =.874 g / cm^3 which is the the density of the amorphous part of pure TPBD, L is about 13 nm, which is 20% greater than that of 11 nm found from shadowing length measurements on the electron microscope picture as discussed in Section 4.3.1. Due to the usual inaccuracies in calculating the thickness from shadowing length, it is believed that the result obtained from epoxidation and C-13 NMR are more accurate. However the ρ_a value of .894 g/cm^3 used in this calculation is the density of the amorphous part of the pure trans-polymer. The ρ_a of 89%-trans-PBD is unknown.

4.3.3. X-Ray Scattering

X-ray scattering was carried out on the 89%-trans-PBD single crystal mats and dried gel to see whether there is a difference in their crystalline structure. Fig 4.8 provides a comparison, where (c) and (d) are corresponding x-ray scattering pattern of the single crystal mats and the gel. The patterns in (a) and (b) are for powder x-ray scattering pictures of single crystal mats and their lamellar aggregates of 99%-trans-PBD. There is no significant difference between (a), (b), (c) and (d).

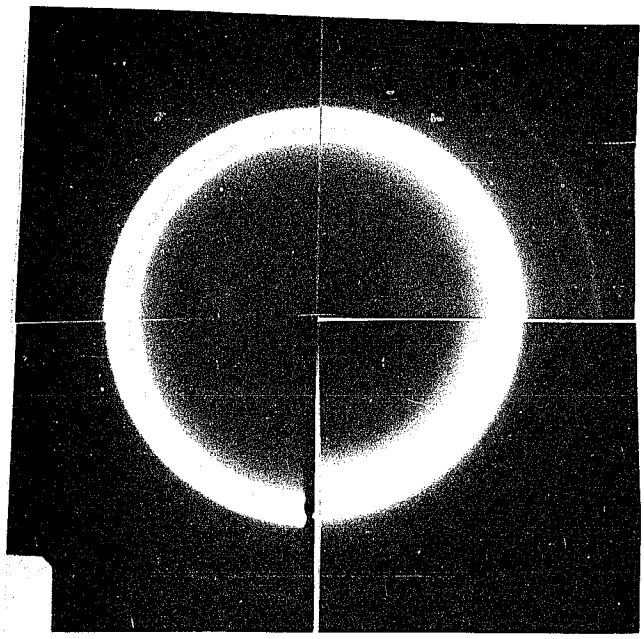

(a)	(b)
(c)	(d)

Fig 4.8 Pattern of x-Ray Scattering
(a) single crystal mat of 99%-trans-PBD, (b) dried gel of 99%-trans-PBD
(c) single crystal mat of 89%-trans-PBD, (d) crystal aggregate of 89%-trans-PBD

4.3.4 Results of Density Measurements

Table 4.5 gives the results of density measurements. Within an experimental error of ± 0.003 g/cm^3 the density of the various preparations are the same. Since there is no available ρ_a data for 89%-trans-PBD, the crystallinity can not be evaluated from the density measurements. If as ρ_a the value of 0.874 g/cm^3 is used, this being the value for 100% trans 1,4 polybutadiene in the amorphous state, the crystallinity from the density measurement is about .49-.54.

Table 4.5

Results of density Measurement

Crystallization Conditions	Density (g / cm^3)	Crystallinity
AA .05% 10°C	.947	.51
AA .05% 10°C	.944	.49
AA 1% 10°C	.944	.49
DEK .05% 10°C	.947	.51
AA .05% 10°C	.949	.50
AA .1% 10°C	.951	.53
AA .3% 10°C	.950	.52
AA .7% 10°C	.950	.52
AA 1% 10°C	.951	.53

AA, amyl acetate; DEK, diethylketone.

4.3.5 DSC Measurement

The DSC technique was used to further compare the single lamellas with the dried gel of 89%-trans-PBD. Fig 4.9 (a) and (b) are two representative DSC plots, plot (a) is for the single crystal mats of 89%-trans-PBD and plot (b) is for the dried gel. Both of them have two clear endotherms. One is for the crystal-crystal transition, and the other is for melting. In Table 4.6 all the results of single crystal mats and gel, and their epoxidized products of 89%-trans-PBD are represented. Table 4.6 shows that there is no difference in the thermal properties between the single crystal mats and the dried gel of 89%-trans-PBD. However, when compared to the thermal properties of the single crystal mats of 99%-trans-PBD, the 89%-trans-PBD crystal mats have much lower T_{tr}, T_m and ΔH_m. This might be attributed to the entering of a small amount of cis-units into the crystalline core as found in C-13 NMR spectrum. It is interested to point out that the epoxidized samples have a much higher T_m and ΔH_m. This will be discussed in Section 4.4.4.

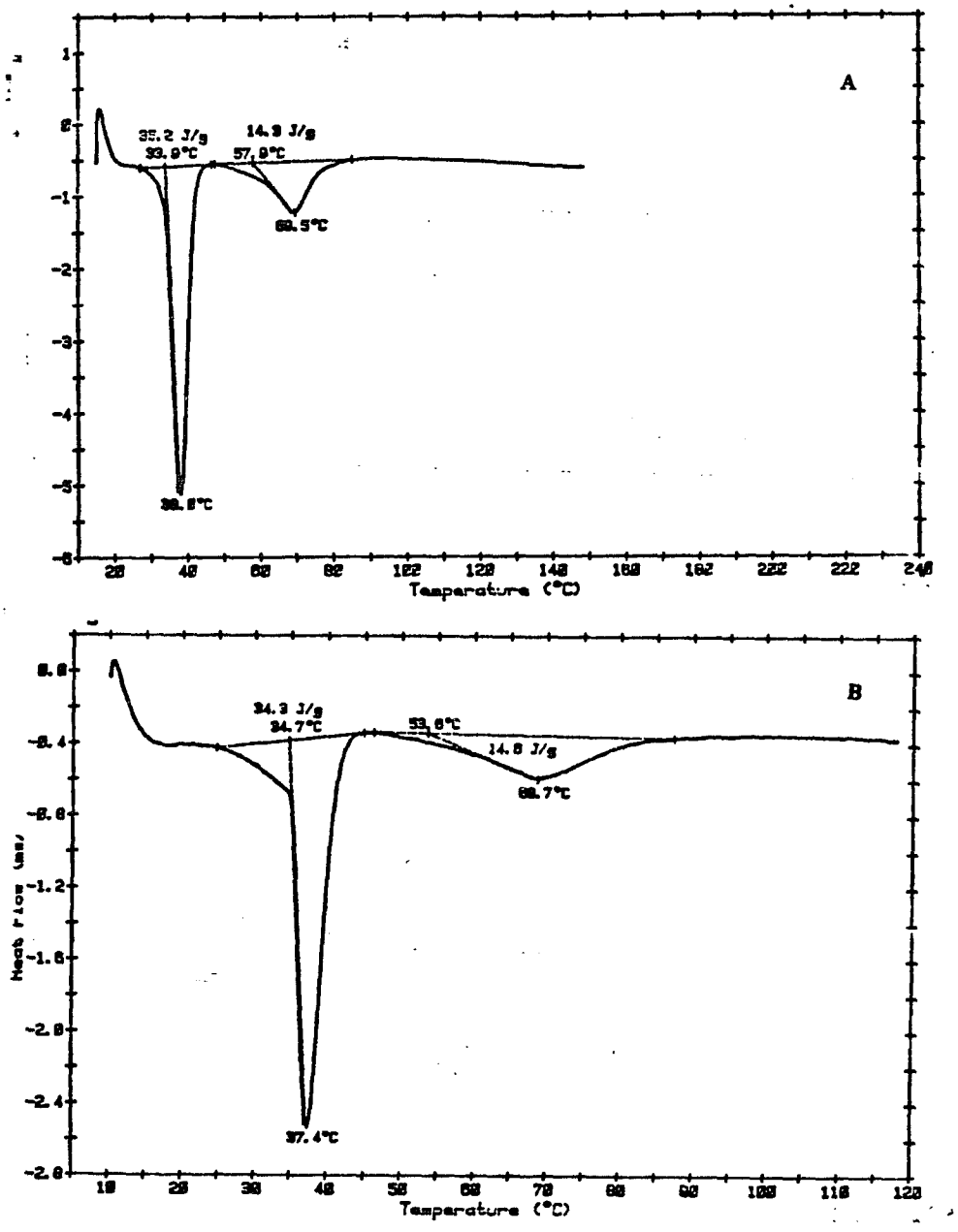

Fig 4.9 Differential scanning calorimetry plots for single lamellar mats and dried gel of 89% trans-polybutadiene. (a) single lamellar mats. (b) dried gel.

Table 4.6

Results of DSC Measurements on Polybutadiene

Sample	Crys. Conds.	*Ttr* °C	ΔH_{tr} (j/g)	T_m °C	ΔH_m (j/g)
99%-trans	.05%, 30°C	54	57	130	48
-PBD	1%, 30°C	53	57	130	49
89%-trans	.05%,10°C	38	35	69	15
-PBD	1%, 10°C	37	35	69	15
epozd. 89%-	.05%, 10°C	36	18	89	22
trans-PBD	1%, 10°C	36	15	88	25

4.4 DISCUSSION

4.4.1 Crystalline Stem Length

From the results of surface epoxidation/NMR analysis it is known that both A and B values remain constant for the lamellas of 89%-trans-PBD, independent of the crystallization temperature, solvent and concentration (See Table 4.4). Similar behavior was observed for 99%-trans-PBD when crystallized from .05% amyl acetate at 20°C and lower (15°C and 10°C) with a value of 19 monomer units being obtained. One possible

cause of this phenomenon is that the supercooling is large as has been observed for other polymers [74], and the crystalline thickness reaches a limited value. Another more likely explanation is that the crystalline stem length is determined by the segment length when it is much shorter by kinetic factors, and is approximately equal to the most probable sequence length (the sequence length is defined as the number of monomer units between two successive noncrystallizing units, i.e, cis units, 1,2 units and chain ends). In Chapter III the probability of a segment with i trans units is given as $p^i(1-p)$, where p is the probability of trans units. Therefore, the length weighted probability of the segment with i trans-units is $ip^i(1-p)$. The maximum of that probability gives x_m = - 1/ln(p). For 89% trans-PBD, x_m is calculated as 9, a value in reasonable agreement with the A value of 11 $\pm$ 1 monomer units. The average segment length is 1/(1-p), which is 9 monomer units also.

4.4.2 Crystallinity and Cis-Content

The B value of 89%-trans-PBD of 16 is significantly higher than that found for 99%-trans-PBD (5-9 monomer units depending on the crystallization temperature and solvent). This increase in B is due to the increase in cis (1,2)-content. The rejection of most cis units and all 1,2 units leads to rejection of some trans-units adjacent to the cis (1,2) units.

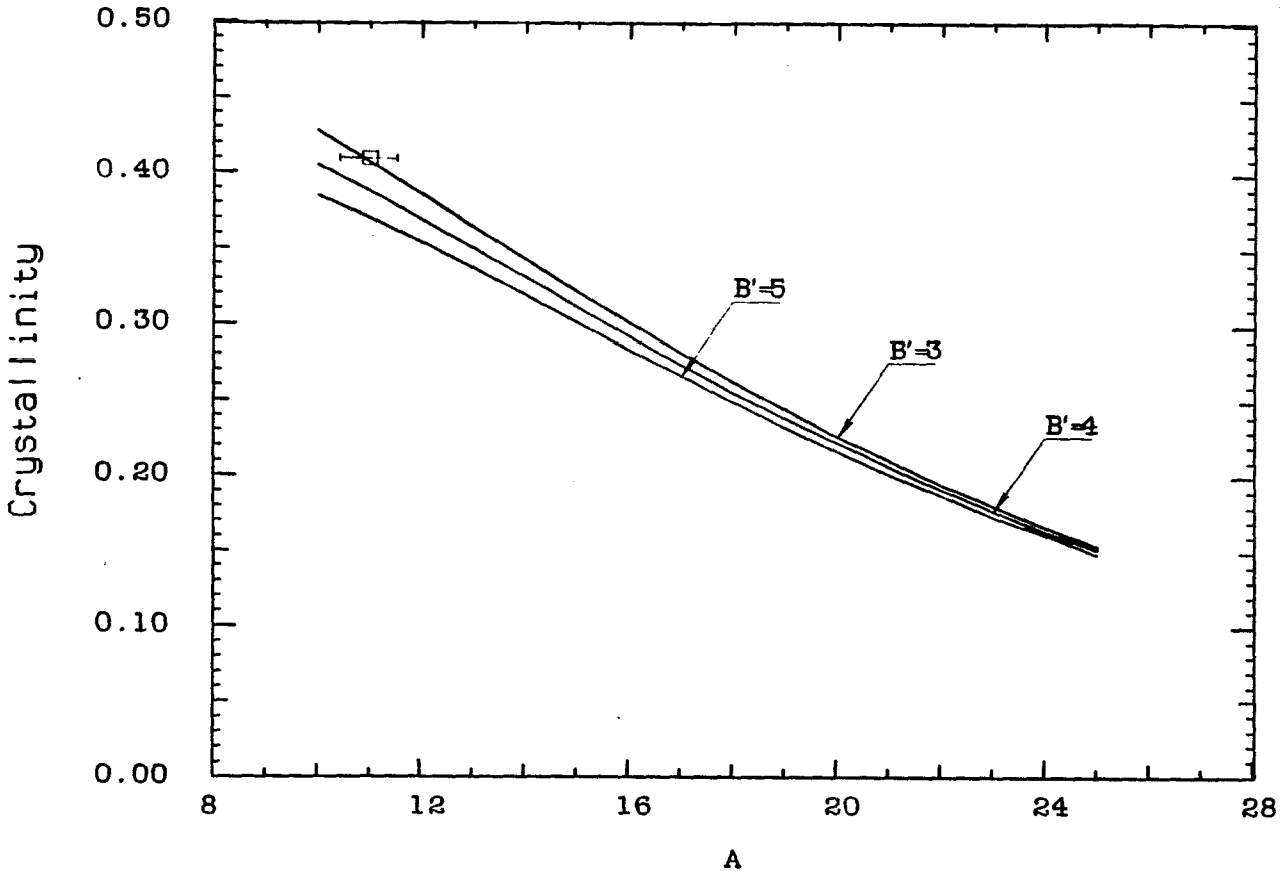

Fig 4.10 A comparison of the calculated and experimental crystallinity

An increase of B means a decrease in crystallinity. It is interesting to compare the results for 89%-trans-PBD with those from the statistical treatment established in Chapter III. For 89%-trans-PBD in addition to the cis-units there are 1.5% 1,2 units. C-13 NMR spectra showed that about 1/20 of the total cis-units remain in the crystalline core. The total equivalent cis-content, therefore, is (1−1/ 20)×10% + 1.5% =11%. Due to high molecular weight, the contribution from chain ends can be ignored. In Fig 4.10 a set of theoretical curves of crystallinity versus A with minimum fold length B' of 3, 4 and 5, the q' of .11 and degree of polymerization of 3700 are compared with the experimental point (A=11, 1-fe = .41). As it is believed that all and only monomer units in the amorphous part can be epoxidized, 1-fe is equal to the crystallinity. The best agreement with the theoretical curves is for B' = 3. This result for a relative high cis/high molecular weight polybutadiene agrees well with those value for samples with a cis-content and molecular weight about 10 times lower. Again this result favors the adjacent reentry mechanism.

4.4.3 Gelation and Fold Length

As was discussed in Sections 4.3.3 gelation takes place when concentration of 89%-trans-PBD solution in amyl acetate at 10°C is greater than 0.7%. X-ray scattering, surface epoxidation, density and DSC results showed that these polymer has the same crystalline structure, same crystalline stem length, and same crystallinity above and below the critical

concentration for gelation. The TEM pic ture (Fig 3 (b)) manifests that the gel is made up of connected multilayers. When the concentration of solution is smaller than 0.7%, only separated multilayers can be found. At this point our research supports Mandelkern's view that "the structural basis for gel formation by crystallization mechanism become clear" [78]. Based on our limited evidence a possible mechanism of gelation is "fold entanglement" of different lamellas as depicted in Fig 4.11.

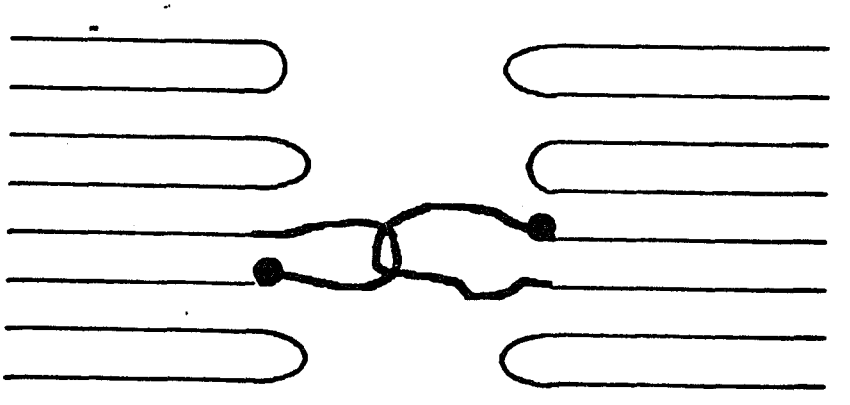

Fig 4.11 A schematic representation of fold entanglement

If on the average each lamella (or each multilayer) has more than two fold entanglements the whole system will become a three dimensional network.

This mechanism is proposed, first, because there is some kind of linkage in a three dimensional network. Second, this mechanism can explain the weak dependence of critical gelation concentration on molecular weight. As Damzy et al [78] indicated $c^* \approx M^{-a}$, where c^* is the critical gelation concentration, M is molecular weight, and a is a fractional number. The range of a-value is about 0.2-0.3 for lower molecular weight, it becomes even smaller for higher molecular weight samples. From the view of the fold entanglement mechanism, lamellas consisting of low molecular weight chains have a higher percentage of cilia which are unavailable to form fold entanglements, thus, a higher critical gelation concentration is needed. A simple consideration gives a cilia correction of critical gelation concentration for samples with higher cis-content: $c^* \approx c_0 \times \frac{\frac{x}{(A+B)}}{(2+\frac{x}{(A+B)})} = c_0(1-\frac{2(A+B)}{x})$, where c_0 is the critical gelation concentration of molecular chains with infinite molecular weight. This expression gives a weak dependence of the critical gelation concentration on the molecular weight, and a trend that the higher the molecular weight, the weaker the dependence. Third, It furnishs a reason why 89%-trans-PBD forms a gel structure easier than the 99%-trans-PBD. Even with a = 1/2 $c^* \approx M^{-1/2}$ the critical gelation concentration for 99%-trans-PBD should be $0.7\% \times (3700/330)^{1/2} \approx 2\%$. However, up to 5% concentration at 10°C, there is not any gel formed for this sample. The two samples differ in their fold length as well as in molecular weight. The average

fold length of 99%-trans-PBD lamellas is much shorter (5-7monomer units versus 15-17monomer units for 89%-trans-PBD) due to the low cis-content, which sharply decreases the possibility of fold entanglement in the former. If the probability of forming a fold entanglement is proportional to the area enclosed by that fold, the entanglement density will be proportional to the square of the fold length. Therefore, gelation takes place much more easily in 89%-trans-PBD solution.

This proposed mechanism appears to conflict with the experimental results for polyethylene, for which the critical gelation concentration increases with the content of short branches [78]. The answer might be that for polyethylene each branch decreases the effective area enclosed by the fold. On the other hand, the cis-content in TPBD lets the folds become large, but doesn't affect the fold effective area (See Fig 4.12).

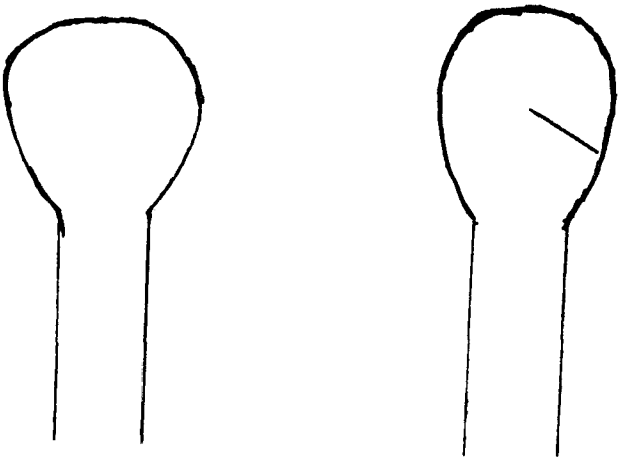

Fig 4.12 The effective area enclosed by folds with or without branch

4.4.3 Submerged Cis-Units and Its Effects

From C-13 NMR before and after surface epoxidation, it was found that about 1/20 total cis-units enter the crystalline core for 89%-trans-PBD crystals. This is not in disagreement with the earlier conclusion that all cis-units are rejected from the crystalline core for the 99%-trans-PBD sample. For that sample one twentieth of the cis content is too low to be detected. However, in 89%-trans-PBD lamellas this small amount of cis-untis submerged in the crystalline part may have a significant effect on the thermal properties. Table 4.6 showed that the transition temperature T_{tr}, melting point T_m, ΔH_{tr} and ΔH_m of 89%-trans-PBD crystals are much lower than that for 99%-trans-PBD crystals. This is because of the shorter crystalline length and the existence of submerged cis-units. Sanchez and Eby provided a theoretical basis for crystallization of a random copolymer [79]. The formula developed by them to calculate the melting point depression is as follows:

$$1/T_m^0 - 1/T_m = -\frac{R}{\Delta H^0}\left[\epsilon\frac{X_c}{RT_m} + (1-X_c)ln\left(\frac{1-X_c}{1-X}\right) + X_c\, ln\left(\frac{X_c}{X}\right)\right] \qquad (4.5)$$

T_m^0 is the melting point for the homopolymer crystal,

T_m is the melting point for the copolymer crystal,

ΔH^0 is the heat of fusion of a perfect crystal,

ϵ is the mixture energy,

X_c is the fraction of the second component in the crystalline part,

X is the total fraction of the second component, and

R is the gas constant.

Even putting $\epsilon = 0$, a cis-content, X_c, of .013 (It is calculated by the fraction of cis-units in the crystalline core ($1/20 \times 0.10 = .005$) divided by the crystallinity of .41) will shift the melting point about 20°C.

Another significant point of Table 4.6 is that the surface-epoxidized 89%-trans-PBD crystals have higher T_{tr}, T_m and higher ΔH_m. It was found that by using 3.72 kJ/mole as $\Delta H_m{}^0$ [47] the crystallinity calculated from heat of fusion is about .20 for unepoxidized crystals and about .40 for the epoxidized crystals. In converting the units for heat of fusion for surface-epoxidized 89%-trans-PBD from (j/g) to (j/mole), an average mole weight of 63.5 is used, This is calculated from $54 \times .41 + 70 \times .59$, where 54 and 70 are molecular weights of epoxidized and unepoxidized butadiene, and .41 and .59 are their number fractions from the surface epoxidation results. The crystallinity of .40 for surface-epoxidized 89%-trans-PBD lamellas calculated from the heat of fusion is very close to the result of (1-fe) from surface epoxidation. A possible explanation of this agreement is that most of the rejected cis-units reenter the crystalline core at higher temperature, which leads to lower T_{tr}, T_m, and ΔHm, but epoxidation blocks this reentering process, keeping the crystalline part unchanged. If the above explanation is accepted it can explain other facts such as the

high temperature crystalline form of TPBD having higher crystallinity [39], a shorter and tighter fold [39], [41] and less mobile portions [42]. Eng and Woodward measured the mobile fraction of polybutadiene single crystal mats in CS_2 by broad-line NMR technique [42]. They found that for two preparations after annealing at 80 °C the mobile fraction of TPBD lamellas decreases significantly (from 23% to 8.7% for one preparation and 13% to 7.6% for another). Since the transition temperature of the two crystalline forms is about 70 °C, after annealing at 80°C TPBD lamellas exist in the high temperature crystalline form. Using an IR technique Tomo-O Oyama [42] found that the low temperature crystalline form has a fold length of 5 monomer units, and for the high crystalline form it becomes 3 monomer units. The latter result is in agreement with our conclusion.

4.5 CONCLUSIONS

The technique of surface epoxidation followed by C-13 NMR analysis showed that the lamellas prepared using a polybutadiene containing 10% cis-, 88.5% trans- and 1.5% 1,2- units and grown from solution under different crystalline conditions have the same crystalline stem length of 11 monomer units and the same crystallinity of 41%.

Calculation of the crystallinity using the statistical treatment proposed in the previous chapter yields a value of three monomer units for

the minimum fold length, B', in agreement with the values obtained for 1% cis- and 99% trans-polybutadiene. This result strongly favors adjacent reentry folding.

Polybutadiene containing 10% cis, 88.5% trans and 1.5% 1,2 units forms a gel structure in amyl acetate solution at 10°C with the critical concentration between 0.3- 0.7% (w/v). X-ray scattering, density, DSC, and surface epoxidation showed that the gel and single lamellas have the same crystalline structure, same crystalline stem length, and same crystallinity. Transmission electron microscopy established that the gel is a connected lamellar structure. Based on the average fold length of 16 monomer units for 89%-trans-PBD, a "fold entanglement" mechanism of gelation is proposed.

About 5% of the cis units in 10% cis-containing polybutadiene enter the crystalline core of the lamellas. This leads to a much lower transition temperature, melting point and enthalpy of fusion than that measured for the polybutadiene sample with 99% trans- and 1% cis- units.

CONCLUSIONS AND SPECULATIONS

The results from Chapter II to Chapter IV are consistent with each other. For 99%-trans-PBD the results from different methods (surface epoxidation, density measurement and electron microscopy) are comparable, and two kinds of treatments (the statistical treatment and the simple cis-content correction) are in agreement. The both polybutadiene samples (99%- and 89%- trans-BPD) and the two quantities (the crystallinity and the tetrad ratio) give the same minimum fold length. Therefore, the conclusions obtained from this research are believed reliable.

The basic technique, surface epoxidation followed by C-13 NMR analysis, seems to be a relatively accurate one. Under favorable conditions, the quantities of A, B and fe can be evaluated with a relative error smaller that 5%.

From the result that the minimum fold length of both 99%- and 89%- trans-polybutadiene is about three to four monomer units, it is believed that solution grown lamellas of trans-polybutadiene do have predominantly tight adjacent folds. Unfortunately, the technique of surface epoxidation cannot be used to investigate melt crystallized trans-polybutadiene, due to crosslinking and the difficulty in completing the reaction. Also this method is unavailable to most other polymers.

The established statistical treatment, however, seems workable not only for trans-polybutadiene. For any systems with data of crystallinity,

crystalline stem length, equivalent "impurity" content, it can be used. A wide comparison of this model with other systems might lead to valuable conclusions.

It is worth trying to conduct a similar research for an absolute trans-polybutadiene. More convincing results could be expected from the tests of this sample. Even a sample which has cis-content smaller than .3% will be very helpful in confirming the tight adjacent reentry folding.

It seems that a research on TPBD lamellas using the technique of surface hydrochlorination followed by C-13 NMR is valuable. This technique is proven effective for TPI lamellas [62]. Due to the disappearing of the diasteroisomers caused by the epoxidized sequences the C-13 NMR spectrum of surface hydrochlorinated TPBD will become simpler.

The proposed fold entanglement mechanism for gelation is attractive, but only is based on limited experimental evidence. It could be verified by a systematical investigation of the effect of cis-content on critical gelation concentration. For example, a plot of critical gelation concentration versus cis content for a set of TPBD samples which contain no 1,2 units and have similar molecular weights will provide a quantitative verification for the mechanism.

APPENDIX I

The Program for the Calculation of the Crystallinty and the Tetrad ratio

```
      real k1,k2
      integer a,b,c
      dimension rc(60),r(60),s3(60),s4(60),s0(60)
      dimension s01(60),s02(60),s03(60),s431(60),s432(69)
      dimension s31(60),s32(60),s331(60),s332(60),s41(60),s42(60)
      l=350
      p=.990-1.0/float(l)
      b=3
      k1=1.0/(1.0+(1-p)*float(l))
      write(6,30)
30    format(' The Calculation of [OOOO]/[DOOO] and crystallinity ' )
      write(6,40)p,l,b
40    format(1x,'p=',f5.3,4x,'x=',i4, 'B', 2x, i4)
      s=0
      do 50 i=1,l
50    s=s+p**(i-1)*float(i)*(1-p)
      do 150 a=1,50
```

```
      c=a+b
      m=1/c
      k2=float(a)/float(c)
      s01(a)=0
      s02(a)=0
      s03(a)=0
      s31(a)=0
      s32(a)=0
      s331(a)=0
      s332(a)=0
      s41(a)=0
      s42(a)=0
      s431(a)=0
      s432(a)=0
      do 100 i=1,m
      do 80 j=0,c-1
      s01(a)=s01(a)+p**(i*c-b+j-1)*float(i)*(1-p)
      do 70 n=1,b-1
70    s02(a)=s02(a)+p**(i*c-b+j+n-1)*float(i)*(1-p)/(b-1)
      do 75 n=0,a-1
75    s03(a)=s03(a)+p**(i*c-b+j+n-1)*float(i)*(1-p)/a
      do 80 n=3,a-1
      s331(a)=s331(a)+p**(i*c-b+j+n-1)*(1-p)
80    s431(a)=s431(a)+p**(i*c-b+j+n-1)*float(n-3)*(1-p)/a
```

```
      do 98 j=3,c-1
      s31(a)=s31(a)+p**(i*c-b+j-1)*(1-p)
      s41(a)=s41(a)+p**(i*c-b+j-1)*float(j-3)*(1-p)
      do 94 n=1,b-1
      s32(a)=s32(a)+p**(i*c-b+j+n-1)*(1-p)/(b-1)
94    s42(a)=s42(a)+p**(i*c-b+j+n-1)*(j-3)*(1-p)/(b-1)
      do 98 n=0,a-1
      s332(a)=s332(a)+p**(i*c-b+j+n-1)*(1-p)/a
98    s432(a)=s432(a)+p**(i*c-b+j+n-1)*float(j-3)*(1-p)/a
100   continue
      s0(a)=k1*s03(a)+(1-k1)*(k2*s01(a)+(1-k2)*s02(a))
      s3(a)=k1*(s331(a)+s332(a))+(1-k1)*(k2*s31(a)+(1-k2)*(s32(a)))
           +2*s0(a)-2
      s4(a)=k1*(s431(a)+s432(a))+(1-k1)*(k2*s41(a)+(1-k2)*(s42(a)))
      rc(a)=a*s0(a)/s
150   r(a)=s4(a)/s3(a)
170   continue
      write(6,200)
200   format('A',4x,'An',4x,'N3',4x,'N4',4x,'Se',4x,'Cry',4x,'Cry*',4x,'r',4x,'r*')
210   write(6,220)a,s0(a),s3(a),s4(a),s,rc(a),rc1(a),r(a),r1(a)
220   format(6x,i7,2x,8f8.3)
      stop
      end
```

Explanation

a is A;

b is B;

q is q;

x is x;

rc is the Crystallinity;

r is the tetrad ratio;

s0 is the segment length;

s1 is the length of the crystalline part of segment;

s3 is the number of DOOO sequences per segment;

s4 is the number of OOOO sequences per segment;

s11, s12, s13 are s1 in the three kinds of segments;

s31, s32, s33 are s3 in the three kinds of segments;

s41, s42, s43 are s4 in the three kinds of segments;

s331 and s332 (s431 and s432) are two parts of s33 (s43) from the tail and head parts when the head of a segment is a chain end, respectively.

REFERENCES

[1] Keller, A., Phil. Mag., 1957, V8, 1171

[2] Fischer, E.W., Naturforsch Z., 1957, V12A, 753

[3] Till, P.H. J. Polym. Sci., 1957, V24, 301

[4] Geil, P.H., J. Polym. Sci., 1960, V44, 449

[5] Blackadder, D.A., J. macromol. Sci., Rev., Macromol. Chem., 1967, VC1, 297

[6] Geil, P.H., Polymer, 1963, V4, 404

[8] Reneker, F. and Geil, P.H., J. Macromol. Sci., 1973, VB7, 1

[9] Padden, F.J., and Keith, H.D., J. Appl. Phys., 1965, V36, 2987

[10] Eppe, R., Fischer, E.W., and Stuart, H.A., J. Polym. Sci., 1959, V34, 721

[11] Kabayashi, K., Kaguka (Chem) 1962, V8, 203

[12] Bunn, C.W., Cobold, A.J., and Palmer, R.D., J. Polym. Sci., 1958, V28, 365

[13] Geil, P.H., J. Polym. Sci., Part VA2, 3813

[14] Wunderlich, B. "Macromolecular Physics", Academic Press, New York, 1973

[15] Khoury, F. and Passaglia, E., "The Morphology of Crystalline Synthetic Polymers", Chapter 6, in Hannay Ed. "Treatise on Solid State Chemistry" vol. 3, Plenum Press, New York, 1976.

[16] Bassett, D.C. Frank, F.C. and Keller, A., Nature, 1964, V184, 801

[17] Reneker, D.H., and Geil, P.H., J. Appl. Phys., 1960, V31, 1916

[18] Lindenmeyer, P.H., J. Polym. Sci., 1963, VC1, 5

[19] Lauritzen, J.I.Jr. and Hoffman, J.D., J. Res. Nat. Bur. St., 1959, V64A, 73

[20] Lauritzen, J.I.Jr. and Hoffman, J.D., J. Chem. Phys., 1959, V31, 1680

[21] Price, F.P., J. Chem. Phys., 1959, V31, 1679

[22] Mandelkern, L. J. Polym. Sci., Symposium, No. 50, 1975, 457

[23] Fischer, E.W., Lorenz, R., Kolloid Z. U. Z. Polymer, 1972, V25, 1094

[24] Jackson, J.B., Flory, P.J., and Chiang, R. Tran.
Faraday Soc., 1963, V59, 1906

[25] Lauritzen, J.I.Jr. and Hoffman, J.D., J. Appl. Phys., 1973, V44, 4340

[26] sadler, D.M. and Keller, A., Macromolecules, 1977, V10, 1128

[27] Calvert, P. Nature, 1976, V263, 371

[28] Flory, J.P., and Yoon, D.Y., Nature, 1976, V272, 226

[29] Guenet,, J.M, Macromolecules, 1980, V13, 387

[30] Williams, J., Blundell, D.J., and Keller, A., and Word, I.M, J.
Polym. Sci., 1967, Part A2, V6, 162

[31] Williams, J., Blundell, D.J., and Keller, A., and Word, I.M, J.
Polym. Sci., Part A2, 1967, V6, 1613

[32] Bank, M.I., and Krimm, S., J. Polym. Sci., Part A2, 1967, V7, 1785

[33] Ching, J.H.C., and Krimm, S., J. Appl. Phys., 1975, V46, 4181

[34] Jing, X., and Krimm S., J. Polem. Sci., Polym letter, 1983, V21, 123

[35] Flory, J.P., and Yoon, D.Y., Macromolecules, 1984, V17, 862

[36] Guttman, C.M, and DiMazio, E.A., Macromolecules, 1982, V15, 525

[37] Natta, G., and Corradini, P., Nuovo Cimeto, Suppl., 1960, V1, 9

[38] Iwayanagi, S, Sakurai, I., and Sakurai, T.,
J. Macromol. Sci.-Phys., 1968, VB2 163

[39] Suehiro, K., and Takayanagi, M, J. Macromol. Sci.-Phys. 1970, VB4, 39

[40] Tatsumi, T., Fukushima, T., Imada, K., and Takayanagi M.,
J. Macromol. Sci.-Phys. 1967, VB1, 459

[41] Hsu, S.H., Moore, W.H., and Krimm, S., J. Appl. Phys., 1975, V46, 4185

[42] Oyama, T., Shiokawa, K., and Murata, Y., Polymer J., 1974, V6, 549

[43] Finter, J., and Wegner, G., Makromol. Chem., 1981, V182, 1859

[44] Marchetti A., and Martuschelli, E., J. Polym. Sci.,
Polym. Phys. Ed., 1976, V14, 323

[45] Grebowiez. J., Aycock,, W., and Wunderlich, B.,
Polymer, 1986, V27, 575

[46] Hendrix, C.,, Whiting, D.A. and Woodward, A.E.,
Macrom., 1971, V4, 571

[48] Evans, H., and Woodward, A.E., Macromolecules, 1978, V11, 685

[49] Nagamura, T. and Woodward, A.E., J. Polym. Sci.,
Polym. Phys. Ed, 1976, V14, 275

[50] Ng, S-B., Stellman, J.M, and Woodward, A.E.,
J. Macromol. Sci., 1973, VB7, 539

[51] Eng, S., and Woodward, A.E., J. Macromol. Sci., 1974, VB10, 627

[52] Eng, S., and Woodward, A.E., J. Macromol. Sci. Phys., 1974, VB10, 627

[53] Schilling, F.C., Bovey, F.A., Tonelli, A.E., Tseng, S.,
and Woodward, A.E., Macromolecules, 1984, V17, 728

[53] Stellman, J.M., and Woodward, A.E., J. Polym. Sci.,
Polym. Letter Ed. 1969, V7, 755

[54] Stellman, J.M., and Woodward, A.E., J. Polym. Sci., Part A2, 1971, 59

[55] Wichacheewa, P. and Woodward, A.E., J. Polym. Sci.,
Polym. Phys. Ed., 1978, V16, 1849

[57] Schilling, F.C., Bovey, F.A., Tseng, S., and Woodward, A.E.,
Macromolecules, 1983, V16, 808

[58] Woodward, A.E., Tseng, S., Schilling, and F.C.,Bovey, F.A.,
Polymer Preprints, 1983, V24, 808

[59] Schilling, F.C.,Bovey, F.A., Anandakumaran, K.,
and Woodward, A.E., Macromolecules, 1985, V18, 2688

[60] Kuo, C.C., and Woodward, A.E., Macromolecules, 1984, V17, 1034

[61] Xu, J.R., and Woodward, A.E., Macromolecules, submitted

[62] Tischler, F., and Woodward, A.E., Macromolecules, 1986, V19, 1328

[63] Corrigan, J. P. and Woodward, unpublished results

[64] Rinehart, R.E., Polymer Preprints, 1966, V7, 556

[65] Canal, A.J., Hewett, W.A., Shryne. T.M., Yougman, E.A., Chemistry and Industry, 1962, 1054

[66] Endo, R., J. Rubber Ind. Japan, 1961, V34, 527

[67] Kamide, K., Miyazaki, Y., Aby, T., British Polymer J., December V1981, 168

[68] Kamide, K., Miyazaki, Y., Makromol. Chem., 1975, V176, 1427

[69] Iwayanagi, S., Sakurai, I, Sakurai, T., Seto, T., J. Macromol., Phys., 1968, VB2, 163

[70] Silverstein, R.M, Bassler, C.C., Norrell, T.C., "Spectroscopic Identification of Organic Compounds", Wiley, New York, 1981, p263

[71] Clouge, A.D.H., Von Broekhoen, J.A.M, Blaauw, L.P., Macromolecules, 1974, V7, 348

[72] Pakula, T., Polymer, 1983, V23, 1300

[73] Harrison, I.R., and Juska, T., J. Polym. Sci., Polym. Phys. Ed., 1974, V17, 491

[74] Popli, R. and Mandelkern, L, J. Polym., Sci., 41 Polym. Phys. Ed., 1987, V25, 4

[75] Keller, A., in "Polymer Liquid Crystals, and Low Dimensional Solids" March, N, Tosi, M, Eds, Plenum Press, New York, 1984, Chapter 3

[76] Domszy, R.C., Alamo, R., Edwards, C.O., Mandelkern, L, Macromolecules, 1986, V19, 310

[77] Sanchez, I.C., Eby, R.K., Macromolecules, 1975, V8, 638